A revised (earliest Vallesian) age for the hominoid-bearing locality of Can Mata 1 based on new magnetostratigraphic and biostratigraphic data from Abocador de Can Mata (Vallès-Penedès Basin, NE Iberian Peninsula)

David M. Alba [a,*], Josep M. Robles [a], Isaac Casanovas-Vilar [a], Elisabet Beamud [b-c], Raymond L. Bernor [d-e], Omar Cirilli [d,f], Daniel DeMiguel [g,a], Jordi Galindo [a], Itziar Llopart [a], Guillem Pons-Monjo [a,] Israel M. Sánchez [a], Víctor Vinuesa [a], Miguel Garcés [c,h]

[a] *Institut Català de Paleontologia Miquel Crusafont, Universitat Autònoma de Barcelona, Edifici ICTA-ICP, c/ Columnes s/n, Campus de la UAB, 08193 Cerdanyola del Vallès, Barcelona, Spain*

[b] *Paleomagnetic Laboratory CCiTUB–Geo3Bcn CSIC, c/ Lluís Solé i Sabarís s/n, 08028 Barcelona, Spain*

[c] *Institut Geomodels, Grup de Recerca Consolidat de Geodinàmica i Anàlisi de Conques, Universitat de Barcelona, c/ Martí i Franqués s/n, 08028, Barcelona, Spain*

[d] *College of Medicine, Department of Anatomy, Laboratory of Evolutionary Biology, 520 W St. N.W., 20059, Washington D.C., USA*

[e] *Human Origins Program, Department of Anthropology, Smithsonian Institution, 20560, Washington D.C., USA*

[f] *Dipartimento di Scienze della Terra, Paleo[Fab]Lab, Università degli Studi di Firenze, Via G. La Pira 4, 50121 Firenze, Italy*

[g] *ARAID foundation / Universidad de Zaragoza, Departamento de Ciencias de la Tierra, and Instituto Universitario de Investigación en Ciencias Ambientales de Aragón (IUCA), Pedro Cerbuna 12, 50009 Zaragoza, Spain*

[h] *Departament de Dinàmica de la Terra i de l'Oceà, Facultat de Ciències de la Terra, Universitat de Barcelona, c/ Martí i Franqués s/n, 08028, Barcelona, Spain*

*Corresponding author.

E-mail address: david.alba@icp.at (D.M. Alba).

A revised (earliest Vallesian) age for the hominoid-bearing locality of Can Mata 1 based on new magnetostratigraphic and biostratigraphic data from Abocador de Can Mata (Vallès-Penedès Basin, NE Iberian Peninsula)

Abstract

The Abocador de Can Mata (ACM) composite stratigraphic sequence (els Hostalets de Pierola, Vallès-Penedès Basin, NE Iberian Peninsula) has yielded a diverse primate assemblage from the late Aragonian (Middle to Late Miocene). Detailed litho-, bio- and magnetostratigraphic control has enabled an accurate dating of these fossil remains. Comparable data, however, were lacking for the nearby locality of Can Mata 1 (CM1), which yielded a dryopithecine canine of a female individual. Given the lack of hipparionin equids and giraffids, CM1 has been correlated to the latest Aragonian (Mammal Neogene [MN] zone MN7+8). Here we revise the age of CM1 based on fieldwork and associated paleomagnetic samplings undertaken in 2018–2021. Our results extend the ACM composite sequence upward and indicate that CM1 correlates to the earliest Vallesian (MN9). The updated ACM sequence is ~300 m-thick and comprises 12 magnetozones correlated to subchrons C5Ar.1r to C5n.2n (~12.6 to 11.1 Ma; latest MN6 to earliest MN9, late Aragonian to earliest Vallesian). CM1 is correlated to C5r.1r (11.146–11.056 Ma), with an interpolated age of 11.11 Ma, thus postdating the dispersal of hipparionin horses into the Vallès-Penedès Basin—which is correlated to the previous subchron C5r.1n, with an interpolated age of 11.18 Ma, and by definition marks the beginning of the Vallesian. CM1 also minimally postdates the earliest record of giraffids at ACM—representing their earliest well-dated occurrence in the basin—being correlated to C5r.1n with an interpolated age of 11.11 Ma. We conclude that CM1 has an earliest Vallesian (MN9) age of ~11.1 Ma, intermediate

between the Aragonian dryopithecins and the Vallesian hispanopithecins. Ongoing paleontological surveillance at ACM thus offers the prospect to yield additional earliest Vallesian ape remains, which are essential to clarify their taxonomic allocation as well as to confirm whether hispanopithecins evolved locally from dryopithecins rather than immigrating from elsewhere during MN9.

Key words: Fossil apes; Dryopithecinae; Bretxa de Can Mata; Magnetostratigraphy; Paleomagnetism; Vallesian.

1. Introduction

1.1. Fossil primates from els Hostalets de Pierola

Thanks to continued paleontological surveillance of the digging activity during the construction of a dump between 2002 and 2014, a diverse primate assemblage (Alba, 2012; Marigó et al., 2014; Alba et al., 2017; DeMiguel et al., 2021; Fortuny et al., 2021) has been recovered from the Middle to Late Miocene stratigraphic sequence of Abocador de Can Mata (ACM; Alba et al. 2006, 2011a, 2017) in the fossiliferous area of els Hostalets de Pierola (Catalonia, Spain). Both small-bodied catarrhines (Alba et al., 2010, 2012a, 2015) and large-bodied apes—*Pierolapithecus* (Moyà-Solà et al., 2004; Almécija et al., 2009; Pérez de los Ríos et al., 2012; Hammond et al., 2013; Pina et al., 2014), *Dryopithecus* (Moyà-Solà et al., 2009a; Alba and Moyà-Solà, 2012; Pina et al., 2019, 2020), and *Anoiapithecus* (Moyà-Solà et al., 2009b; Alba et al., 2013)—have been recovered there, spanning from ~12.4–12.3 to ~11.6 Ma (Alba et al., 2017). While litho-, bio-, and magnetostratigraphic correlation has enabled an accurate dating of the fossil primate remains from ACM (Moyà-Solà et al.,

2009a; Casanovas-Vilar et al., 2011, 2016a, 2016b; Alba et al., 2017), this does not apply to all the previous hominoid finds from the same area.

A mandibular fragment with M_2–M_3 (IPS1826+1827) found in 1941 at Can Vila (Villalta Comella and Crusafont Pairó, 1941a, 1944) is the holotype of '*Sivapithecus*' *occidentalis*, which is considered a species inquirenda (Alba et al., 2020; Fortuny et al., 2021)—i.e., of uncertain taxonomic validity due to the lack of comparable elements in other species. This specimen comes from minimally older levels than ACM/BCV1 (Barranc de Can Vila 1, the type locality of *Pierolapithecus catalaunicus*) and thus has an age of ~12.0 Ma (Alba et al., 2013, 2017, 2020). However, the age of the two other previous finds is more uncertain. Thus, the stratigraphic provenance of an M^2 (MGSB48486) from Can Mata s.l. (Van der Made and Ribot, 1999), currently assigned to *Dryopithecus fontani* (Alba et al., 2013, 2017, 2020; Fortuny et al., 2021), is unknown. Therefore, it can only be considered broadly younger than the hominoid finds from ACM (Alba et al., 2013), but it is impossible to determine whether it is latest Aragonian (Mammal Neogene [MN] zone MN7+8) or earliest Vallesian (MN9) in age (i.e., ~11.3–11.0 Ma). The third previous hominoid find from the area is a C_1 of a female individual (IPS1766; Fig. 1) from the locality of Can Mata 1 (CM1) or Bretxa de Can Mata. It was originally assigned to *Hispanopithecus laietanus* (Crusafont-Pairó and Golpe-Posse, 1973; Golpe-Posse, 1993) or *Dryopithecus laietanus* (Begun et al., 1990; Harrison, 1991; Andrews et al., 1996), but most recently it was left unassigned to genus as Hominidae indet. (Casanovas-Vilar et al., 2011; Alba, 2012) or Dryopithecinae indet. (Alba et al., 2013, 2020; Marigó et al., 2014). This canine has been excluded from the hypodigm of *H. laietanus* because this species is not recorded until much later (~10.0 Ma; Alba et al., 2018) and also because the specimen cannot be directly compared with any of the ACM dryopithecine taxa. Although the provenance of IPS1766 from CM1 is well documented

(Crusafont-Pairó and Golpe-Posse, 1973), its age is uncertain owing to the lack of magnetostratigraphic data and poor stratigraphic control of historical finds of hipparionin equids from the area of els Hostalets de Pierola.

1.2. Uncertainties about the age of Can Mata localities

The localities of Can Mata are situated nearby the farmhouse of Can Mata de la Garriga within the fossiliferous area of els Hostalets de Pierola, in the Penedès sector of the Vallès-Penedès Basin (Fig. 2; Casanovas-Vilar et al., 2016a; for details on the geological background, see Casanovas-Vilar et al., 2008; Alba et al., 2009, 2017; Moyà-Solà et al., 2009a). Three Can Mata localities (CM1, CM2 and CM3) have been reported in the literature (Supplementary Online Material [SOM] S1.1), although only CM1 has yielded a rich fossil assemblage. The locality of CM1 (Fig. 3) was discovered in 1941 close to the farmhouse of Can Mata de la Garriga (Fig. 4), being considered pre-Vallesian given the absence of hipparionins and giraffids (Villalta Comella and Crusafont Pairó, 1941b, 1943; Crusafont and Truyols, 1954). In turn, CM2 was initially considered Vallesian in age due to the record of giraffids and the presence of *Hippotherium* molars in the same area (Crusafont Pairó, 1952; Crusafont and Truyols, 1954). Finally, CM3 corresponds to an isolated find of *Hippotherium* ~200 m in NE direction from CM1 (Fig. 4c; Alba et al., 2006; SOM S1.1), which represents the oldest hipparionin find of known provenance from the area of Can Mata. Over the years, and only with a few exceptions (Mein, 1990; Andrews et al., 1996; Pickford, 2013), most authors have correlated CM1 to the latest Aragonian on biostratigraphic grounds (Crusafont-Pairó and Golpe-Posse, 1973; Golpe-Posse, 1974, 1982, 1993; Agustí et al., 1985; de Bruijn et al., 1992; Alba et al., 2006, 2011a, 2017; Moyà-Solà et al., 2009b; Casanovas-Vilar et al., 2011, 2016a, 2016b; Robles et al., 2013), and the same applies to CM2

(Crusafont Pairó and Golpe Posse, 1971; Golpe-Posse, 1974; Agustí et al., 1985, 1997, 2001) with the exception of de Bruijn et al. (1992).

The published faunal list of large mammals from CM1 needs to be updated and revised to confirm the identity of multiple taxa that is confusing according to published sources (see S1.2 for further details). However, it is generally indicative of an age close to the Aragonian/Vallesian boundary. The frequent correlation of CM1 to MN7+8 instead of MN9 almost entirely relies on the lack of *Hippotherium* and giraffids. These large mammals have even been formally considered in the local biozonation of the Vallès-Penedès Basin (Casanovas-Vilar et al., 2016b). Even the claim that CM2 was located above CM1 (e.g., Agustí et al., 1985) might be exclusively based on the fact that Golpe-Posse (1974) roughly correlated CM1 with La Grive-Saint-Alban in France (MN7+8) and CM2 with Castell de Barberà (then considered latest MN7+8, but currently considered earliest MN9; Alba et al., 2019), based on the presence of giraffids in the latter locality. Along the same line of reasoning, Agustí et al. (1985) remarked that not only *Hippotherium*, but also giraffids—traditionally considered to predate the arrival of hipparionins in the Vallès-Penedès Basin (e.g., Golpe-Posse, 1974; Crusafont Pairó, 1975; Agustí et al., 1985, 1997, 2001)—were missing from CM1.

The important role played by hipparionins and giraffids in the local biozonation of the Vallès-Penedès Basin across the Aragonian/Vallesian transition might seem surprising given that most of the local biozones are based on rodents (e.g., Agustí et al., 1997; Casanovas-Vilar et al., 2016b). However, besides the role played by hipparionins in the definition of the Vallesian, there are other historical reasons that explain this situation. In particular, CM1 only yielded very scarce micromammal remains, contrasting with the hundreds of micromammal specimens recovered from the so-called 'bloc de marga' (marl block)—

originally attributed to nearby Mas d'Ocata (Schaub, 1944, 1947), but actually coming from Can Flequer (Agustí, 1981; Agustí et al., 1985), which is Vallesian based on the presence of *Hippotherium.* Agustí and colleagues (Agustí, 1981, 1999; Agustí and Gibert, 1982; Agustí et al., 1985, 1997, 2001; Agustí and Moyà-Solà, 1991) relied on a composite micromammal faunal list for all the purportedly pre-Vallesian outcrops from the area, collectively denoted as Hostalets Inferior. These authors noted similarities with micromammals from the unambiguously Vallesian localities (Hostalets Superior) and concluded that their composition remained virtually unchanged through the Aragonian/Vallesian boundary (see also Casanovas-Vilar et al., 2011, 2016a, 2016b). Needless to say, this practice might lead to circular reasoning (particularly if Vallesian levels are mistaken as pre-Vallesian due to the absence of *Hippotherium*). Nevertheless, ever since then, it has been customarily accepted that the latest Aragonian and earliest Vallesian rodent assemblages from the Vallès-Penedès Basin are virtually indistinguishable (Agustí et al., 1997; Alba et al., 2006; Casanovas-Vilar et al., 2011, 2016a, 2016b).

Alba et al. (2006) remained skeptical about whether CM2 was latest Aragonian or earliest Vallesian, but given that CM1 is a well-sampled locality, they assumed that the absence of *Hippotherium* was not a sampling bias and accepted its customary correlation to MN7+8. Under such an assumption, Moyà-Solà et al. (2009b: Fig. 5) and Casanovas-Vilar et al. (2011) correlated CM1 to the upper part of the reverse polarity subchron C5r.2r (postdating the short-duration normal polarity cryptochron C5r.2r-1), implying an age comprised between 11.263 and 11.188 Ma (Ogg, 2020). Casanovas-Vilar et al. (2016a) further correlated CM1 to the *Democricetodon crusafonti–Hippotherium* interval subzone of the Vallès-Penedès Basin (Casanovas-Vilar et al., 2016b), whose top boundary in this basin is defined by the first local occurrence (FLO) of *Hippotherium* at 11.18 Ma (Garcés et al., 1996, 1997; Agustí et al., 1997;

144 Casanovas-Vilar et al., 2016a, 2016b; Alba et al., 2019). In turn, based on the assumption
145 that CM3 was located ~40 m above CM1 (Alba et al., 2006), Moyà-Solà et al. (2009a)
146 tentatively correlated the former to C5r.1r, although such a correlation was revised to
147 C5n.2n by Casanovas-Vilar et al. (2016b: Fig. 3), following some corrections on the then
148 available composite magnetostratigraphic sequence for ACM and Ecoparc de Can Mata
149 (ECM; Alba et al., 2012b).
150 The tentative magnetostratigraphic correlation of CM1 by Moyà-Solà et al. (2009b) was
151 based on its geographic location and its lithostratigraphic correlation with paleomagnetic
152 samplings in the nearby Riera de Claret—as CM1 was then located outside the area of the
153 Can Mata landfill. Nevertheless, Robles et al. (2013: 999) noted that "paleomagnetic
154 sampling would be required in order to confirm correlation [of CM1] with C5r.2r [...] rather
155 than C5r.1n". The resumption of the digging activity at ACM in 2018, to enlarge further the
156 landfill, provided the opportunity to extend the sequence upward toward the Vallesian—
157 including the stratigraphic section where CM1 is located, as well as to measure in situ the
158 stratigraphic distance between CM1 and CM3. New paleomagnetic samples were therefore
159 taken in 2020 to update the ACM composite stratigraphic sequence (so as to accurately date
160 the fossil remains recovered between 2018–2020) and provide a revised
161 magnetostratigraphic correlation and interpolated ages for CM1 and CM3. Given their
162 biochronological implications, the oldest well-dated hipparionin and giraffid remains from
163 the area of els Hostalets de Pierola are also reported. Finally, our results are discussed in
164 relation to phylogenetic and paleobiogeographic uncertainties regarding the evolutionary
165 origin of Vallesian dryopithecines from Western Europe.
166
167 **2. Methods**

168 *2.1. Location and paleomagnetic sampling of Can Mata 1*

169 Although no detailed coordinates of CM1 are available from the literature, some of the
170 authors of this paper were able to locate it during a field visit in February 2004 (Fig. 3c), with
171 the help of published pictures (Villalta Comella and Crusafont Pairó, 1941b: Pl. XVI, 1943: Pl.
172 XV; see our Fig. 3a–d). Back in 2004, CM1 was well outside the area of the then planned
173 enlargement of the Can Mata landfill (Fig. 4), but this situation changed when a new
174 enlargement phase started after the publication of Alba et al. (2017). The new outcrops
175 exposed during 2019–2020 allowed us to extend the ACM composite sequence upward
176 toward the Vallesian. The new paleomagnetic samplings were performed in July 2020,
177 including the short section of CM1, which was finally affected by the construction works of
178 the landfill in 2021. With the help of an excavator machine, the outcrop was excavated
179 under paleontological surveillance in May 2021 (Fig. 5). This allowed us to find the original
180 spot of the excavation filled with debris (Fig. 5g), thereby confirming that the CM1 bone bed
181 had been completely excavated by Crusafont and collaborators several decades ago.

182 Magnetostratigraphic sampling was carried out in the perimeter of the newly excavated
183 Cell 13 and the future Cell 14 of the landfill. A total of 44 sites were sampled along a 78 m-
184 thick composite section, which yielded an average sampling resolution of 1.77 m/site. The
185 locality of CM1 was located at meter 62 of the section. 32 paleomagnetic samples were
186 collected along the ~65 m-thick Cell 13 (C13) section, 6 sites in the Préstec de Terres de
187 l'Abocador (PTA) sector, and another 6 sites in the overlying 15 m-thick Bretxa de Can Mata
188 section (Fig. 6). Fresh unaltered red-brown mudstones and fine-grained sandstones were
189 drilled by means of a battery-powered drill with a water-cooled diamond bit. The samples
190 were oriented in situ with a magnetic compass fixed to an orienting device with a
191 clinometer. Magnetic measurements were carried out at the Paleomagnetic Laboratory of

192 Barcelona (CCiTUB-Geo3Bcn CSIC). Laboratory procedures consisted of stepwise thermal
193 demagnetization and measurement of the natural remanent magnetization of one sample
194 per site. A thermal demagnetizer TD48EU (ASC Scientific) and a 755SRM superconducting
195 rock magnetometer (2G Enterprises) were used. The measurement routine included 12
196 increasing temperature steps, applied to all samples up to 630 °C or complete
197 demagnetization (100, 200, 250, 350, 400, 440, 480, 520, 550, 580, 610, and 630 °C).
198 Magnetic susceptibility was measured with a KLY-2 (Geofyzika Brno) after each
199 demagnetization step with no remarkable changes observed (SOM Table S1), which ensures
200 no significant formation of undesired secondary magnetic minerals during heating. Samples
201 showed a low temperature component that was usually removed below 200 °C, which we
202 interpret as a viscous recent overprint (SOM Fig. S1). Above this temperature, characteristic
203 components were calculated by principal component analysis (Kirschvink, 1980) after visual
204 inspection of the demagnetization diagrams using 'Paleomagnetism.org 2.2.0' interpretation
205 portal (Koymans et al., 2016). Characteristic components were usually defined between 250
206 and 580 °C (SOM Table S2), pointing to magnetite as the main remanence carrier. Only in
207 three samples the characteristic component reached higher temperatures (610 or 630 °C),
208 suggesting a mixture of magnetite and hematite. Characteristic components were ranked
209 into three classes according to their quality. Quality 1 components (42%) showed a straight
210 and complete decay directed towards the origin. Class 2 components (37%) were clearly
211 isolated from the viscous component and were defined by at least three demagnetization
212 steps showing an incomplete demagnetization trend. When only two temperature steps
213 were used to calculate the characteristic components, or polarity was difficult to assess due
214 to unstable behavior and erratic trajectories, they were classified as quality 3 (21%), and
215 were not considered for further magnetostratigraphic analysis.

Mean paleomagnetic directions and associated Fisher parameters (Fisher, 1953) were calculated using the PmagPy software (Tauxe et al., 2016). No fold test could be performed due to the homogeneous gentle dip of the beds, but a significant better agreement with the expected north-directed paleomagnetic direction was obtained after correction for the tilt of beds (SOM Fig. S2; SOM Table S3). The total number of samples of quality 1 and 2 resulted in a good stratigraphic resolution, so that occurrence of missing magnetozones can be considered unlikely. The obtained paleomagnetic directions were used to calculate the latitude of the virtual geomagnetic pole (VGP) for each site. Positive VGP latitudes were interpreted as normal polarity whereas negative VGP latitudes were interpreted as reversed polarity, and a sequence of polarity zones was represented accordingly in the local magnetostratigraphy (black for normal magnetozones and white for the reversed ones).

2.3. Correlation methods

Lithostratigraphic correlation As in Alba et al. (2017), we mostly relied on intensely red-colored horizons interpreted as paleosols for lithostratigraphic correlation in the ACM composite series. The composite lithostratigraphic sequence reported by Alba et al. (2017) was constructed on the basis of 38 local sections ranging from 7 to 150 m in thickness, of which 5 included the magnetostratigraphic data previously reported by Moyà-Solà et al. (2009a). Here we provide an updated version of the ACM composite sequence that incorporates 13 additional local sections, of which the one including CM1 has new magnetostratigraphic data. The new lithostratigraphic sections largely overlapped and were correlated by means of 9 additional correlation levels, resulting in a total of 51 correlation levels in the composite sequence of ACM.

239 Magnetostratigraphic correlation and interpolated ages The magnetostratigraphic
240 correlation of the ACM composite sequence with the Geomagnetic Polarity Time Scale
241 (GPTS; Ogg, 2020) is based on the 366 paleomagnetic samples reported by Moyà-Solà et al.
242 (2009a) and analyzed by Alba et al. (2017) plus the 44 samples newly reported in the
243 present work. The samples originally analyzed by Moyà-Solà et al. (2009a) were distributed
244 in three different sections from ACM—Barranc de Can Vila, Vial Intern, and Camí de Can
245 Vila–Cells 3–4 (the latter being the composite of three different sections)—plus the nearby
246 section of Riera de Claret. The newly sampled section of Cells 13–14 (including CM1) is
247 added here. The stratigraphic position of each ACM fossil locality was recorded relative to
248 its closest lithostratigraphic section(s), thereby being correlated on lithostratigraphic
249 grounds to the composite magnetostratigraphic sequence.
250 As in Alba et al. (2017), given short-term variation in sedimentation rates (due to the
251 intermittent nature of sedimentation in alluvial environments), an estimated age was
252 calculated for each locality using linear interpolation based on the sedimentation rate
253 computed for each subchron (Barry et al., 2002; Casanovas-Vilar et al., 2014: Fig. 3); for the
254 top and bottom subchrons, sedimentation rate was approximated by that of the adjacent
255 subchron. Alba et al. (2017) concluded that errors associated with interpolated ages are
256 lower than 100 ka, so that estimated ages for ACM localities can be considered reliable to
257 the nearest 0.1 Ma. However, interpolated ages to the nearest 0.01 Ma are also provided,
258 as they are still informative with regard to the relative age among ACM localities.
259 Biostratigraphic correlation The local biozonation of the Vallès-Penedès Basin during the
260 late Aragonian and Vallesian is based on Casanovas-Vilar et al.'s (2016b) biostratigraphic
261 scheme, which provides a formal diagnosis and description of each zone and is almost
262 exclusively based on rodents—except for the FLOs of *Hippotherium* and giraffids. The fossils

from els Hostalets de Pierola referred to in this paper are housed in the Institut Català de Paleontologia Miquel Crusafont (ICP) in Sabadell (Catalonia, Spain). The fossils described are referred to by their catalog numbers, which are preceded by the acronom 'IPS' ('Institut de Paleontologia de Sabadell', the former name of the ICP).

3. Results

3.1. Magnetostratigraphy

Our paleomagnetic results for the Cells 13–14 section, where CM1 is located, allowed us to identify the presence of six magnetozones (three normal and three reversed, with the lowermost one having a reversed polarity) defined at least by two consecutive sites of the same polarity (Fig. 6). The reliability of the magnetic zonation could be validated by a cross-correlation with the neighboring overlapping sections of the Riera de Claret and Camí de Can Vila–Cells 3–4 (SOM Fig. S3; Moyà-Solà et al., 2009a; Alba et al., 2017), which can be traced by lithostratigraphic correlation (SOM Fig. S4), supporting a primary origin of the magnetization.

A unique correlation of the local magnetostratigraphy of the Cells 13–14 section with the GPTS (Ogg, 2020) can be established based on its integration with other sections in the ACM area (Fig. 7), and refines earlier results (Alba et al., 2017). Given these constraints, the occurrence of two very short intervals of normal polarity within a period of dominantly reversed polarity points to a correlation of the Cells 13–14 section with the upper end of chron C5r. The lower normal magnetozone would represent the cryptochron C5r.2r-1n, and the second one subchron C5r.1n. The normal magnetozone on top of Cells 13–14 section would then be correlated to the lowermost portion of subchron C5n.2n. Despite not being

286 listed in the time scale until recently, the cryptochron C5r.2r-1 is a short event of
287 comparable duration to C5r.1n (Abdul Aziz et al., 2003; Ogg, 2020).
288 The lower portion of C5r.2r was previously the uppermost magnetozone recorded at the
289 ACM composite sequence s.s., which terminated a few meters above locality ACM/CCV1
290 (Camí de Can Vila 1; Moyà-Solà et al., 2009a; Alba et al., 2017; locality indicated in Fig. 7 and
291 SOM Fig. S3). Therefore, the five polarity reversals documented at the Cells 13–14 section
292 had not previously been recorded within the area of the landfil back in 2014—although they
293 had been documented at the Riera de Claret section, as well as partly (the first two
294 reversals) at the Camí de Can Vila section outside the landfill (Fig. 7; SOM Fig. S3; Moyà-Solà
295 et al., 2009a; Alba et al., 2017). The outcrops exposed subsequently within the area affected
296 by the landfill allowed us to extend the ACM composite section s.s. up to the lowermost
297 portion of the long normal polarity subchron C5n.2n (11.056–9.984 Ma), typical of the early
298 Vallesian. The locality of CM1 is located in the uppermost reversed polarity zone recorded
299 (Figs. 7 and 8), correlated with C5r.1r (11.146–11.056 Ma). The latter subchron
300 approximately extends from meters 278 to 293 of the ACM composite sequence (Table 1),
301 whereas CM1 is located on meter 284, resulting in an interpolated age of 11.11 Ma.
302 In turn, although no paleomagnetic samples were taken there, computations based on
303 both geographical location and field measurements indicate that CM3 is located ~8 m above
304 CM1 (based on the coordinates reported in Fig. 4 and a strike/dip of 180°/13° W), thus being
305 similarly correlated with C5r.1r with an interpolated age of 11.06 Ma. Finally, these results
306 made us reconsider previous correlations between the ECM and ACM composite sections
307 (Casanovas-Vilar et al., 2016b). Unfortunately, magnetostratigraphic data are only available
308 for the uppermost part of the section, where no polarity reversal is recorded. However, the
309 stratigraphic thickness between the base of the ECM and CM1, based on geographical

location (see coordinates in Fig. 4) and the aforementioned strike/dip figure, is estimated to be 63 m. According to this, the base of the ECM section would be roughly equivalent to ACM/CCV1 (~11.5 Ma), with the oldest localities (e.g., ECM/VCE-A1 [VCE = Variant de la Carretera de l'Ecoparc]) being latest Aragonian (correlated to the upper portion of C5r.2r, with an estimated age of ~11.2 Ma) instead of earliest Vallesian (~10.9 Ma) as previously thought (Alba et al., 2012b). In contrast, the remaining ECM localities would be earliest Vallesian, but older than previously thought (Alba et al., 2012b; Casanovas-Vilar et al., 2016b). In particular, based on the sedimentation rate calculated for the preceding subchron, ECM/VCE-Bb would have an estimated age of ~10.9 Ma, whereas ECM/VCE-B2 would date to ~10.8 Ma and ECM/VCE-C1 to ~10.7 Ma. Only the estimated ages for the ECM localities mentioned later in this paper are provided, as fieldwork during the following years will likely enable a refinement of their dating based on a more secure tie-point of the ECM base to the upper portion of the ACM composite section.

3.2. Biochronology

Small mammals The small mammal collection from the Aragonian levels of els Hostalets de Pierola includes rodent, lagomorph, and insectivoran remains that are mostly labeled as 'Hostalets inferior'or 'Hostalets vindobonien'. Only three specimens are accompanied by the label 'Can Mata 1' and can be unambiguously related to this locality. The remainder of the small mammal sample certainly mixes material from different sites, as already stated by Agustí and Gibert (1982), but probably includes additional specimens from CM1. The assemblage is overwhelmingly dominated by the cricetids *Hispanomys lavocati, Hispanomys dispectus*, and *Megacricetodon ibericus*. In addition, the cricetid *Dem. crusafonti*, the terrestrial sciurid *Csakvaromys bredai* and the lagomorph *Prolagus oeningensis* also occur in

lower numbers. The same taxa are also present in the collection from Vallesian levels of the area (Hostalets Superior), largely originating from the 'bloc de marga' (Can Flequer).

Given that the cricetids *His. lavocati, His. dispectus*, and *M. ibericus* are present in the small mammal collections from both Hostalets Inferior and Superior, it is not surprising that no significant difference was previously noticed across the Aragonian/Vallesian boundary in the area (e.g., Agustí et al., 1985). However, our magnetostratigraphic results—indicating that CM1 is earliest Vallesian and providing an accurate dating for ACM localities—suggest otherwise. At ACM, the FLO of *M. ibericus* is recorded from ACM/C1-E9 (with an interpolated age of 12.29 Ma), whereas the FLO of *His. lavocati* is recorded from various localities dated to ~11.6 Ma (e.g., ACM/C6-A2, with an interpolated age of 11.61 Ma), indicating that both species appeared well before the Aragonian/Vallesian boundary. In contrast, *His. dispectus* has not been reported from the ACM composite section (Casanovas-Vilar et al., 2016b), at least as defined in Alba et al. (2017)—i.e., up to ~11.4 Ma. *Hispanomys dispectus* is neither present at the oldest micromammal site from ECM (ECM/VCE-A1), which records *His. lavocati* and, as noted above, is probably latest Aragonian in age (~11.2 Ma, correlated with the upper portion of C5r.2r). Similarly, the roughly coeval locality ACM/PTA-A2, with an interpolated age of 11.21 Ma (Alba et al., 2022), records *His.* cf. *lavocati* but not *His. dispectus*, thus suggesting that the latter species might have not appeared until the Vallesian.

Large mammals We were unable to find among the ICP collections any *Hippotherium* remains labeled as coming from CM3. However, in all probability, the specimen found by Jordi Agustí in 1976 corresponds to a left mandibular fragment with very worn M_2–M_3 (IPS30897; SOM Fig. S5d–f). This specimen was found in the ICP collections inventoried together with an isolated left M_3 (currently IPS124307) of the same taxon (SOM Fig. S5a–c)

358 despite belonging to two different individuals, and collectively labeled as coming from “Can
359 Mata, levels superior than those of the breccia” (our translation from Spanish). According to
360 its discoverer, the specimen from CM3 most likely corresponds to IPS30897 (pers. comm. to
361 J.G., December 2021). However, pending a more complete revision of all the *Hippotherium*
362 remains from Hostalets Superior, both specimens are taken into account here (see
363 description in SOM S2.1). The presence of a well-developed pli caballinid in IPS124307 hints
364 at similarities between the Can Mata sample and Pannonian C remains from the Vienna
365 Basin (Austria) assigned to *Hippotherium* sp. (Bernor et al., 2017, 2021).
366 With regard to giraffids, CM1 slightly postdates the oldest well-dated record of this
367 family at ACM, which corresponds to two M^3 germs from a single individual (IPS121859;
368 SOM Fig. S6a–f) found isolated (i.e., not associated with additional fossil remains) in April
369 2020 at sector ACM/C13/C14-A. The specimen’s provenance is located only 1.3 m below
370 CM1 (i.e., approximately at meter 283 of the ACM sequence), thereby being correlated to
371 the same subchron and having the same interpolated age as CM1. In turn, the giraffid
372 material from ECM consists of a few teeth from locality ECM/VCE-Bb (SOM Fig. S6g–r),
373 which despite the lack of *Hippotherium* has an unambiguous Vallesian age somewhat
374 younger than CM3 (~10.9 Ma, updated from Alba et al., 2012b; see above for further
375 details). A description of IPS121859, together with other giraffid material from the area of
376 els Hostalets de Pierola, is provided in SOM S2.2. Although the scarce remains from ACM
377 and ECM are not informative enough to provide a taxonomic attribution to genus rank, they
378 likely correspond to the same taxon previously identified as *Palaeotragus* sp. by Crusafont
379 Pairó (1952) based on Can Mata (including CM2) remains. Deciphering the taxonomic
380 affinities of these giraffids is hindered by the lack of ossicones and the fact that they display
381 a mix of apparently primitive and derived characters. Some of the latter are similar to those

present in taxa allied to the samothere-sivathere lineage, although future systematic work is needed to test this hypothesis. In any case, it is noteworthy that the Can Mata giraffid displays some dental and postcranial differences relative to *Decennatherium pachecoi*, present in the early Vallesian of the Calatayud-Montalbán and Duero basins (Crusafont-Pairó, 1952; Ríos et al., 2016), despite being only slightly older than the material from its type locality (Nombrevilla 1, which has an age of ~10.8 Ma; Van Dam et al., 2014). This supports Crusafont Pairó's (1952) early assessment that a different (even if poorly known) giraffid species is recorded during the earliest Vallesian in the Vallès-Penedès Basin.

4. Discussion

4.1. The age of Can Mata localities based on the updaed Abocador de Can Mata sequence

The previous ACM composite sequence, based on the fieldwork undertaken between 2002 and 2014 (Alba et al., 2017), was 234 m in thickness, comprised seven magnetozones that were correlated with C5Ar.1r to C5r.2r, and covered a time span between ~12.6 and ~11.4 Ma. With the addition of the new magnetostratigraphic section of Cells 13–14 and other lithostratigraphic sections excavated since 2017, the ACM composite sequence now has a thickness of 300 m (Fig. 8) and includes up to 12 magnetozones (Table 1), ranging in time from ~12.6 to ~11.1 Ma. The newly added magnetostratigraphic section allows us to refine the interpolated ages of previously known ACM localities from the uppermost portion of the composite sequence. These interpolated ages were formerly based on the stratigraphic situation of the top of C5r.2r in the nearby sequence of Camí de Can Vila (Alba et al., 2017), which has been slightly corrected based on our new results (Table 1). Furthermore, our magnetostratigraphic analyses for the Cells 13–14 section enable an accurate dating of the new fossil localities (and isolated finds) from ACM that have been

406 discovered since 2017, as well as of CM1. A comprehensive updated list of ACM localities
407 and sectors, based on the subchron chronological and stratigraphic boundaries reported in
408 Table 1, is provided in SOM Tables S4 and S5, respectively. In turn, an updated list of ACM
409 primate-bearing localities as compared with CM1 is also reported in Figure 8 and SOM Table
410 S6.

411 Our results necessitate us to reconsider the previously published correlations for the
412 hominoid-bearing locality of CM1, as they support an unambiguous correlation with C5r.1r.
413 These results contradict the commonly held notion that CM1 (and CM2) are late Aragonian
414 (MN7+8) in age (see the Introduction) and indicate an estimated age of ~11.1 Ma for both
415 CM1 and CM3. Indeed, CM1 slightly postdates the short normal magnetic polarity subchron
416 C5r.1n (11.188–11.146 Ma), where *Hippotherium* is first recorded in the Vallès-Penedès
417 Basin (Garcés et al., 1996, 1997; Agustí et al., 1997; Casanovas-Vilar et al., 2016a, 2016b;
418 Alba et al., 2019). According to this, CM1 and CM3 would be slightly younger than both Creu
419 de Conill 20 and Castell de Barberà (~11.2 Ma), but older than most of the ECM composite
420 sequence—with the exception of its lowermost portion (e.g., ECM/VCE-A1), which on
421 lithostratigraphic grounds appears to be latest Aragonian in age (contra Alba et al., 2012b;
422 Casanovas-Vilar et al., 2016b). The age of CM2 cannot be estimated with certainty, given
423 that its exact geographic location and stratigraphic position above CM1 are unknown.
424 However, given the geographical proximity to the Can Mata farmhouse, CM2 must be
425 roughly penecontemporaneous with CM1 (~11.1 Ma), in agreement with Crusafont-Pairó's
426 (1952) original dating based on the presence of hipparionin remains in the same area
427 (although not in the same stratigraphic horizon).
428
429 *4.2. Biostratigraphic and biochronological implications*

Small mammals The earliest Vallesian micromammal assemblages have previously been found to be taxonomically identical to the late Aragonian ones (see Section 1.2 as well as SOM S3.1 for further details). Similarly, the local zone H of the Calatayud-Montalbán Basin was originally correlated to the earliest Vallesian (Daams and Freudenthal, 1981) but is currently considered to span the latest Aragonian and the early Vallesian (Álvarez Sierra et al., 2003; Van Dam et al., 2014; García-Paredes et al., 2016). This interpretation is based on the fact that neither Nombrevilla 9 nor 10 (~11.2 Ma) record *Hippotherium*, which is not found there until Nombrevilla 1 (~10.8 Ma). A pre-Vallesian age for Nombrevilla 9 is further supported by its magnetostratigraphic correlation to the uppermost portion of C5r.2r with an interpolated age of 11.20 Ma, whereas Nombrevilla 10 correlates with C5r.1n with an interpolated age of 11.18 Ma (Garcés et al., 2003; Van Dam et al., 2014) has not yielded large mammal remains (Álvarez-Sierra et al., 2003). *Megacricetodon ibericus* is recorded in the latest Aragonian and the earliest Vallesian both in the Vallès-Penedès Basin and the Calatayud-Montalbán Basin (SOM S3.1), being thus irrelevant for determining the Aragonian/Vallesian boundary. Only the later appearance of the cricetid *Cricetulodon hartenbergeri* denotes a significant change in the rodent faunas (SOM S3.2), roughly coinciding with the extinction of the cricetids *Dem. crusafonti* and *M. ibericus*, which were generally dominant elements of the latest Aragonian and earliest Vallesian rodent faunas in both basins (SOM S3.2).

Nevertheless, the revised correlation of CM1 to the earliest Vallesian highlights the potential biostratigraphic significance of *Hispanomys* species during the latest Aragonian and earliest Vallesian, which had been previously neglected due to incorrect correlation of various localities (including CM1) to the latest Aragonian. In the Calatayud-Montalbán and Duero basins (López-Guerrero et al., 2014, 2019; Van Dam et al., 2014; Castillo et al., 2018;

SOM S3.3), *His. lavocati* is restricted to the late Aragonian (zone G3), whereas *His. nombrevillae* is recorded around the Aragonian/Vallesian transition (zone H), and *His. aragonensis* appears later in early Vallesian (zone I). In contrast, in the Vallès-Penedès Basin *His. lavocati* persists into the earliest Vallesian, which is characterized by two different species of this genus: *His. dispectus* and *Hispanomys daamsi*. Neither of these species has been thus far recorded from Aragonian levels from ACM, being restricted to earliest Vallesian localities of the Vallès-Penedès Basin (and also the Empordà basin in the case of *His. dispectus*; Casanovas-Vilar et al., 2016a; SOM S3.3). The only exception is the presence of *His. dispectus* at Hostalets Inferior. However, the fact that the latter assemblage potentially includes Vallesian material from levels previously considered to predate the dispersal of *Hippotherium* (such as CM1) make it uncertain the record of the species before the Vallesian. In contrast, later early Vallesian localities from ECM record *His. aragonensis*, which is first recorded at ~10.8 Ma (Alba et al., 2012b; Casanovas-Vilar et al., 2016b; SOM S3.3). In summary, both *His. dispectus* and *His. daamsi* appear conclusively recorded only from a short time period during the earliest Vallesian (accurately dated localities between ~11.2–11.0 Ma), thus potentially being a biochronological marker of the Vallesian in its type area (see SOM S3.3 for further details).

Hipparionins European *Hippotherium* originated from a single dispersal event of *Cormohipparion* from North America sometime after 11.5 Ma (Woodburne, 2007, 2009; Bernor et al., 2017, 2020, 2021). *Cormohipparion* has been recorded in the Old World since 10.8 Ma in Asia (Bernor et al., 2003; Wolf et al., 2013) and 10.7 Ma in Africa (Bernor et al., 2004; Bernor and White, 2009), but not in Europe, where *Hippotherium* is recorded earlier and almost simultaneously in the Vallès-Penedès Basin in Spain at ~11.2 Ma (Garcés et al., 1996; Agustí et al., 1997; Casanovas-Vilar et al., 2016a, 2016b; Alba et al., 2019) and in the

Pannonian C sites of the Vienna Basin (Gaiselberg, Atzelsdorf, and Mariathal) in Austria at ~11.4–11.0 Ma (Bernor et al., 2017). An earlier age of ~11.5 Ma has been proposed for the first occurrence of hipparionins in China (Fang et al., 2016; Sun et al., 2022), thus being slightly older than the record of *Hippotherium* in the Vienna and Vallès-Penedès basins. However, the corresponding magnetostratigraphy (Fang et al., 2016) is missing many relevant subchrons, such that alternative correlations—including C5r.1r, which could imply a younger age roughly coeval with the European *Hippotherium* datum—cannot be discounted (SOM S4.1).

Different species of *Hippotherium* are recorded in the Vallesian of the Vallès-Penedès and Calatayud-Montalbán basins. In the former, *Hippotherium catalaunicum* is customarily recognized as a distinct species (Bernor et al., 1980, 1996, 2021; Woodburne and Bernor, 1980), whereas *Hippotherium koenigswaldi* is recorded at Nombrevilla 1 (~10.8 Ma). Both species have been interpreted as derived in facial and dental morphology compared with *Hippotherium primigenium* from Central Europe (Bernor et al., 1996). A third species, *Hippotherium melendezi*, is recorded from MN9 of the Duero Basin (SOM S4.2), although its cranial morphology rather supports its inclusion in *Hipparion* s.s. (Bernor et al., 1996), which is otherwise first recorded at MN10 in Iran (Bernor et al., 2017). Available evidence thus indicates that vicariant speciation events occurred during MN9 after the initial dispersal of *Hippotherium* into the Iberian Peninsula. Nevertheless, the identity of the earliest Vallesian (~11.2–11.0 Ma) hipparionins from the Vallès-Penedès Basin, which are older than either *Hip. catalaunicum* and *Hip. koenigswaldi* and include the remains from els Hostalets de Pierola (this paper) and Castell de Barberà (Rotgers and Alba, 2011; Alba et al., 2019), remains to be clarified (Alba et al., 2019). The dental specimens from Can Mata reported in this paper show a similar morphology to the Pannonian C *Hippotherium* remains from the

Vienna Basin, which are more plesiomorphic than those of *Hipp. primigenium* (Woodburne 2009; Bernor et al., 2017), and may be thus identified as *Hippotherium* sp.

Giraffids and other large mammals The giraffid remains from CM2 described by Crusafont-Pairó (1952), and the whole giraffid sample from earliest Vallesian sites of the Vallès-Penedès Basin, have traditionally been assigned to *Palaeotragus* instead of *Decennatherium* (e.g., Agustí et al., 1985, 2001)—albeit it is noteworthy that Crusafont-Pairó (1952) noted similarities with species currently included in *Schansitherium* sp. (SOM S4.3). Nevertheless, like the new dental remains reported here from ACM and ECM, the remainder of the Vallès-Penedès giraffid sample from the earliest Vallesian only includes scarce dental and postcranial remains, which are not informative enough to justify an attribution to genus rank. Both *Schansitherium* and *Decennatherium* belong to the samothere-sivathere clade and the former only appears slightly more basal than *Decennatherium* in cladistic analyses (Ríos et al., 2017). *Decennatherium* has been reported not only from the Vallesian of Spain (Ríos et al., 2016, 2017) but also of Pakistan (Ríos et al., 2019; see SOM S4.3 for further details), where it is first tentatively recorded at 13.5 Ma (Ríos et al., 2019). The combination of more primitive features than in *Decennatherium* with some apparently derived characters raises the possibility that '*Palaeotragus*' sp. from the Vallès-Penedès Basin might belong to a very basal species of *Decennatherium*, or at least to a genus closely related to the latter. Therefore, both '*Palaeotragus*' sp. from the Vallès-Penedès and *Dec. pachecoi* from elsewhere in Spain might have originated from the earliest giraffid immigrants that dispersed from the east.

Despite the lack of giraffids and *Hippotherium* at CM1, our results conclusively indicate that this locality postdates, even if slightly, the earliest well-dated record of giraffids in the area of els Hostalets at ~11.1 Ma (Fig. 8) and elsewhere in the Vallès-Penedès Basin (Castell

de Barberà at ~11.2 Ma; Alba et al., 2019). This indicates that the lack of both giraffids and hipparionins at CM1 is either a sampling bias and/or must be attributed to local paleoenvironmental reasons. Giraffid remains assigned to *Palaeotragus* have also been cited from multiple Vallès-Penedès localities of controversial age (latest Aragonian or earliest Vallesian; see SOM 4.3. for further details). Many of these localities were initially correlated to the Vallesian given that Crusafont Pairó (1950) conceived this land mammal age as characterized by the presence of both hipparionins and giraffids. However, the subsequent more detailed characterization of the Vallesian by Crusafont Pairó and Truyols Santonja (1960) only emphasized the dispersal of hipparionins as a biochronological marker—even though the association with giraffids was still noted. Ultimately, Crusafont Pairó and Golpe Posse (1971) defined a new pre-Vallesian biozone characterized by the lack of hipparionins and the presence of giraffids, to which CM2 and other localities of uncertain age around the Aragonian/Vallesian boundary were correlated (e.g., Golpe-Posse, 1974; Crusafont Pairó, 1975; SOM S4.3). This view was subsequently followed by Agustí and coauthors (Agustí et al., 1985, 1997, 2001; Agustí and Moyà-Solà, 1990), leading to the idea that giraffids of genus *Palaeotragus* would constitute a biochronological marker of MN7+8 and that only the giraffid *Decennatherium* would be indicative of the Vallesian (see SOM S4.3 for additional details). In contrast, during the last decade an earliest Vallesian age has been favored for many of these localities (Casanovas-Vilar et al., 2016a, 2016b; Alba et al., 2019). Our results further indicate that a latest Aragonian age is no longer tenable for CM2, as CM1 correlates to the Vallesian despite the lack of *Hippotherium*. The fact that giraffids, as shown here, are recorded slightly before *Hippotherium* at els Hostalets de Pierola might simply result from insufficient sampling, paleoecological biases, and the lack of stratigraphic control for most historical finds of *Hippotherium* in the area. At ACM, giraffids have yet to

550 be found in the late Aragonian levels (Alba et al., 2006, 2017), suggesting that giraffids and
551 hipparionins might have dispersed approximately at the same time (as previously supported
552 by Casanovas-Vilar et al., 2016b).
553 In the Calatayud-Montalbán Basin, the earliest record of giraffids corresponds to *Dec.*
554 *pachecoi* from Nombrevilla 9, correlated to C5r.2r with an interpolated age of 11.20 Ma and
555 been considered latest Aragonian in age due to the lack of *Hippotherium* (Álvarez-Sierra et
556 al., 2003; Van Dam et al., 2014). If such a correlation is accurate, it implies that giraffids
557 might have immigrated into Iberia during the latest Aragonian immediately before the entry
558 of *Hippotherium* (as recorded in the Vallès-Penedès Basin at 11.18 Ma). On the other hand,
559 Nombrevilla 9 already records several typically Vallesian elements, such as *Dec. pachecoi*,
560 *Deinotherium giganteum*, *Tetralophodon longirostris*, and *His. nombrevillae* (Álvarez Sierra
561 et al., 2003; Van Dam et al., 2014; García-Paredes et al., 2016; Ríos et al., 2016). Given that
562 the dispersal of *Hippotherium* seems to have been roughly synchronous across Europe
563 (Vasiliev et al., 2011; Bernor et al., 2017; this paper), it is conceivable that *Hippotherium* had
564 already dispersed into Iberia when Nombrevilla 9 was deposited, being absent from this
565 locality because of the same (likely paleoenvironmental) reasons as to why this taxon is
566 missing or very rare in many earliest MN9 sites of the Vallès-Penedès Basin.
567 While the presence of *Hippotherium* indicates a Vallesian age by definition, its absence
568 cannot be taken as unambiguously indicating a pre-Vallesian age (Alba et al., 2019). For
569 example, no hipparionin remains have thus far been identified from the nearby ECM
570 composite series despite the unambiguous Vallesian age of most of the series (Alba et al.,
571 2012b; this paper). The cases of CM2 and Castell de Barberà further highlight the risk of
572 relying almost exclusively on the purported absence of *Hippotherium* when making
573 biostratigraphic correlations for sites located close to the Aragonian/Vallesian boundary—

574 particularly because other large mammal taxa, such as giraffids, also appear indicative of a
575 Vallesian age.
576 There are other eastern immigrants that first appear in the Iberian Peninsula and
577 elsewhere in Europe coinciding with the beginning of the Vallesian, such as the
578 machairodontine felid *Machairodus* and the suid *Propotamochoerus palaeochoerus* (see
579 SOM S4.4 for further details). These taxa co-occur with *Hippotherium* at Creu de Conill 20
580 are also present at presumably Vallesian levels from els Hostalets de Pierola, although it is
581 uncertain when they are first recorded there (SOM S4.4). Further research would be
582 required to discern if the dispersal of *Hippotherium* and other Vallesian faunal elements was
583 synchronous or part of a more protracted faunal turnover across the Aragonian/Vallesian
584 transition. Nevertheless, currently available data indicate that the large mammal
585 assemblages from the earliest Vallesian of the Vallès-Penedès Basin were characterized by
586 an array of new immigrants including at least *Hippotherium*, giraffids, *Propotamochoerus*,
587 and *Machairodus*, even if these taxa do not always co-occur.
588
589 *4.3. Implications for primate evolution*
590 In the past decades, dryopithecines have been variously interpreted as pongines,
591 hominines, and stem hominids, so that conclusively deciphering their closest phylogenetic
592 affinities would be key for deciding among competing scenarios about the place of origin of
593 crown hominids (see discussion in Almécija et al., 2021; Pugh, 2022). Not so long ago, late
594 Middle and early Late Miocene dryopithecines from Europe were still included in a single
595 genus *Dryopithecus* (e.g., Andrews et al., 1996; Begun, 2002), largely as a result of the
596 limited knowledge of Middle Miocene dryopithecines at the time. This constrasts with the
597 panoply of genera that are currently recognized, following the discovery of more complete

598 Middle Miocene ape remains at ACM in the 2000s, which prompted the realization that
599 dryopithecine diversity could not be accommodated within the single genus (Begun, 2009;
600 Moyà-Solà et al., 2009a). Two alternative proposals were then put forward: Moyà-Solà et al.
601 (2004, 2009a, 2009b) distinguished various Middle Miocene genera (*Pierolapithecus*,
602 *Anoiapithecus*, *Dryopithecus*) and included the Late Miocene material from Spain and
603 Hungary into a single genus *Hispanopithecus*; in contrast, Begun (2009) and Begun et al.
604 (2012) considered that *Pierolapithecus* and *Anoiapithecus* could be synonyms of
605 *Dryopithecus* and distinguished instead *Hispanopithecus* from *Rudapithecus* in the Late
606 Miocene. The distinction between the two latter genera is currently also favored by Alba,
607 Moyà-Solà and colleagues (e.g., Almécija et al., 2021; Fortuny et al., 2021; Urciuoli et al.,
608 2021), while the existence of more than a single genus at ACM is also generally
609 acknowledged (e.g., Böhme et al., 2019; Andrews, 2020). To recognize the fact that the Late
610 Miocene dryopithecines appear more derived and closely related than the Middle Miocene
611 ones, Alba (2012) distinguished the tribes Dryopithecini and Hispanopithecini, although this
612 picture became more complicated after the description of *Danuvius*, which is dated to ~11.6
613 Ma (Kirscher et al., 2016; Böhme et al., 2019) and thus roughly coeval with the youngest
614 dryopithecines from ACM (Alba et al., 2017).
615 On paleobiogeograpic grounds, it would be most reasonable to assume that
616 hispanopithecins from the Vallesian evolved locally in central and/or western Europe from
617 Middle Miocene dryopithecin ancestors. However, this cannot be conclusively asserted,
618 owing to phylogenetic uncertainties surrounding the internal phylogeny of dryopithecines
619 coupled with the fragmentary nature of the hominoid fossil record in Europe throughout
620 the Aragonian/Vallesian boundary. Regarding phylogeny, it is generally considered that
621 hispanopithecins are more derived than dryopithecins (e.g., Alba, 2012), but it is currently

622 uncertain whether dryopithecines as a whole constitute a clade or a paraphyletic
623 assemblage (Almécija et al., 2021), because few cladistic analyses have analyzed
624 dryopithecins and hispanopithecins separately. Alba et al.'s (2015) analysis recovered
625 *Hispanopithecus* and *Pierolapithecus* as stem hominids, whereas Pugh's (2022) analyses
626 more conclusively showed that dryopithecines are best interpreted as stem hominids, with
627 hispanopithecins appearing more closely related to crown hominids than dryopithecins.
628 *Danuvius* appears intermediate in the degree of suspensory adaptations and other
629 morphological features between dryopithecins and hispanopithecins (Almécija et al., 2021),
630 thus favoring the regional continuity hypothesis by strengthening the view that the more
631 suspensory hispanopithecins might have evolved from the Middle Miocene dryopithecins.
632 However, *Danuvius* predates the beginning of the Vallesian by more than 0.5 Myr and the
633 earliest record of hispanopithecin genera by about 1.5 Myr. Therefore, *Danuvius* cannot be
634 automatically taken as an evolutionary link between dryopithecins and hispanopithecins—at
635 least, until a formal cladistic analysis shows that this genus is more closely related to the
636 latter.
637 The hypothetical phylogenetic link between dryopithecins and hispanopithecins is further
638 complicated by the fact that Pugh's (2022) analyses sometimes recovered a close link
639 between dryopithecines and kenyapithecines (*Kenyapithecus* and *Griphopithecus*), as
640 previously argued by Moyà-Solà et al. (2009b), whereas '*Lufengpithecus*' *hudienensis* from
641 the Late Miocene (8.2–7.2 Ma) of China (Kelley and Gao, 2012) tended to group with
642 hispanopithecins instead of *Lufengpithecus lufengensis* (the type species of the genus),
643 which clusters with other Asian hominids in a pongine clade (Pugh, 2022). This closer
644 phylogenetic of '*L.*' *hudienensis* with hispanopithecins instead of pongines agrees with the
645 lack of pongine synapomorphies in this species (Kelley and Gao, 2012) and the possession of

some dental similarities (in canine and incisor morphology; Begun and Kelley, 2016). Coupled with faunal similarities suggesting "a strong biogeographic link between Europe and China" by the Late Miocene (Begun, 2013: 143; see also Begun and Kelley, 2016), currently available evidence suggests that dryopithecines might have been present in both Europe and Asia during the Late Miocene and at the very least supports more complex paleobiogeographic scenarios than customarily assumed (Gilbert et al., 2020). Although '*L.*' *hudienensis* is younger than the European hispanopithecins, the the oldest and less well-known species included in the same genus—*Lufengpithecus keiyuanensis* from the Middle Miocene of China (12.5–11.6 Ma; Kelley, 2002; Ji et al., 2013)—has not been analyzed from a cladistic viewpoint yet and it is thus uncertain whether it belongs to the pongine radiation. Such a possibility is supported by the fact that closer morphological similarities between the samples of *L. keiyuanensis* from Xiaolongtan and '*L.*' *hudienensis* from Yuanmou (as opposed to *L. lufengensis* from Shihuiba, Lufeng) have been noted by previous authors, who even included the two former within a single species (Gao, 1998; Harrison et al., 2002). Given that the beginning of the Vallesian, as discussed above, is not only marked by the dispersal of hipparionin horses, but also by the more or less simultaneous arrival of other taxa that dispersed from the east—including the machairodontine felid *Machairodus*, giraffids, and the suid *Propotamochoerus*—the possibility that hispanopithecins did not locally evolve from dryopithecins but dispersed from elsewhere roughly coinciding with the Aragonian/Vallesian boundary deserves further consideration.

Unfortunately, the identity of earliest Vallesian hominoids from Europe is not well known. In particular, during the time interval between the latest Aragonian (~11.5 Ma, i.e., after *Danuvius*) and the earliest well-dated occurrences of *Hispanopithecus* (~10.3–10.0 Ma; Alba et al., 2018) and *Rudapithecus* (~10.0–9.8 Ma; Casanovas-Vilar et al., 2011) in the

Vallesian, the record of European hominids is very scarce. In the Vallès-Penedès Basin, earliest Vallesian dryopithecines are known from Castell de Barberà (~11.2 Ma; Alba et al., 2019) and CM1 (~11.1 Ma; this paper). The former material was assigned to cf. *D. fontani* based on its inferred body mass when Castell de Barberà was still correlated to the latest Aragonian (Alba et al., 2011b; Alba, 2012; Marigó et al., 2014), but such an allocation is tentative given the lack of craniodental specimens (Almécija et al., 2012; Alba et al., 2019; Pina et al., 2019). With regard to the CM1 canine (Crusafont-Pairó and Golpe-Posse, 1973), a secure taxonomic allocation is not possible (as it cannot be directly compared with ACM dryopithecin taxa). Elsewhere in Europe, when poorly dated localities are excluded, the earliest Vallesian material is restricted to an isolated molar from Mariathal, Austria (Thenius, 1982), which has yielded a form of *Hippotherium* (*Hip.* aff. *primigenium*) slightly more derived than those from Gaiselberg and Atzelsdorf (*Hippotherium* sp.), suggesting a slightly younger age within Pannonian C (but still be older than 11 Ma; Bernor et al., 2017). The Mariathal hominoid molar was formerly assigned to *Dryopithecus brancoi* by several authors (Thenius, 1982; Begun, 2002), or alternatively to *Dryopithecus carinthiacus* by Andrews et al. (1996), but more recently it was considered of uncertain attribution (Casanovas-Vilar et al., 2011; Pickford, 2012).

Discovering additional fossil great ape finds from the time span comprised between ~11.5 and ~10.5 Ma is thus required to determine their taxonomic identity as well as to further clarify the phylogenetic relationships between the late Aragonian dryopithecins, *Danuvius*, '*L.*' *hudienensis* and other species of *Lufengpithecus* from China, and the Vallesian hispanopithecins from Europe. Given that the fossiliferous accumulations from both Castell de Barberà (Almécija et al., 2019) and CM1 (this paper) are exhausted, fieldwork efforts should be redirected to other earliest Vallesian sites. In this regard, the site of Creu de Conill

694 20 (representing the earliest appearance of *Hippotherium* in western Europe) has some
695 potential, even though it displays marked paleoenvironmental differences as compared with
696 Castell de Barberà (Alba et al., 2019) and has not yielded any hominoid remains yet despite
697 several successive fieldwork campaigns since 2016. Thus far, Vallès-Penedès hominoids
698 dating to the Vallesian were considered to be restricted to the Vallès Sector of the basin.
699 Redating CM1 is thus important because it conclusively shows that these primates were also
700 recorded in the earliest Vallesian of the Penedès Sector, thereby opening new research
701 prospects for the future. In particular, ongoing works of paleontological surveillance during
702 the new phase of enlargement of the Can Mata landfill—mostly focused on deposits that
703 cover the Aragonian/Vallesian transition (~11.5–11.0 Ma)—represent one of the best
704 opportunities to find additional dryopithecine remains that might clarify their taxonomic
705 and phylogenetic status in years to come.
706
707 **5. Conclusions**
708 We revisit the age of the hominoid-bearing locality of CM1 (or Bretxa de Can Mata),
709 where a dryopithecine canine of a female individual was found in the 1970s. Can Mata 1 is
710 located in the Penedès sector of the Vallès-Penedès Basin (NE Iberian Peninsula), in the
711 fossiliferous area of els Hostalets de Pierola. This locality has traditionally been considered
712 latest Aragonian (pre-Vallesian) in age, supposedly predating the earliest record of giraffids
713 (CM2) and hipparionins (CM3) in the area. Currently, CM1 is included with the area affected
714 by the enlargement works of the Can Mata landfill (i.e., the ACM macrosite), which thanks
715 to paleontological surveillance and rescue excavations has delivered tens of thousands of
716 fossil vertebrate remains from the late Aragonian during the last two decades. Here we
717 report new magnetostratigraphic data that include CM1 and extend the ACM composite

718 section upward toward the Vallesian. The updated composite section is 300 m-thick and
719 spans from ~12.6 to 11.1 Ma (latest MN6 to earliest MN9), with CM1 being correlated to
720 subchron C5r.1r, with an estimated age of 11.1 Ma. Our results indicate that, despite slightly
721 predating the oldest well-dated record of *Hippotherium* in the area of els Hostalets de
722 Pierola (CM3), CM1 is younger than the first appearance datum of this taxon in the Vallès-
723 Penedès Basin (correlated with C5r.1n, with an estimated age of 11.2 Ma), on which the
724 definition of the Vallesian land mammal age hinges. Our results thus unambiguously
725 indicate that CM1 does not correlate to the latest Aragonian (MN7+8)—as previously
726 assumed based on the absence of *Hippotherium* and giraffids—but to the earliest Vallesian.
727 We note that *Hippotherium* remains from Can Mata show resemblances to the roughly
728 coeval remains from Pannonian C sites of the Vienna Basin (Austria). We further show,
729 based on new remains from ACM, that the oldest well-dated record of giraffids in the area
730 of Can Mata is not younger (as previouly thought) but slightly older than CM1, with a similar
731 estimated age of 11.1 Ma. A critical assessment of Vallès-Penedès localities with giraffids,
732 previously considered latest Aragonian owing to the lack of *Hippotherium*, indicates that this
733 view is no longer tenable. In contrast, hipparionins and giraffids might have dispersed more
734 or less simultaneously across Europe ~11.2 Ma, together with other large mammal
735 immigrants from eastern Eurasia. All in all, our results highlight the need to stop considering
736 the lack of *Hippotherium* as a reliable criterion for correlation with the latest Aragonian
737 without the aid of magnetostratigraphic data or, at least, without taking into consideration
738 other biochronologically important taxa. These include other large mammals and the
739 cricetid *Hispanomys*, since based on currently available data both *His. dispectus* and *His.*
740 *daamsi* might be characteristic of the earliest Vallesian.

741 Further research is necessary to ascertain to what extent the Aragonian/Vallesian
742 transition was a relatively protracted faunal turnover or a more punctuted event. From a
743 paleobiogeographic viewpoint, this has potential implications for hominoid evolution,
744 because it is currently uncertain whether Vallesian dryopithecines evolved locally from their
745 late Aragonian counterparts or immigrated from elsewhere at the beginning of the Vallesian
746 (along with other eastern immigrants such as giraffids, *Machairodus*, or *Propotamochoerus*).
747 Testing these competing hypotheses is hampered by the incompleteness and fragmentary
748 nature of the hominoid fossil record, which is particularly meager for the earliest Vallesian
749 (including scarce remains from CM1, Castell de Barberà, and Mariathal). Our study thus
750 highlights the need to strengthen fieldwork efforts focused on this particular time interval,
751 approximately between 11.5 and 10.5 Ma. In this sense, the revised (earliest Vallesian) age
752 for CM1 conclusively shows that dryopithecines were also present in this sector of the basin
753 by this time. Therefore, currently ongoing paleontological surveillance at ACM offers the
754 most promising prospects to recover additional fossil ape remains from this key interval in
755 years to come. This might help disentangle the controversial phylogenetic relationships
756 among dryopithecine taxa, as well as the potential link between hispanopithecins and Late
757 Miocene species from China that appear to be excluded from the pongine radiation.
758
759 **Acknowledgments**
760 This publication is the result of R+D+I projects PID2020-117289GB-I00, PID2020-
761 116908GB-I00, PID2020-116220GB-I00, PID2020-117118GB-I00, and PID2019-106440GB-
762 C21, funded by the Ministerio de Ciencia e Innovación/Agencia Estatal de
763 Investigación/10.13039/501100011033/. The research has been funded also by the
764 Generalitat de Catalunya, including: CERCA Programme; Agència de Gestió d'Ajuts

765 Universitaris i de Recerca (Consolidated Research Groups 2017 SGR 086, 2017 SGR 116, and
766 2017 SGR 596); and Departament de Cultura (CLT009/18/00071). Fieldwork at ACM was
767 defrayed by CESPA Gestión de Residuos S.A.U. and UTE Ampliació Can Mata. We are grateful
768 to Jordi Agustí for sharing his remembrances about the *Hippotherium* find from CM3 as well
769 as the numerous field paleontologists that worked at ACM over the years. We further
770 acknowledge the collaboration of the Centre d'Interpretació i Restauració Paleontològica
771 (Ajuntaments dels Hostalets de Pierola) and the Servei d'Arqueologia i Paleontologia of the
772 Generalitat de Catalunya. Finally, we thank the co-Editor-in-Chief (Clément Zanolli), the
773 Associate Editor, and three anonymous reviewers for helpful comments that helped improve
774 a previous version of this manuscript.
775
776 **References**
777 Abdul Aziz, H., Krijgsman, W., Hilgen, F., Wilson, D.S., Calvo, J.P., 2003. An astronomical
778 polarity timescale for the late middle Miocene based on cyclic continental sequences. J.
779 Geophys. Res. 108, 2159.
780 Agustí, J., 1981. Roedores miomorfos del Neógeno de Cataluña. Ph.D. Dissertation,
781 Universidad de Barcelona.
782 Agustí, J., 1999. A critical re-evaluation of the Miocene mammal units in Western Europe:
783 Dispersal events and problems of correlation. In: Agustí, J., Rook, L., Andrews, P. (Eds.),
784 The Evolution of Neogene Terrestrial Ecosystems in Europe. Cambridge University Press,
785 Cambridge, pp. 84–112.
786 Agustí, J., Gibert, J., 1982. Roedores e insectívoros del Mioceno superior dels Hostalets de
787 Pierola (Vallès-Penedès, Cataluña). Butll. Inf. Inst. Paleontol. Sabadell 14, 19–37.

788 Agustí, J., Moyà-Solà, S., 1990. Mammal extinctions in the Vallesian (Upper Miocene). Lect.
789 Not. Earth Sci. 30, 425–432.
790 Agustí, J., Moyà-Solà, S., 1991. Spanish Neogene Mammal succession and its bearing on
791 continental biochronology. Newslett. Stratigr. 25, 91–114.
792 Agustí, J., Cabrera, L., Moyà-Solà, S., 1985. Sinopsis estratigráfica del Neógeno de la fosa del
793 Vallés-Penedés. Paleontol. Evol. 18, 57–81.
794 Agustí, J., Cabrera, L., Garcés, M., Parés, J.M., 1997. The Vallesian mammal succession in the
795 Vallès-Penedès basin (northeast Spain): Paleomagnetic calibration and correlation with
796 global events. Palaeogeogr. Palaeoclimatol. Palaeoecol. 133, 149–180.
797 Agustí, J., Cabrera, L., Garcés, M., Krijgsman, W., Oms, O., Parés, J.M., 2001. A calibrated
798 mammal scale for the Neogene of Western Europe. State of the art. Earth Sci. Rev. 52,
799 247–260.
800 Alba, D.M., 2012. Fossil apes from the Vallès-Penedès Basin. Evol. Anthropol. 21, 254–269.
801 Alba, D.M., Moyà-Solà, S., 2012. On the identity of a hominoid male upper canine from the
802 Vallès-Penedès Basin figured by Pickford (2012). Estud. Geol. 68, 149–153.
803 Alba, D.M., Moyà-Solà, S., Casanovas-Vilar, I., Galindo, J., Robles, J.M., Rotgers, C., Furió, M.,
804 Angelone, C., Köhler, M., Garcés, M., Cabrera, L., Almécija, S., Obradó, P., 2006. Los
805 vertebrados fósiles del Abocador de Can Mata (els Hostalets de Pierola, l'Anoia,
806 Cataluña), una sucesión de localidades del Aragoniense superior (MN6 y MN7+8) de la
807 cuenca del Vallès-Penedès. Campañas 2002-2003, 2004 y 2005. Estud. Geol. 62, 295–312.
808 Alba, D.M., Robles, J.M., Rotgers, C., Casanovas-Vilar, I., Galindo, J., Moyà-Solà, S., Garcés,
809 M., Cabrera, L., Furió, M., Carmona, R., Bertó Mengual, J.V., 2009. Middle Miocene
810 vertebrate localities from Abocador de Can Mata (els Hostalets de Pierola, Vallès-

Penedès Basin, Catalonia, Spain): An update after the 2006-2008 field campaigns. Paleolusitana 1, 59–73.

Alba, D.M., Moyà-Solà, S., Malgosa, A., Casanovas-Vilar, I., Robles, J.M., Almécija, S., Galindo, J., Rotgers, C., Bertó Mengual, J.V., 2010. A new species of *Pliopithecus* Gervais, 1849 (Primates: Pliopithecidae) from the Middle Miocene (MN8) of Abocador de Can Mata (els Hostalets de Pierola, Catalonia, Spain). Am. J. Phys. Anthropol. 141, 52–75.

Alba, D.M., Casanovas-Vilar, I., Robles, J.M., Moyà-Solà, S., 2011a. Parada 3. El Aragoniense superior y la transición con el Vallesiense: Can Mata y la exposición paleontological de els Hostalets de Pierola. Paleontol. Evol. Memòria especial 6, 95–109.

Alba, D.M., Moyà-Solà, S., Almécija, S., 2011b. A partial hominoid humerus from the middle Miocene of Castell de Barberà (Vallès-Penedès Basin, Catalonia, Spain). Am. J. Phys. Anthropol. 144, 365–381.

Alba, D.M., Moyà-Solà, S., Robles, J.M., Galindo, J., 2012a. Brief Communication: The oldest pliopithecid record in the Iberian Peninsula based on new material from the Vallès-Penedès Basin. Am. J. Phys. Anthropol. 147, 135–140.

Alba, D.M., Carmona, R., Bertó Mengual, J.V., Casanovas-Vilar, I., Furió, M., Garcés, M., Galindo, J., Luján, À.H., 2012b. Intervenció paleontològica a l'Ecoparc de Can Mata (els Hostalets de Pierola, conca del Vallès-Penedès). Trib. Arqueol. 2010–2011, 115–130.

Alba, D.M., Fortuny, J., Pérez de los Ríos, M., Zanolli, C., Almécija, S., Casanovas-Vilar, I., Robles, J.M., Moyà-Solà, S., 2013. New dental remains of *Anoiapithecus* and the first appearance datum of hominoids in the Iberian Peninsula. J. Hum. Evol. 65, 573–584.

Alba, D.M., Almécija, S., DeMiguel, D., Fortuny, J., Pérez de los Ríos, M., Pina, M., Robles, J.M., Moyà-Solà, S., 2015. Miocene small-bodied ape from Eurasia sheds light on hominoid evolution. Science 350, aab2625.

Alba, D.M., Casanovas-Vilar, I., Garcés, M., Robles, J.M., 2017. Ten years in the dump: An updated review of the Miocene primate-bearing localities from Abocador de Can Mata (NE Iberian Peninsula). J. Hum. Evol. 102, 12–20.

Alba, D.M., Casanovas-Vilar, I., Furió, M., García-Paredes, I., Angelone, C., Jovells-Vaqué, S., Luján, À.H., Almécija, S., Moyà-Solà, S., 2018. Can Pallars i Llobateres: A new hominoid-bearing locality from the late Miocene of the Vallès-Penedès Basin (NE Iberian Peninsula). J. Hum. Evol. 121, 193–203.

Alba, D.M., Garcés, M., Casanovas-Vilar, I., Robles, J.M., Pina, M., Moyà-Solà, S., Almécija, S., 2019. Bio- and magnetostratigraphic correlation of the Miocene primate-bearing site of Castell de Barberà to the earliest Vallesian. J. Hum. Evol. 132, 32–46.

Alba, D.M., Fortuny, J., Robles, J.M., Bernardini, F., Pérez de los Ríos, M., Tuniz, C., Moyà-Solà, S., Zanolli, C., 2020. A new dryopithecine mandibular fragment from the middle Miocene of Abocador de Can Mata and the taxonomic status of '*Sivapithecus*' *occidentalis* from Can Vila (Vallès-Penedès Basin, NE Iberian Peninsula). J. Hum. Evol. 145, 102790.

Alba, D.M., Robles, J.M., Valenciano, A., Abella, J., Casanovas-Vilar, I., 2022. A new species of *Eomellivora* from the latest Aragonian of Abocador de Can Mata (NE Iberian Peninsula). Hist Biol. 34, 694–703.

Almécija, S., Alba, D.M., Moyà-Solà, S., 2009. *Pierolapithecus* and the functional morphology of Miocene ape hand phalanges: Paleobiological and evolutionary implications. J. Hum. Evol. 57, 284–297.

Almécija, S., Alba, D.M., Moyà-Solà, S., 2012. The thumb of Miocene apes: New insights from Castell de Barberà (Catalonia, Spain). Am. J. Phys. Anthropol. 148, 436–450.

858 Almécija, S., Pina, M., Vinuesa, V., DeMiguel, D., Moyà-Solà, S., Alba, D.M., 2019. Memòria
859 sobre la intervenció paleontològica programada a Creu Conill (Terrassa): Campanyes
860 2016-2017. Institut Català de Paleontologia Miquel Crusafont, unpublished report.
861 Almécija, S., Hammond, A.S., Thompson, N.E., Pugh, K.D., Moyà-Solà, S., Alba, D.M., 2021.
862 Fossil apes and human evolution. Science 372, eabb4363.
863 Álvarez Sierra, M. A., Calvo, J. P., Morales, J., Alonso-Zarza, A., Azanza, B., García Paredes, I.,
864 Hernández Fernández, M., van der Meulen, A.J., Peláez-Campomanes, P., Quiralte, V.,
865 Salesa, M.J., Sánchez, I.M., Soria, D., 2003. El tránsito Aragoniense-Vallesiense en el área
866 de Daroca-Nombrevilla (Zaragoza, España). Coloquios de Paleontología Vol. Ext. 1, 25–33.
867 Andrews, P., 2020. Last common ancestor of apes and humans: Morphology and
868 environment. Folia Primatol. 91, 122–148.
869 Andrews, P., Harrison, T., Delson, E., Bernor, R.L., Martin, L., 1996. Distribution and
870 biochronology of European and Southwest Asian Miocene catarrhines. In: Bernor, R.L.,
871 Fahlbusch, V., Mittmann, H.-W. (Eds.), The Evolution of Western Eurasian Neogene
872 Mammal Faunas. Columbia University Press, New York, pp. 168–207.
873 Barry, J.C., Morgan, M.E., Flynn, L.L., Pilbeam, D., Behrensmeyer, A.K., Raza, S.M., Khan, I.A.,
874 Badgley, C., Hicks, J., Kelley, J., 2002. Faunal and environmental change in the late
875 Miocene Siwaliks of Northern Pakistan. Paleobiology 28 (S2), 1–71.
876 Begun, D.R., 2002. European hominoids. In: Hartwig, W.C. (Ed.), The Primate Fossil Record.
877 Cambridge University Press, Cambridge, pp. 339–368.
878 Begun, D.R., 2009. Dryopithecins, Darwin, de Bonis, and the European origin of the African
879 apes and human clade. Geodiversitas 31, 789–816.
880 Begun, D.R., 2013. A new interpretation of relationships among Euraisan and African Late
881 Miocene hominids. In: Çagatay, N., Zabci, C. (Eds.), RCMNS 14th Congress. Regional

Comittee on Mediterranean Neogene Stratigraphy. 8-12 September 2013 Istanbul, Turkey. Neogene to Quaternary Geological Evolution of the Mediterranean, Paratethys and Black Sea. Book of Abstracts of the RCMNS 2013. Istanbul Technical University.

Begun, D., Kelley, J., 2016. Hominid localities from the Pannonian Basin (Hungary) and Yunnan Province (China) and relations among Eurasian Miocene apes. J. Vertebr. Paleontol. Program and Abstracts 2016, 95.

Begun, D.R., Moyá-Sola, S., Kohler, M., 1990. New Miocene hominoid specimens from Can Llobateres (Vallès Penedès, Spain) and their geological and paleoecological context. J. Hum. Evol. 19, 255–268.

Begun, D.R., Nargolwalla, M.C., Kordos, L., 2012. European Miocene hominids and the origin of the African ape and human clade. Evol. Anthropol. 21, 10–23.

Bernor, R.L., White, T.D., 2009. Systematics and biogeography of "*Cormohipparion*" *africanum*, early Vallesian (MN 9, ca. 10.5 Ma) of Bou Hanifa, Algeria. Mus. North. Arizona Bull. 65, 635–657.

Bernor, R.L., Woodburne, M.O., Van Couvering, J.A., 1980. A contribution to the chronology of some Old World Miocene faunas based on hipparionine horses. Geobios 13, 705–739.

Bernor, R.L., Koufos, G.D., Woodburne, M.O., Fortelius, M., 1996. The evolutionary history and biochronology of European and Southwest Asian Late Miocene and Pliocene Hipparionine horses. In: Bernor, R.L., Fahlbusch, V., Mittmann, H.-W. (Eds.), The Evolution of Western Eurasian Neogene Faunas. Columbia University Press, New York, pp. 307–338.

Bernor, R.L., Scott, R.S., Fortelius, M., Kappelman, J., Sen, S., 2003. Equidae (Perissodactyla). In: Fortelius, M., Kappelman, J., Sen, S., Bernor, R.L. (Eds.), Geology and Paleontology of

905 the Miocene Sinap Formation, Turkey. Columbia University Press, New York, pp. 220–
906 281.
907 Bernor, R.L., Kaiser, T.M., Nelson, S.V., 2004. The oldest Ethiopian Hipparion (Equinae,
908 Perissodactyla) from Chorora: Systematics, paleodiet and paleoclimate. Cour. Forsch.-
909 Inst. Senck. 246, 213–226.
910 Bernor, R.L., Göhlich, U., Harzhauser, M., Semprebon, G.M., 2017. The Pannonian C
911 hipparions from the Vienna Basin. Palaeogeogr. Palaeoclimatol. Palaeoecol. 476, 28–41.
912 Bernor, R.L., Boaz, N., Cirilli, O., El-Shawaihdi, M., Rook, L., 2020. Sahabi *Eurygnathohippus*
913 *feibeli*: its systematic, stratigraphic, chronologic and biogeographic contexts. Riv. Ital.
914 Paleontol. Stratigr. 126, 561–581.
915 Bernor, R.L., Kaya, F., Kaakinen, A., Saarinen, J., Fortelius, M., 2021. Old world hipparion
916 evolution, biogeography, climatology and ecology. Earth Sci. Rev. 221, 103784.
917 Böhme, M., Spassov, N., Fuss, J., Tröscher, A., Deane, A.S., Prieto, J., Kirscher, U., Lechner, T.,
918 Begun, D.R., 2019. A new Miocene ape and locomotion in the ancestor of great apes and
919 humans. Nature 575, 489–493
920 Cande, S.C., Kent, D.V., 1992. A new geomagnetic polarity time scale for the Late Cretaceous
921 and Cenozoic. J. Geophys. Res. 97, 13917–13951.
922 Casanovas-Vilar, I., Alba, D.M., Moyà-Solà, S., Galindo, J., Cabrera, L., Garcés, M., Furió, M.,
923 Robles, J.M., Köhler, M., Angelone, C., 2008. Biochronological, taphonomical and
924 paleoenvironmental background of the fossil great ape *Pierolapithecus catalaunicus*
925 (Primates, Hominidae). J. Hum. Evol 55, 589–603.
926 Casanovas-Vilar, I., Alba, D.M., Garcés, M., Robles, J.M., Moyà-Solà, S., 2011. Updated
927 chronology for the Miocene hominoid radiation in Western Eurasia. Proc. Natl. Acad. Sci.
928 USA 108, 5554–5559.

929 Casanovas-Vilar, I., Van den Hoek Ostende, L.W., Furió, M., Madern, P.A., 2014. The range
930 and extent of the Vallesian Crisis (Late Miocene): new prospects based on the
931 micromammal record from the Vallès-Penedès basin (Catalonia, Spain). J. Iber. Geol. 40,
932 29–48.
933 Casanovas-Vilar, I., Madern, A., Alba, D.M., Cabrera, L., García-Paredes, I., Van den Hoek
934 Ostende, L.W., DeMiguel, D., Robles, J.M., Furió, M., Van Dam, J., Garcés, M., Angelone,
935 C., Moyà-Solà, S., 2016a. The Miocene mammal record of the Vallès-Penedès Basin
936 (Catalonia). C. R. Palevol 15, 791–812.
937 Casanovas-Vilar, I., Garcés, M., Van Dam, J., García-Paredes, I., Robles, J.M., Alba, D.M.,
938 2016b. An updated biostratigraphy for the late Aragonian and the Vallesian of the Vallès-
939 Penedès Basin (Catalonia). Geol. Acta 14, 195–217.
940 Castillo, A., López-Guerrero, P., Álvarez-Sierra, M.Á., 2018. New Insights on Cricetodontini
941 (Rodentia, Mammalia) from the Duero Basin, Spain. Hist. Biol. 30, 392–403.
942 Crusafont Pairó, M., 1950. La cuestión del llamado Meótico español. Arrahona 1950, 41–48.
943 Crusafont Pairó, M., 1952. Los jiráfidos fósiles de España. Mem. Com. Inst. Geol. Prov. 8, 1–
944 239.
945 Crusafont Pairó, M., 1975. Topografia paleontològica del Vallès. In: Societat Catalana de
946 Geografia (Ed.), Miscel·lània Pau Vila: Biografia, Bibliografia, Treballs d'Homenatge.
947 Editorial Montblanc-Martín, Granollers, pp. 249–254.
948 Crusafont, M., Truyols, J., 1954. Catálogo Paleomastológico del Mioceno del Vallés-Penedés
949 y de Calatayud-Teruel. Segundo Cursillo Internacional de Paleontología. Museo de la
950 Ciudad de Sabadell, Sabadell.
951 Crusafont Pairó, M., Truyols Santonja, J., 1960. Sobre la caracterización del Vallesiense. Not.
952 Com. Inst. Geol. Min. Esp. 60, 109–125.

953 Crusafont Pairó, M., Golpe Posse, J.M., 1971. Biozonation des Mammifères néogènes
954 d'Espagne. In: V Congrés du Néogène Mediterranéen. Mém. Bur. Recher. Géol. Min. 78,
955 121–129.
956 Crusafont-Pairó, M., Golpe-Posse, J.M., 1973. New pongids from the Miocene of Vallès
957 Penedès Basin (Catalonia, Spain). J. Hum Evol. 2, 17–24.
958 Daams, R., Freudenthal, M., 1981. Aragonian: the stage concept versus Neogene Mammal
959 zones. Scripta Geol. 62, 1–17.
960 de Bruijn, H., Daams, R., Daxner-Höck, G., Fahlbusch, V., Ginsburg, L., Mein, P., Morales, J.,
961 Heinzmann, E., Mayhew, D.F., van der Meulen, A.J., Schmidt-Kittler, N., Telles Antunes,
962 M., 1992. Report of the RCMNS working group on fossil mammals, Reisensburg 1990.
963 Newsl. Stratigr. 26, 65–118.
964 DeMiguel, D., Domingo, L., Sánchez, I.M., Casanovas-Vilar, I., Robles, J.M., Alba, D.M., 2021.
965 Palaeoecological differences underlie rare co-occurrence of Miocene European primates.
966 BMC Biol. 19, 6.
967 Evans, H.F., Westerhold, T., Paulsen, H., Channell, J.E.T., 2007. Astronomical ages for
968 Miocene polarity chrons C4Ar–C5r (9.3–11.2 Ma), and for three excursion chrons within
969 C5n.2n. Earth Planet. Sci. Lett. 256, 455–465.
970 Fang, X., Wang, J., Zhang, W., Zan, J., Song, C., Yan, M., Appel, E., Zhang, T., Wu, F., Yang, Y.,
971 Lu, Y., 2016. Tectonosedimentary evolution model of an intracontinental flexural
972 (foreland) basin for paleoclimatic research. Global Planet. Change 145, 78–97.
973 Fisher, R., 1953. Dispersion on a sphere. Proc. R. Soc. A 217, 295–305.
974 Fortuny, J., Zanolli, C., Bernardini, F., Tuniz, C., Alba, D.M., 2021. Dryopithecine
975 paleobiodiversity in the Iberian Miocene revisited on the basis of molar endostructural
976 morphology. Palaeontology 64, 531–554.

977 Gao, F., 1998. Phylogeny for the large-bodied hominoid of Yunnan, China and its significance
978 in human origin. In: Cheng, J., Jian, Z., Ji, X. (Eds.), Collected Works for “The 30th
979 Anniversary of Yuanmou Man Discovery and the International Conference on
980 Palaeoanthropological Studies”. Yunnan Science & Technology Press, Kunming, pp. 231–
981 232.
982 Garcés, M., Agustí, J., Cabrera, L., Parés, J.M., 1996. Magnetostratigraphy of the Vallesian
983 (late Miocene) in the Vallès-Penedès Basin (northeast Spain). Earth Planet. Sci. Lett. 142,
984 381–396.
985 Garcés, M., Cabrera, L., Agustí, J., Parés, J. M., 1997. Old World first appearance datum of
986 *"Hipparion"* horses: Late Miocene large-mammal dispersal and global events. Geology 25,
987 19–22.
988 Garcés, M., Krijgsman, W., Peláez-Campomanes, P., Álvarez Sierra, M.A., Daams, R., 2003.
989 *Hipparion* dispersal in Europe: magnetostratigraphic constraints from the Daroca area
990 (Spain). Coloquios de Palentología Vol. Ext. 1, 171–178.
991 García-Paredes, I., Álvarez-Sierra, M.Á., Van den Hoek Ostende, L., Hernández-Ballarín, V.,
992 Hordijk, K., López-Guerrero, P., Oliver, A., Peláez-Campomanes, P., 2016. The Aragonian
993 and Vallesian high-resolution micromammal succession from the Calatayud-Montalbán
994 Basin (Aragón, Spain). C. R. Palevol 15, 781–789.
995 Gilbert, C.C., Pugh, K.D., Fleagle, J.G., 2020. Dispersal of Miocene hominoids (and
996 pliopithecoids) from Africa to Eurasia in light of changing tectonics and climate. In:
997 Prasad, G.V., Patnaik, R. (Eds.), Biological Consequences of Plate Tectonics. New
998 Perspectives on post-Gondwana Break-Up—A Tribute to Ashok Sahni. Springer, Cham,
999 pp. 393–412.

1000 Golpe-Posse, J.M., 1974. Faunas de yacimientos con suiformes en el Terciario español.
1001 Paleontol. Evol. 8, 1–87.
1002 Golpe Posse, J.M., 1982. Los hispanopitecos (Primates, Pongidae) de los yacimientos del
1003 Vallès Penedès (Cataluña - España). I: Material ya descrito. Butll. Inf. Inst. Paleontol.
1004 Sabadell 14, 63–69.
1005 Golpe-Posse, J.M., 1993. Los Hispanopitecos (Primates, Pongidae) de los yacimientos del
1006 Vallès-Penedès (Cataluña, España). II: Descripción del material existente en el Instituto de
1007 Paleontología de Sabadell. Paleontol. Evol. 26–27, 151–224.
1008 Hammond, A.S., Alba, D.M., Almécija, S., Moyà-Solà, S., 2013. Middle Miocene
1009 *Pierolapithecus* provides a first glimpse into early hominid pelvic morphology. J. Hum.
1010 Evol. 64, 658–666.
1011 Harrison, T., 1991. Some observations on the Miocene hominoids from Spain. J. Hum. Evol.
1012 19, 515–520.
1013 Harrison, T., Ji, X., Su, D., 2002. On the systematic status of the late Neogene hominoids
1014 from Yunnan Province, China. J. Hum. Evol. 43, 207–227.
1015 ICGC (Institut Cartogràfic i Geològic de Catalunya), 2021. VISSIR v3.26 (VISor del Servidor
1016 d'Imatges Ràster). Generalitat de Catalunya. http://www.icc.cat/vissir3/ (Accessed May
1017 30, 2021).
1018 Ji, X.P., Jablonski, N.G., Su, D.F., Deng, C. L., Flynn, L.J., You, Y.S., Kelley, J., 2013. Juvenile
1019 hominoid cranium from the terminal Miocene of Yunnan, China. Chin. Sci. Bull. 58, 3771–
1020 3779.
1021 Kelley, J., 2002. The hominoid radiation in Asia. In: Hartwig, W.C. (Ed.), The Primate Fossil
1022 Record. Cambridge University Press. Cambridge, pp. 369–384.

1023 Kelley, J., Gao, F., 2012. Juvenile hominoid cranium from the late Miocene of southern China
1024 and hominoid diversity in Asia. Proc. Natl. Acad. Sci. USA 109, 6882–6885.
1025 Kirscher, U., Prieto, J., Bachtadse, V., Aziz, H. ., Doppler, G., Hagmaier, M., Böhme, M., 2016.
1026 A biochronologic tie-point for the base of the Tortonian stage in European terrestrial
1027 settings: Magnetostratigraphy of the topmost Upper Freshwater Molasse sediments of
1028 the North Alpine Foreland Basin in Bavaria (Germany). Newslett. Stratigr. 49, 445–467.
1029 Kirschvink, J.L., 1980. The least-squares line and plane and the analysis of palaeomagnetic
1030 data. Geophys. J. R. Astronom. Soc. 62, 699–718.
1031 Koymans, M.R., Langereis, C.G., Pastor-Galan, D., van Hinsbergen, D.J.J., 2016.
1032 Paleomagnetism.org: An online multi-platform open source environment for
1033 paleomagnetic data analysis. Comput. Geosci. 93, 127–137.
1034 López-Guerrero, P., García-Paredes, I., Álvarez-Sierra, M.Á., Peláez-Campomanes, P., 2014.
1035 Cricetodontini from the Calatayud–Daroca Basin (Spain): A taxonomical description and
1036 update of their stratigraphical distributions. C. R. Palevol 13, 647–664.
1037 López-Guerrero, P., Álvarez-Sierra, M. Á., García-Paredes, I., Carro-Rodríguez, P. M., Peláez-
1038 Campomanes, P., 2019. Species of *Hispanomys* from the late Aragonian and early
1039 Vallesian (middle-late Miocene) of the Calatayud–Daroca Basin, Zaragoza, Spain. J. Iber.
1040 Geol. 45, 163–180.
1041 Marigó, J., Susanna, I., Minwer-Barakat, R., Madurell-Malapeira, J., Moyà-Solà, S.,
1042 Casanovas-Vilar, I., Robles, J.M., Alba, D.M., 2014. The primate fossil record in the Iberian
1043 Peninsula. J. Iber. Geol. 40, 179–211.
1044 Mein, P., 1990. Updating of MN zones. In: Lindsay, E.H., Fahlbusch, V., Mein, P. (Eds.),
1045 European Neogene Mammal Chronology. Plenum Press, New York, pp. 73–90.

1046 Moyà-Solà, S., Köhler, M., Alba, D.M., Casanovas-Vilar, I., Galindo, J., 2004. *Pierolapithecus*
1047 *catalaunicus*, a new Middle Miocene great ape from Spain. Science 306, 1339–1344.
1048 Moyà-Solà, S., Köhler, M., Alba, D.M., Casanovas-Vilar, I., Galindo, J., Robles, J.M., Cabrera,
1049 L., Garcés, M., Almécija, S., Beamud, E., 2009a. First partial face and upper dentition of
1050 the Middle Miocene hominoid *Dryopithecus fontani* from Abocador de Can Mata (Vallès-
1051 Penedès Basin, Catalonia, NE Spain): taxonomic and phylogenetic implications. Am. J.
1052 Phys. Anthropol. 139, 126–145.
1053 Moyà-Solà, S., Alba, D.M., Almécija, S., Casanovas-Vilar, I., Köhler, M., De Esteban-Trivigno,
1054 S., Robles, J.M., Galindo, J., Fortuny, J., 2009b. A unique Middle Miocene European
1055 hominoid and the origins of the great ape and human clade. Proc. Natl. Acad. Sci. USA
1056 106, 9601–9606.
1057 Ogg, J.G., 2020. Geomagnetic Polarity Time Scale. In: Gradstein, F.M., Ogg, J.G., Schmitz,
1058 M.D., Ogg, G.M. (Eds.), Geologic Time Scale 2020. Elsevier, Amsterdam, pp. 159–192.
1059 Pérez de los Ríos, M., Moyà-Solà, S., Alba, D.M., 2012. The nasal and paranasal architecture
1060 of the Middle Miocene ape *Pierolapithecus catalaunicus* (Primates: Hominidae):
1061 Phylogenetic implications. J. Hum. Evol. 63, 497–506.
1062 Pickford, M., 2012. Hominoids from Neuhausen and other Bohnerz localities, Swabian Alb,
1063 Germany: evidence for a high diversity of apes in the Late Miocene of Germany. Estud.
1064 Geol. 68, 113–147.
1065 Pickford, M., 2013. Reassessment of Dinotheriensande Suoidea: Biochronological and
1066 biogeographic implications (Miocene Eppelsheim Formation). Mainz. Naturwiss. Arch. 50,
1067 155–193.

1068 Pina, M., Almécija, S., Alba, D.M., O'Neil, M.C., Moyà-Solà, S., 2014. The Middle Miocene
1069 ape *Pierolapithecus catalaunicus* exhibits extant great ape-like morphometric affinities
1070 on its patella: Inferences on knee function and evolution. PLoS One 9, e91944.
1071 Pina, M., Alba, D.M., Moyà-Solà, S., Almécija, S., 2019. Femoral neck cortical bone
1072 distribution of dryopithecin apes and the evolution of hominid locomotion. J. Hum. Evol.
1073 136, 102651.
1074 Pina, M., DeMiguel, D., Puigvert, F., Marcé-Nogué, M., Moyà-Solà, S., 2020. Knee function
1075 through finite element analysis and the role of Miocene hominoids in our understanding
1076 of the origin of antipronograde behaviours: The *Pierolapithecus catalaunicus* patella as a
1077 case study. Palaeontology 63, 459–475.
1078 Pugh, K.D., 2022. Phylogenetic analysis of Middle-Late Miocene apes. J. Hum. Evol. 165,
1079 103140.
1080 Ríos, M., Sánchez, I. M., Morales, J., 2016. Comparative anatomy, phylogeny, and
1081 systematics of the Miocene giraffid *Decennatherium pachecoi* Crusafont, 1952
1082 (Mammalia, Ruminantia, Pecora): State of the art. J. Vertebr. Paleontol. 36, e1187624.
1083 Ríos, M., Sánchez, I.M., Morales, J., 2017. A new giraffid (Mammalia, Ruminantia, Pecora)
1084 from the late Miocene of Spain, and the evolution of the sivathere-samothere lineage.
1085 PLoS One, 12, e0185378.
1086 Ríos, M., Danowitz, M., Solounias, N., 2019. First identification of *Decennatherium*
1087 Crusafont, 1952 (Mammalia, Ruminantia, Pecora) in the Siwaliks of Pakistan. Geobios 57,
1088 97–110.
1089 Roberts, A.P., Lewin-Harris, J.C., 2000. Marine magnetic anomalies: Evidence that 'tiny
1090 wiggles' represent short-period geomagnetic polarity intervals. Earth Planet. Sci. Lett.
1091 183, 375–388.

1092 Robles, J.M., Alba, D.M., Fortuny, J., De Esteban-Trivigno, S., Rotgers, C., Balaguer, J.,
1093 Carmona, R., Galindo, J., Almécija, S., Bertó, J.V., Moyà-Solà, S., 2013. New craniodental
1094 remains of the barbourofelid *Albanosmilus jourdani* (Filhol, 1883) from the Miocene of
1095 the Vallès-Penedès (NE Iberian Peninsula) and the phylogeny of the Barbourofelini. J.
1096 Syst. Palaeontol. 11, 993–1022.
1097 Rotgers, C., Alba, D.M., 2011. The genus *Anchitherium* (Equidae: Anchitheriinae) in the
1098 Vallès-Penedès Basin (Catalonia, Spain). In: Pérez-García, A., Gascó, F., Gasulla, J.M.,
1099 Escaso, F. (Eds.), Viajando a Mundos Pretéritos. Ayuntamiento de Morella, Morella, pp.
1100 347–354.
1101 Schaub, S., 1944. Cricetodontiden der Spanischen Halbinsel. Eclogae geol. Helvet. 37, 453–
1102 457.
1103 Schaub, S., 1947. Los cricetodóntidos del Vallés-Panadés. Estud. Geol. 6, 55–67.
1104 Sun, B., Liu, Y., Chen, S., Deng, T., 2022. *Hippotherium* Datum implies Miocene
1105 palaeoecological pattern. Sci. Rep. 12, 3605.
1106 Tauxe, L., Shaar, R., Jonestrask, L., Swanson-Hysell, N.L., Minnett, R., Koppers, A.A.P.,
1107 Constable, C.G., Jarboe, N., Gaastra, K., Fairchild, L., 2016. PmagPy: Software package for
1108 paleomagnetic data analysis and a bridge to the Magnetics Information Consortium
1109 (MagIC) Database. Geochem. Geophys. Geosyst. 17, 2450–2463.
1110 Thenius, E., 1982. Ein Menschenaffenfund (Primates: Pongidae) aus dem Pannon (Jung-
1111 Miozän) von Niederösterreich. Folia Primatol. 39, 187–200.
1112 Urciuoli, A., Zanolli, C., Almécija, S., Beaudet, A., Dumoncel, J., Morimoto, N., Nakatsukasa,
1113 M., Moyà-Solà, S., Begun, D.R., Alba, D.M., 2021. Reassessment of the phylogenetic
1114 relationships of the late Miocene apes *Hispanopithecus* and *Rudapithecus* based on
1115 vestibular morphology. Proc. Natl. Acad. Sci. USA 118*,* e2015215118.

1116 Van Dam, J.A., Krijgsman, W., Abels, H.A., Álvarez-Sierra, M.Á., García-Paredes, I., López-
1117 Guerrero, P., Peláez-Campomanes, P., Ventra, D., 2014. Updated chronology for middle
1118 to late Miocene mammal sites of the Daroca area (Calatayud-Montalbán Basin, Spain).
1119 Geobios 47, 325–334.
1120 Van der Made, J., Ribot, F., 1999. Additional hominoid material from the Miocene of Spain
1121 and remarks on hominoid dispersals into Europe. Contrib. Tert. Quat. Geol. 36, 25–39.
1122 Vasiliev, I., Iosifidi, A.G., Khramov, A. N., Krijgsman, W., Kuiper, K., Langereis, C.G., Popov,
1123 V.V., Stoica, M., Tomsha, V.A., Yudin, S.V., 2011. Magnetostratigraphy and radio-isotope
1124 dating of upper Miocene–lower Pliocene sedimentary successions of the Black Sea Basin
1125 (Taman Peninsula, Russia). Palaeogeogr. Palaeoclimatol. Palaeoecol. 310, 163–175.
1126 Villalta Comella, J.F. de, Crusafont Pairó, M., 1941a. Hallazgo del "*Dryopithecus fontani*",
1127 Lartet, en el Vindoboniense de la cuenca Vallés-Penedés. Bol. Inst. Geol. Min. Esp. 55,
1128 131–142.
1129 Villalta Comella, J.F. de, Crusafont Pairó, M., 1941b. Noticia preliminar sobre la fauna de
1130 carnívoros del Mioceno continental del Vallés-Penedés. Bol. R. Soc. Esp. Hist. Nat. 39,
1131 201–208.
1132 Villalta Comella, J.F. de, Crusafont Pairó, M., 1943. Los vertebrados del Mioceno continental
1133 de la cuenca del Vallés-Panadés (provincia de Barcelona). I. Insectívoros. II. Carnívoros.
1134 Bol. Inst. Geol. Min. Esp. 56, 145–336.
1135 Villalta Comella, J.F. de, Crusafont Pairó, M., 1944. Dos nuevos antropomorfos del Mioceno
1136 español y su situación dentro de la moderna sistemática de los símidos. Not. Com. Inst.
1137 Geol. Min. Esp. 13, 91–139.

Wolf, D., Bernor, R.L., Hussain, S.T., 2013. A systematic, biostratigraphic, and paleobiogeographic reevaluation of the Siwalik hipparionine horse assemblage from the Potwar Plateau, Northern Pakistan. Palaeontographica A 300, 1–115.

Woodburne, M.O., 2007. Phyletic diversification of the *Cormohipparion occidentale* complex (Mammalia; Perissodactyla, Equidae), Late Miocene, North America, and the origin of the Old World *Hippotherium* datum. Bull. Am. Mus. Nat. Hist. 306, 1–138.

Woodburne, M.O., 2009. The early Vallesian vertebrates of Atzelsdorf (Late Miocene, Austria) 9. *Hippotherium* (Mammalia, Equidae). Ann. Naturhist. Mus. Wien 111A, 585–604.

Woodburne, M.O., Bernor, R.L., 1980. On superspecific groups of some Old World hipparionine horses. J. Paleontol. 54, 1319–1348.

Figure captions

Figure 1. Right C_1 of a female individual from CM1 IPS1766 (old Nos. IPS49, H.223, VP339), in occlusal (a), lingual (b), mesial(c), buccal (d), and distal (e) views.

Figure 2. Simplified geological map of the Vallès-Penedès Basin: a) location of the Vallès-Penedès Basin within the Iberian Peninsula; b) location of Abocador de Can Mata (denoted by a black dot, including Can Mata 1) within the basin. Modified from Casanovas-Vilar et al. (2016a: Fig. 1).

Figure 3. Photographs of Can Mata 1 (CM1) in the early 1940s (a–d) and in 2004 (e): a, b) general views; c–e) detail of CM. The location of the fossiliferous level is indicated by the

paleontologists excavating in panels b and d (denoted by arrows); I.C.V. denotes the approximate location of CM1 in February 2004, although the excavation spot is covered by debris. Photographs in panels a and c by Crusafont, reproduced from Villalta Comella and Crusafont Pairó (1943: Pl. XV); photographs in panels b and d by Bataller, reproduced from Villalta Comella and Crusafont Pairó (1941b: Pl. XVI Figs. 1 and 2, respectively); photograph in panel e by D.M.A., © Institut Català de Paleontologia Miquel Crusafont.

Figure 4. Aerial photographs showing the location of CM1 relative to ACM and the nearby farmhouses of Can Mata de la Garriga and Can Vila; the ACM hominoid-bearing locality of BCV1 is also provided for reference. a, b) Orthophotos taken in 1946 (a) and 2019 (b) to the same scale; the extension of the Can Mata landfill is shown in semitransparency in green (up to 2017) and pink (portion enlarged since 2017 and until early 2021), while the extension of the works performed at ECM a decade ago is marked in orange. c) Orthophoto taken in 2021, depicting the inset marked in panel b at a greater scale; the location of CM1 is here denoted by a yellow circle, while that of CM3 is denoted by a white square; the base of the lithostratigraphic composite section of ECM is marked by a red triangle. Universal Transverse Mercator (UTM) coordinates (European Terrestrial Reference System 1989 [ETRS89]): CM1 = 31N 399765E, 4598400N, 285 m a.s.l.; CM3 = 31N 399848E, 4598585N, 312 m a.s.l.; base of ECM = 31 N 400221E, 4598659N, 325 m a.s.l. Base orthophotomaps: © Institut Cartogràfic i Geològic de Catalunya, downloaded from VISSIR v. 3.26 and reproduced with permission by means of a Creative Commons license CC BY 4.0 (ICGC, 2021). Abbreviations: ACM = Abocador de Can Mata; BCV1 = Barranc de Can Vila 1; CM1 = Can Mata 1; ECM = Ecoparc de Can Mata.

Figure 5. Photographs of Can Mata 1 (CM1) in 2001 (b–f) compared with 2004 (a): a) the dashed line indicates the break along which a large block of rock was detached sometime before 2021, while the circle denotes the approximate location of the CM1 fossiliferous accumulation (see Fig. 3); b, c) panoramic (b) and detailed (c) view of CM1 in January 2021, before the area was deforested; d–f) different perspectives on the excavation of CM1 with the help of a digger machine in May 2021; g) detail of the original excavation spot once exposed. Note that, within the circle in panel g, the stratigraphic layer of intense red coloration (denoted by a dashed line) is partly interrupted by a hole filled with debris that corresponds to the original excavation; this spot was excavated until the whole depth of the layer was exposed, and no further fossil finds were found anywhere nearby. The numbers have been added to facilitate the recognition of the same physiographic structures across different panels and despite different perspectives. Photographs by D.M.A. (a–c), J.M.R. (e, f), and V.V. (d, g), © Institut Català de Paleontologia Miquel Crusafont.

Figure 6. New magnetostratigraphic results for the Cells 13–14 section at Abocador de Can Mata, where the locality of Can Mata 1 (CM1, denoted by a four-pointed red star) is located. Sideways triangles denote the stratigraphic position of paleomagnetic samples. Normal polarity (positive VGP latitude) and reversed polarity (negative VGP latitutide) magnetozones are denoted in black and white, respectively. Abbreviations: M = mudstones; S = sandstones; CG = conglomerates; VGP = virtual geomagnetic pole.

Figure 7. Magnetostratigraphic correlation of the Abocador de Can Mata (ACM) and Riera de Claret sections with the Geomagnetic Polarity Time Scale (GPTS) after Ogg (2020), as well as European land mammal ages (ELMA) and local biozones of the Vallès-Penedès Basin

(after Casanovas-Vilar et al., 2016b). The location of Can Mata 1 (CM1)—being correlated to the *Hippotherium–Cricetulodon hartenbergeri* interval subzone—is denoted by a four-pointed red star. Note that the boundary between this subzone and the preceding *Dem. crusafonti–Hippotherium* interval subzone is defined by the first local occurrence of *Hippotherium* in the Vallès-Penedès Basin at the base of C5r.1n (see Fig. 8 for further details). Short white lines in the GPTS represent short geomagnetic excursions within C5n.2n after Evans et al. (2007). Short horizontal lines to the left of the polarity column represent 'tiny wiggles' from sea floor magnetic anomaly stacks (Cande and Kent, 1992) that have been interpreted to represent geomagnetic polarity intervals (e.g., Roberts and Lewin-Harris, 2000). Note the inclusion in the GPTS of cryptochron C5r.2r-1 within C5r.2r (Abdul-Aziz et al., 2003; Ogg, 2020) and that the bottom boundary of the lowermost local biozone is unknown. See SOM Figure S3 for detailed magnetostratigraphic results of the three sampled sections that cover the uppermost portion of the ACM sequence. Abbreviations: M = mudstones; S = sandstones; CG = conglomerates.

Figure 8. Synthetic correlation of the composite local magnetostratigraphy of ACM and nearby areas with the Geomagnetic Polarity Time Scale (GPTS; after Ogg, 2020), as well as European land mammal ages (ELMA), Mammal Neogene units (MN9), and local biozones of the Vallès-Penedès Basin after Casanovas-Vilar et al. (2016b)—note that, for the local biozonation, a plus symbol denotes a concurrent range subzone, whereas an en dash denotes an interval subzone. The stratigraphic position of CM1, CM3 and the ACM primate-bearing localities (reported in SOM Table S4) is shown to the right on the composite lithostratigraphic column (black arrows), together with the first local occurrences of some biochronologically relevant taxa commented in the text (red arrows). The first local

occurrence of hipparionins (*Hippotherium* datum) in the Vallès-Penedès Basin as recorded in Creu de Conill 20 [CCN20]) is denoted by a green discontinuous arrow. Modified after Alba et al. (2017: Fig. 3) based on the results reported in Figure 7 (see the caption for further details) and in the main text. The ACM primate-bearing localities were listed by Alba et al. (2017: Table 2) except for ACM/C8-Au, where a damaged upper premolar of Dryopithecinae indet. (IPS121187) was recently identified while preparing a deinothere tooth, with an interpolated age of 11.77 Ma.

Table 1

Subchrons correlated with the ACM composite section, including their boundaries and duration according to the Geomagnetic Polarity Time Scale (Ogg, 2020), their stratigraphic position and thickness in the composite sequence, and their computed within-subchron sedimentary rate. Updated from Alba et al. (2017) based on fieldwork performed during 2018–2021. CM1 is located in meter 284 of the sequence and correlated with C5r.1r, which postdates the first subchron on the Vallesian (C5r.1n), while CM3 is located 8 m above CM1 (meter 292 of the sequence) and hence approximately correlated to the top of C5r.1r.

Subchron	Bottom (Ma)	Top (Ma)	Duration (Myr)	Bottom (m)	Top (m)	Thickness (m)	Sedimentation (cm/kyr)
C5n.2n	11.056	9.984	1.072	292.8[a]	—	—	—
C5r.1r	11.146	11.056	0.090	277.5[a]	292.8[a]	15.3[a]	17.0[a]
C5r.1n	11.188	11.146	0.042	272.9[a,c]	277.5[a]	4.6[a]	11.0[a]
C5r.2r (2nd portion)	11.263	11.188	0.075	251.5[a]	272.9[a,c]	21.4[a]	28.5[a]
C5r.2r-1	11.308	11.263	0.045	238.6[a]	251.5[a]	12.9[a]	28.7[a]
C5r.2r (1st portion)	11.592	11.308	0.284	204.2[b]	238.6[a]	34.4[a]	12.1[a]
C5r.2n	11.657	11.592	0.065	177.1[b]	204.2[b]	27.1	41.7
C5r.3r	12.049	11.657	0.392	84.1[b]	177.1[b]	93.0	23.7
C5An.1n	12.174	12.049	0.125	68.6[b]	84.1[b]	15.5	12.4
C5An.1r	12.272	12.174	0.098	47.2[b]	68.6[b]	21.4	21.8
C5An.2n	12.474	12.272	0.202	15.9[b]	47.2[b]	31.3	15.5
C5Ar.1r	12.735	12.474	0.261	—	15.9[b]	≥16.0	—

[a] New results reported in this paper.

[b] Results previously reported by Alba et al. (2017).

[b] Alba et al. (2017) noted that the top of C5r.2r was not recorded at ACM but reported its top at 262.2 m based on the nearby sequence of Camí de Can Vila. New samplings within the ACM area sensu stricto enable to refine the subchron top within the ACM composite series.


a
b
c
d
e
1 cm

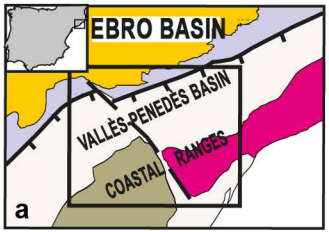

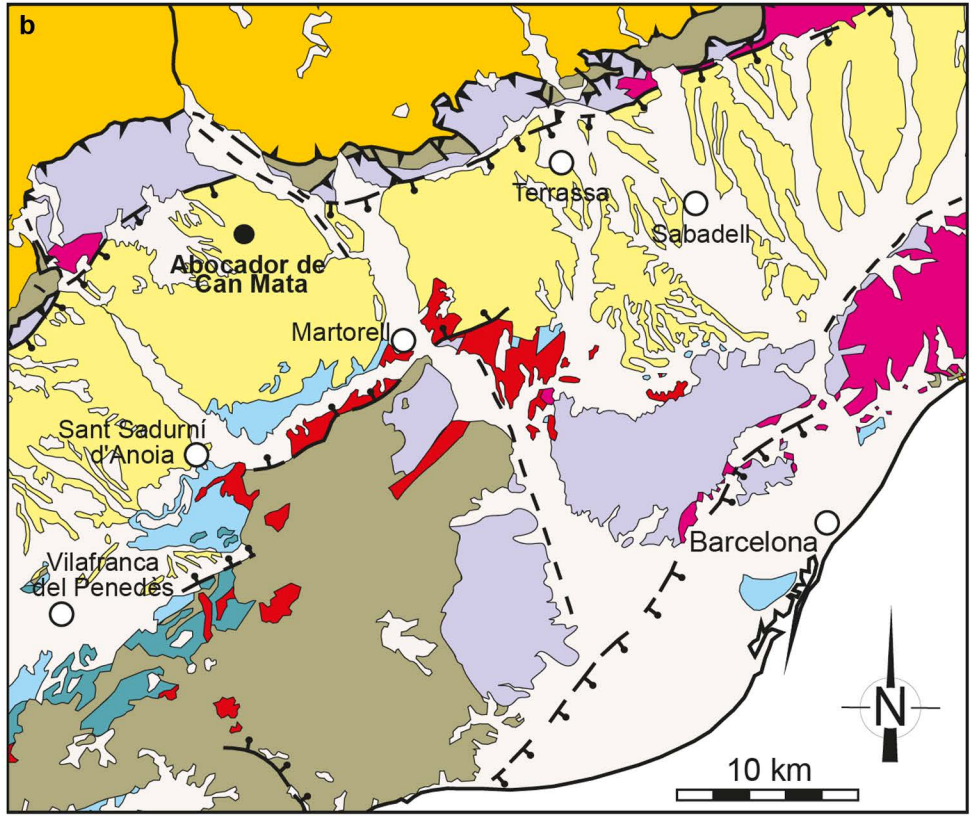

NEOGENE-QUATERNARY

- Pliocene and Quaternary sediments
- Middle to Late Miocene continental units (Langhian-Tortonian): alluvial fan facies
- Miocene marine and transitional units (Burdigalian-Langhian): coralgal carbonate facies
- Miocene marine and transitional units (Late Burdigalian-Serravallian): marls, silts, bioclastic sands and sandstones
- Early Miocene continental units (Early and Late Burdigalian): alluvial fan and shallow lacustrine facies

EBRO FORELAND BASIN INFILL

- Paleogene (conglomerates, sandstones, lutites)

PALEOZOIC BASEMENT AND MESOZOIC COVER

- Mesozoic (carbonates, sandstones, lutites)
- Hercynian intrusive rocks (mostly granitoids)
- Paleozoic sedimentary and metamorphic rocks

- Fault
- Inferred fault
- Normal fault
- Thrust fault


a

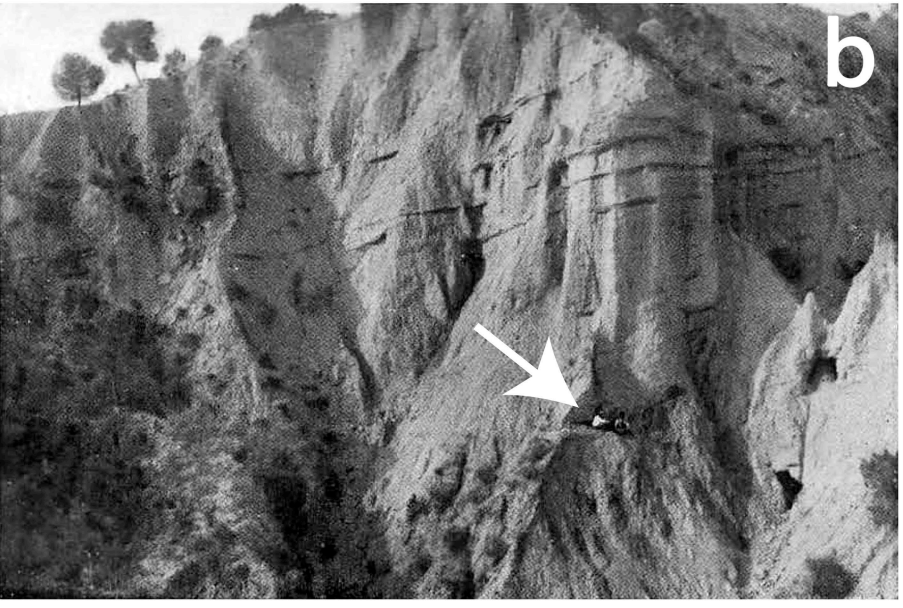
b


e

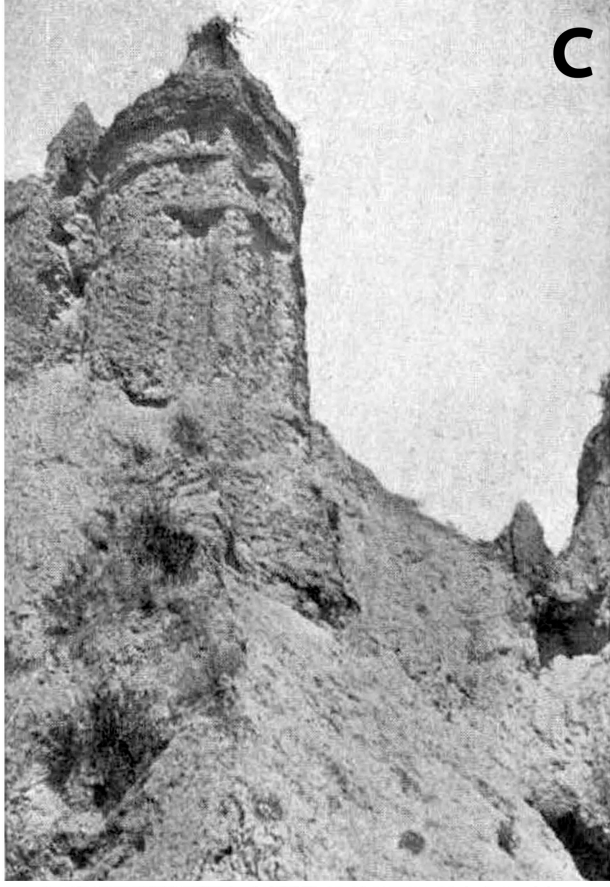
c

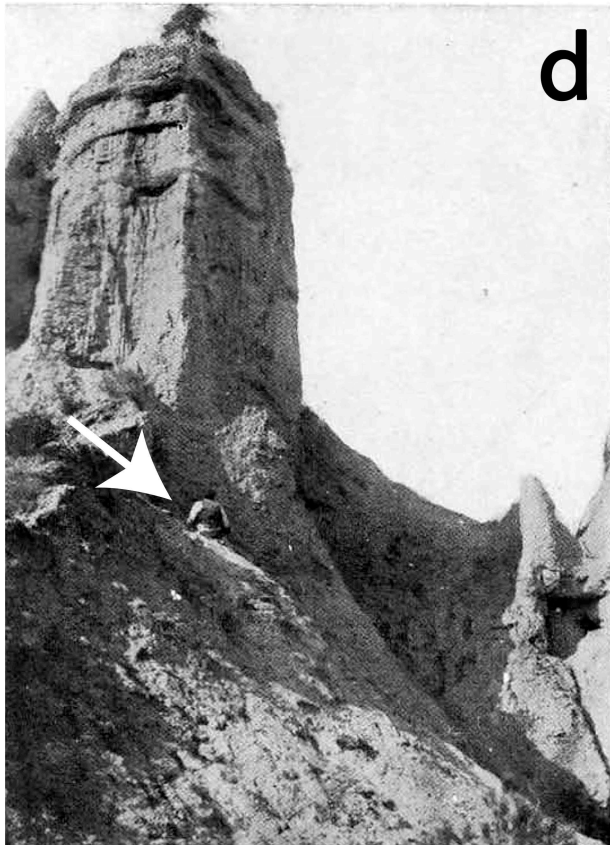
d

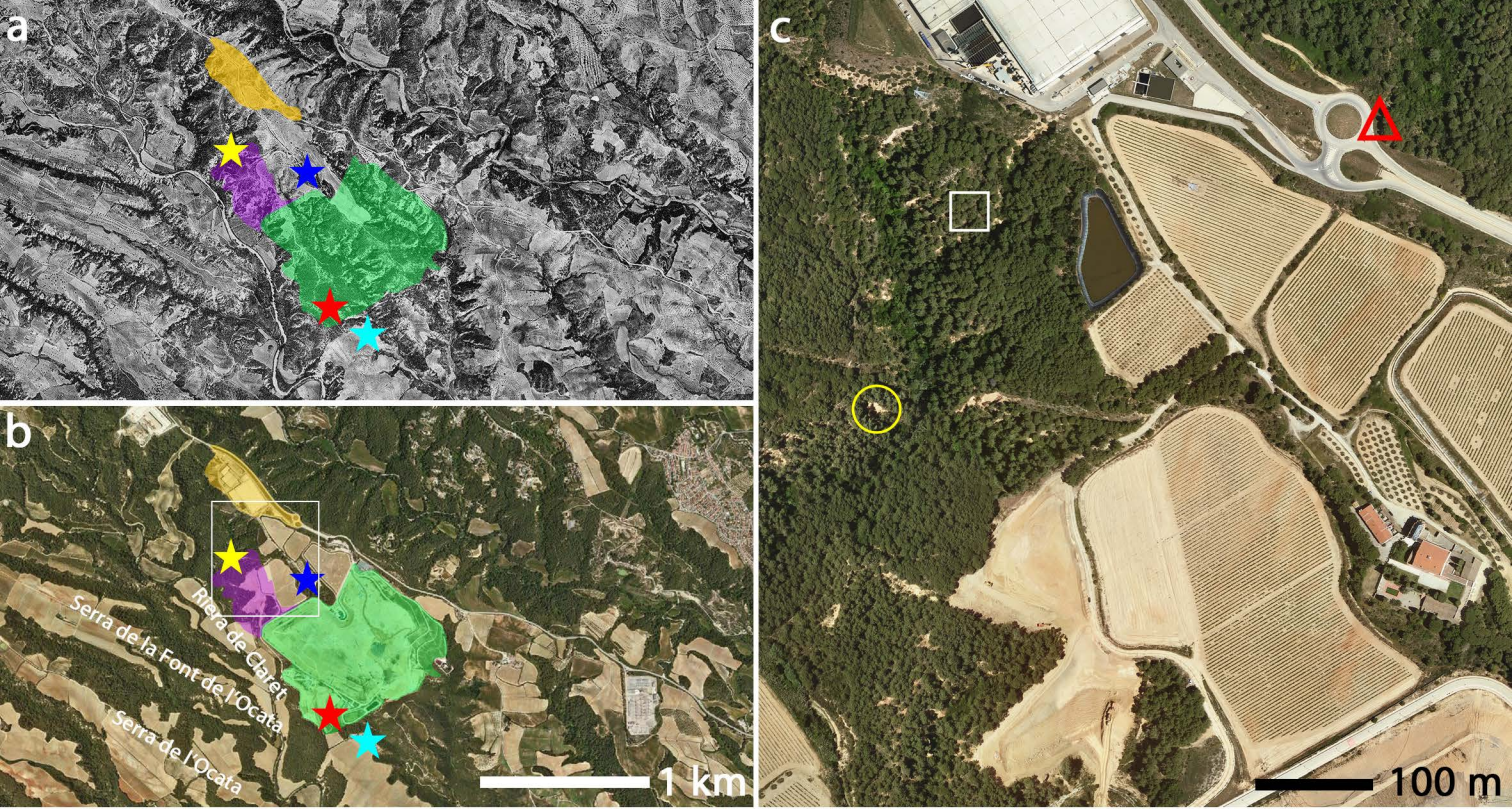
a
b
c
Riera de Caret
Serra de la Font de l'Ocata
Serra de l'Ocata
1 km
100 m
CM1
ACM/BCV1
Can Vila
Can Mata de la Garriga
ACM
ECM


a
1
2
3


b


c
1
2
3
4


d
2
3


e
2
3
4


f
2
3


g

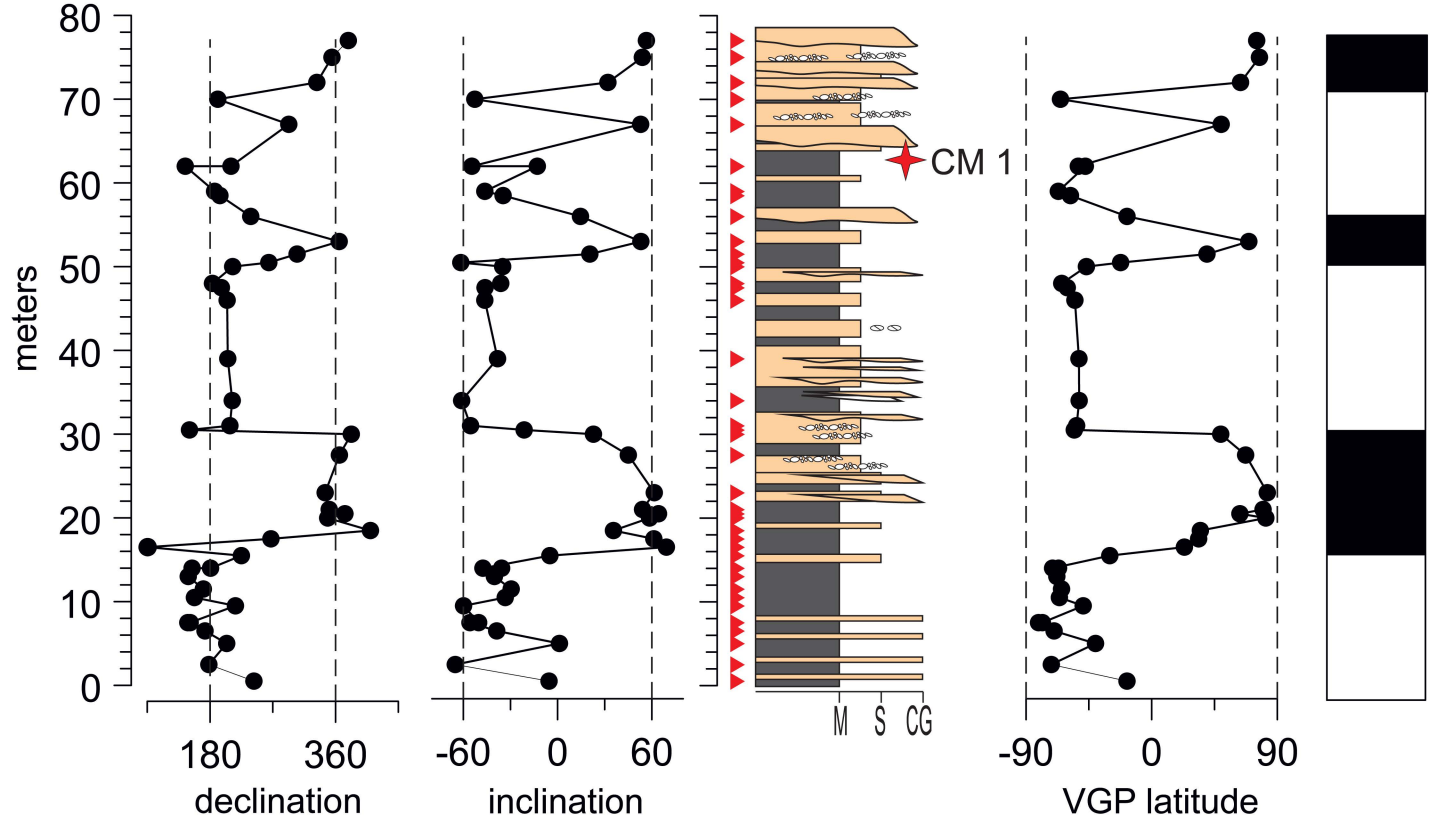
meters
0
10
20
30
40
50
60
70
80
180
360
declination
-60
0
60
inclination
CM 1
M
S
CG
-90
0
90
VGP latitude

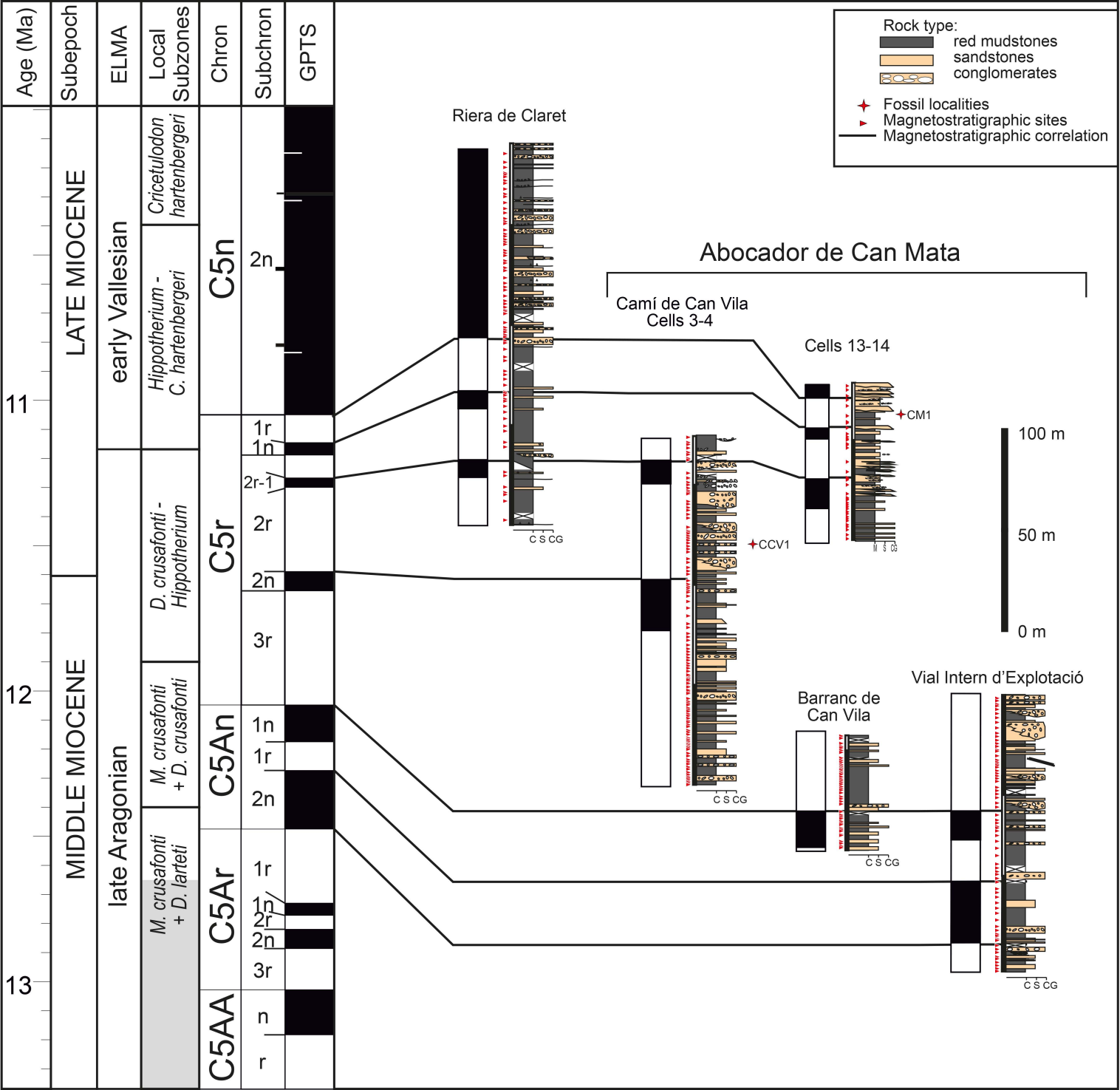
Age (Ma)
Subepoch
ELMA
Local Subzones
Chron
Subchron
GPTS
LATE MIOCENE
MIDDLE MIOCENE
early Vallesian
late Aragonian
Cricetulodon hartenbergeri
Hippotherium - C. hartenbergeri
D. crusafonti - Hippotherium
M. crusafonti + D. crusafonti
M. crusafonti + D. larteti
C5n
C5r
C5An
C5Ar
C5AA
2n
1r
1n
2r-1
2r
2n
3r
1n
1r
2n
1r
1n
2r
2n
3r
n
r
11
12
13
Rock type:
red mudstones
sandstones
conglomerates
Fossil localities
Magnetostratigraphic sites
Magnetostratigraphic correlation
Riera de Claret
Abocador de Can Mata
Camí de Can Vila
Cells 3-4
Cells 13-14
CM1
CCV1
100 m
50 m
0 m
Barranc de Can Vila
Vial Intern d'Explotació
C S CG

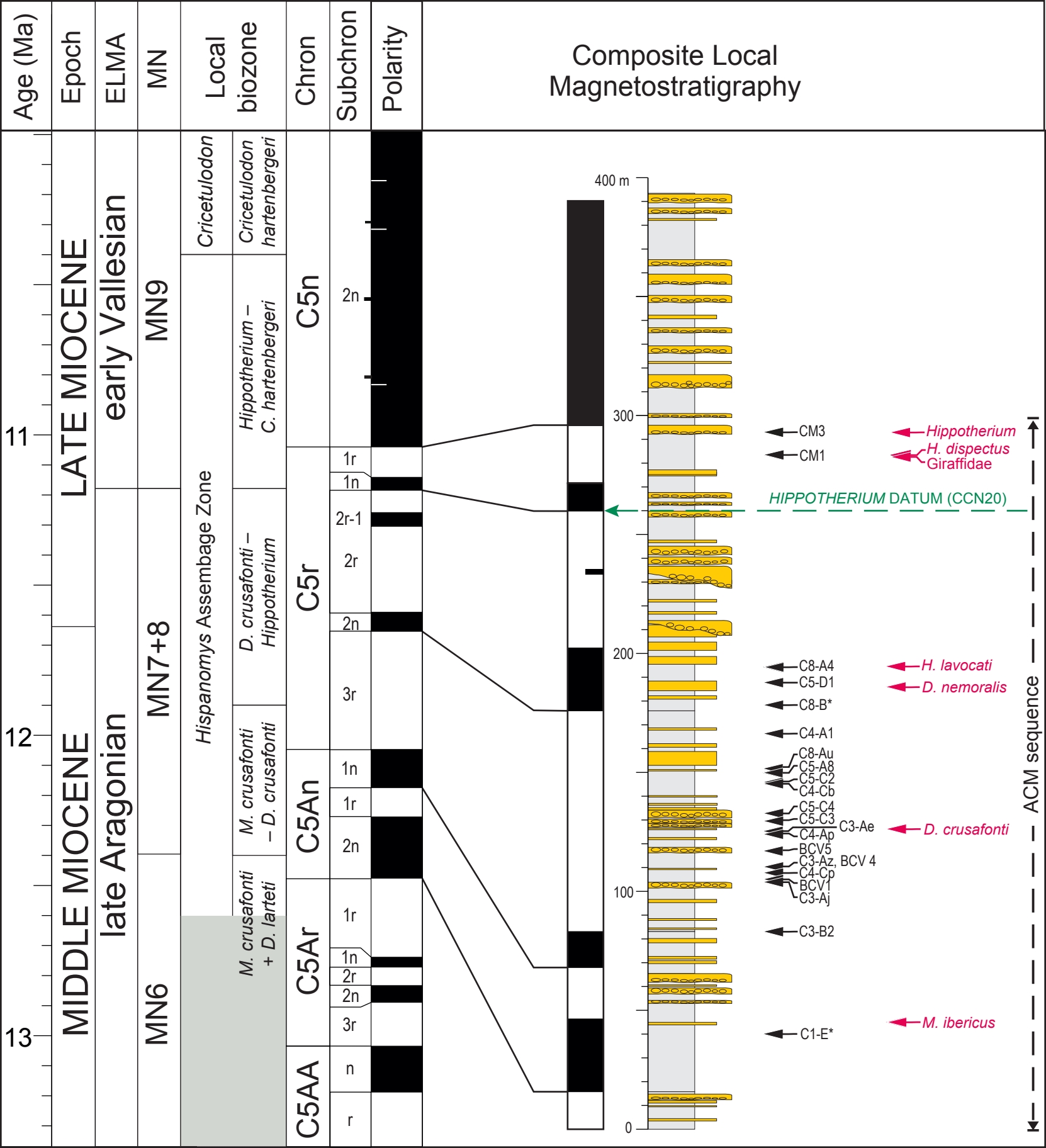
Age (Ma)
Epoch
ELMA
MN
Local biozone
Chron
Subchron
Polarity
Composite Local Magnetostratigraphy
MIDDLE MIOCENE
LATE MIOCENE
late Aragonian
early Vallesian
MN6
MN7+8
MN9
11
12
13
Hispanomys Assembage Zone
Cricetulodon
Cricetulodon hartenbergeri
Hippotherium – C. hartenbergeri
D. crusafonti – Hippotherium
M. crusafonti – D. crusafonti
M. crusafonti + D. larteti
C5n
C5r
C5An
C5Ar
C5AA
2n
1r
1n
2r-1
2r
3r
n
r
400 m
300
200
100
0
CM3
CM1
HIPPOTHERIUM DATUM (CCN20)
C8-A4
C5-D1
C8-B*
C4-A1
C8-Au
C5-A8
C5-C2
C4-Cb
C5-C4
C5-C3
C3-Ae
C4-Ap
BCV5
C3-Az, BCV 4
C4-Cp
BCV1
C3-Aj
C3-B2
C1-E*
Hippotherium
H. dispectus
Giraffidae
H. lavocati
D. nemoralis
D. crusafonti
M. ibericus
ACM sequence

Supplementary Online Material (SOM):

A revised (earliest Vallesian) age for the hominoid-bearing locality of Can Mata 1 based on new magnetostratigraphic and biostratigraphic data from Abocador de Can Mata (Vallès-Penedès Basin, NE Iberian Peninsula)

David M. Alba [a,*], Josep M. Robles [a], Isaac Casanovas-Vilar [a], Elisabet Beamud [b-c], Raymond L. Bernor [d-e], Omar Cirilli [d,f], Daniel DeMiguel [g,a], Jordi Galindo [a], Itziar Llopart [a], Guillem Pons-Monjo [a,] Israel M. Sánchez [a], Víctor Vinuesa [a], Miguel Garcés [c,h]

[a] *Institut Català de Paleontologia Miquel Crusafont, Universitat Autònoma de Barcelona, Edifici ICTA-ICP, c/ Columnes s/n, Campus de la UAB, 08193 Cerdanyola del Vallès, Barcelona, Spain*

[b] *Paleomagnetic Laboratory CCiTUB–Geo3Bcn CSIC, c/ Lluís Solé i Sabarís s/n, 08028 Barcelona, Spain*

[c] *Institut Geomodels, Grup de Recerca Consolidat de Geodinàmica i Anàlisi de Conques, Universitat de Barcelona, c/ Martí i Franqués s/n, 08028, Barcelona, Spain*

[d] *College of Medicine, Department of Anatomy, Laboratory of Evolutionary Biology, 520 W St. N.W., 20059, Washington D.C., USA*

[e] *Human Origins Program, Department of Anthropology, Smithsonian Institution, 20560, Washington D.C., USA*

[f] *Dipartimento di Scienze della Terra, Paleo[Fab]Lab, Università degli Studi di Firenze, Via G. La Pira 4, 50121 Firenze, Italy*

[g] *ARAID foundation / Universidad de Zaragoza, Departamento de Ciencias de la Tierra, and Instituto Universitario de Investigación en Ciencias Ambientales de Aragón (IUCA), Pedro Cerbuna 12, 50009 Zaragoza, Spain*

[h] *Departament de Dinàmica de la Terra i de l'Oceà, Facultat de Ciències de la Terra, Universitat de Barcelona, c/ Martí i Franqués s/n, 08028, Barcelona, Spain*

*Corresponding author.

E-mail address: david.alba@icp.at (D.M. Alba).

SOM S1

Details about the Can Mata localities

1.1. Historical details about the discovery and definition of Can Mata localities

The locality of CM1 was discovered in 1941 and initially referred to as "an ossiferous breccia" in the surroundings of the farmhouse of Can Mata de la Garriga (Villalta Comella and Crusafont Pairó, 1941: 206, Pl. XVI Figs. 1 and 2) or as "the breccia from Hostalets de Pierola" (Villata Comella and Crusafont Pairó, 1943: 172, Pl. XV)—our translations from Spanish. The term "ossiferous breccia" used by the authors implied a rich fossil bone bed rather than a breccia in the geological sense of the term. In turn, Crusafont and Truyols (1954) first mentioned the locality of Can Mata 2 (CM2), from which they reported the giraffid *Palaeotragus* sp., in all probability corresponding to the find of scarce dentognathic and postcranial remains previously reported by Crusafont Pairó (1952: Pls. XVIII Fig. 1 and XIX Figs. 1–5). These remains had been recovered from "the inferiormost layers of the Meotian [i.e., Vallesian] in the region of Hostalets de Pierola, nearby «Can Mata» and, thus, almost on the contact with Vindobonian [i.e., Aragonian] levels, […] in a small breccia located almost on the bottom of a ravine" (Crusafont Pairó, 1952: 71, our translation from the original in Spanish). They were found together with molars of the bovid *Protragocerus chantrei* and considered Vallesian based on the find of *Hippotherium* molars in the same area (Crusafont Pairó, 1952). Finally, the locality of Can Mata 3 (CM3) was first mentioned by Alba et al. (2006), corresponding to an isolated find of *Hippotherium* that thus far represents the oldest hipparionin find of known provenance from the area of Can Mata. Indeed, among the collections of the Institut Català de Paleontologia Miquel Crusafont in Sabadell there are multiple dental or postcranial remains of *Hippotherium* labeled as coming from Vallesian levels of els Hostalets de Pierola, including a few from nearby Can Mata or its surroundings. However, they mostly correspond to finds made by Crusafont and Villalta, whose exact geographic and stratigraphic provenance is unknown. In contrast, according to Alba et al. (2006) CM3 would be located ~200 m in NE direction from CM1, based on a personal communication of Jordi Agustí to J.G. Consulted again by the same author in December 2021, Agustí confirmed that the *Hippotherium* specimen was found during a survey undertaken by him with Josep Gibert in 1976.

1.2. Considerations about the faunal list from Can Mata 1

The published faunal list of large mammals CM1 (Crusafont-Pairó and Golpe-Posse, 1973; Golpe-Posse, 1974; Agustí et al., 1985) needs to be updated and revised, to confirm the

identity of multiple taxa that is confusing according to published sources. In particular, from a biostratigraphic viewpoint it would be interesting to ascertain whether CM1 records typically Aragonian taxa instead of their respective Vallesian counterparts. The former includes the gomphothere *Gomphotherium*, the deinothere *Deinotherium levius*, the chalicothere *Anisodon grande*, or the cervid *Euprox* aff. *furcatus* (Golpe-Posse, 1974; Agustí et al., 1985; Azanza and Menéndez, 1990)—compared with *Tetralophodon*, *Deinotherium giganteum*, *Chalicotherium goldfussi*, or *Euprox dicranoceros*, which are typically Vallesian (Azanza and Menéndez, 1990; Anquetin et al., 2007; Mazo and van der Made, 2012; Pickford and Pourabrishami, 2013). Nevertheless, despite being mostly Vallesian in age, both *Tetralophodon* (Mazo and Van der Made, 2012) and *Chalicotherium* (Anquetin et al., 2007), are first recorded within MN7+8. In turn, both *Dei. levius* (Konidaris and Koufos, 2019; Alba et al., 2020) and *E. furcatus* (Azanza and Menéndez, 1990; Vislobokova, 2007) apparently persisted since the Aragonian until the earliest Vallesian. Therefore, the usefulness of all these taxa to date localities around the Aragonian/Vallesian boundary is restricted. In contrast, it would probably be more relevant the identification of the large non-listriodontine suid from CM1, customarily attributed to *Propotamochoerus palaeochoerus* (Villalta Comella and Crusafont Pairó, 1943; Golpe-Posse, 1971, 1972, 1974; Crusafont-Pairó and Golpe-Posse, 1973; Agustí et al., 1985), which is currently considered to be conclusively recorded only from the early Vallesian (MN9) across Europe (Pickford, 2016a). Revising the faunal list of CM1 is outside the scope of this paper and will not be an easy task because Crusafont and coauthors seldom provided collection numbers and many of the remains from CM1 housed in the collections of the Institut Català de Paleontologia Miquel Crusafont (ICP) are not labeled as such, but merely referred to Hostalets or Hostalets Inferior.

SOM S2

Descriptions and comparisons of equid and giraffid material from Can Mata

2.1. Hipparionins

The best preserved M_3 (IPS124307; SOM Fig. S5a–c) shows a well-developed pli caballinid on the labial side of the hypoconid—a primitive feature that can be found among the Pannonian C *Hippotherium* from Atzeldorf, Gaiselberg, and Mariathal in the Vienna Basin, Austria (Bernor et al., 2017, 2021). Bernor et al. (2017) provided a detailed summary of the upper and lower dental morphology of the Pannonian C hipparionins from the Vienna Basin, identifying the presence of pli caballinids and ectostylids. However, these occlusal and buccal structures of the lower cheek teeth are not always present (Bernor et al., 2017), as their

occurrence may be related to dental wear stage and preservation of the specimens (e.g., pli caballinids may be obliterated in late wear stages and ectostylids may be short, welded to the buccal enamel wall, and buried within the cementum). Although the sample does not include maxillary cheek teeth, the presence of a well-developed pli caballinid in IPS124307 hints at similarities between the Austrian and Iberian samples.

2.2. Giraffids

The P^2 and P^3 from CM2 assigned by Crusafont-Pairó (1952: Pl. XVIII Fig. 1) to *Palaeotragus* sp., like the P^3 and P^4 from les Martines assigned by the same author to a different but unnamed species of the same genus (Crusafont-Pairó, 1952: Pl. XVIII Figs. 2 and 3), are buccolingually extended (not only the P^4). In this regard, the Vallès-Penedès remains differ from those of species such as *Palaeotragus primaevus* that have more or less elongated P^2 and P^3 as well as rounded/subtriangular P^4. Instead, they more closely resemble, among others, *Giraffokeryx punjabiensis*, *Palaeotragus germaini*, *Decennatherium* spp., and the extant *Giraffa* and *Okapia* (see, e.g., Colbert, 1933; Churcher, 1978; Ríos et al., 2017), which have derived rounded upper premolars that are buccolingually extended. The M^3s from ACM (SOM Fig. S6a–f), in turn, are characterized by well-developed cristae, column-like and very rectilinear styles and buccal structures, and presence of protoconal folds. The upper molars from les Martines described by Crusafont-Pairó (1952: Pl. XVIII Figs. 4 and 5) also closely resemble those from ACM in the possession of relatively high and internally flattish cristae, thin and column-like buccal structures, and a strong protoconal fold. A minor difference between the ACM and les Martines upper molars consists in the alignment of the cusps in the buccal wall, which is totally straight in ACM and slightly angled in the latter.

The lower molars from Ecoparc de Can Mata (ECM; SOM Fig. S6m–r) also have extended cristids, higher than those of *Injanatherium* (e.g., Morales et al., 1987), among others. Also, the cuspids in the ECM material are flatter and the third lobe of the M_3 is relatively larger than in *Injanatherium*. The M_3 displays a protruding metastylid which projects distally above the pre-entocristid, as in *Giraffokeryx punjabiensis*. The P_4 (SOM Fig. S6j–l) is similar to that of *Palaeotragus*: rectangular, short, and with a complex occlusal surface that has all cuspids united by their cristids. As in these forms, the P_4 has a large distal region, as noted by Hamilton (1978). However, the posterior wing (distolingual conid and distolabial stylid) is short, being covered lingually by an extended distolingual cristid that reaches the distolingual corner of the crown. In contrast, both *Giraffokeryx* and *Palaeotragus* have a very large posterior wing that occupies the entire distal lobe. Furthermore, contrary to

Palaeotragus and many other giraffids, in the ECM giraffid the distal lobe is not particularly separated from the rest of the crown by a marked constriction, being more similar to the standard ruminant morphology. On the other hand, *Decennatherium*, a basal member of the samothere-sivathere clade recorded from the Vallesian of the Iberian Peninsula (Ríos et al., 2016, 2017), has flatter cuspids in the lower molars and more elongated P_4 with clear posterior lobe separation, although the metastylid projection is very similar to the form recorded at ECM.

The transversal section of the metacarpal III–IV from Can Mata described by Crusafont-Pairó (1952: Pl. XIX Fig. 1) shows a medium deep palmar trough (as described by Ríos et al., 2017: character 97, state 0) very similar to that of the early Vallesian *Decennatherium rex*—a character state that can be considered basal for giraffids (Ríos et al, 2017). The (derived) deep condition of the palmar trough is diagnostic of the clade including *Birgerbohlinia* + *Bramatherium* (Ríos et al., 2017) and thus the Can Mata form can be excluded from that lineage of very derived giraffids. However, its relationship with more basal samotheres-sivatheres (as pointed out by Crusafont-Pairó, 1952) should be subjected to further scrutiny in the future. Similarly, the proximal phalanx of the Can Mata giraffid (Crusafont-Pairó, 1952: Pl. XIX Fig. 3) is somewhat primitive—i.e., elongated and more similar to a regular pecoran phalanx—compared to that of basal members of the samothere-sivathere clade such as *Dec. rex*, which have proximally broadened and overly blunter proximal phalanges. Also, the proximal surface of the metacarpal III–IV shows a more triangular and laterally elongated unciform facet than that of *Dec. rex*. However, as in the latter, the Can Mata giraffid displays a totally enclosed nonarticular fossette (or synovial fossa) between the facets for the unciform and the magnotrapezoid. Finally, the astragalus (Crusafont-Pairó, 1952: Pl. XIX Fig. 5) has equally deep proximal and distal trochleae, being different from the stouter astragalus of giraffids such as *Decennatherium*, in which the distal trochlea is shorter than the proximal one, and the astragalus is overall short and square.

SOM S3

Biostratigraphic remarks based on rodents

3.1. Similarities between latest Aragonian and earliest Vallesian rodent assemblages

According to the most recent local rodent biozonation of the Vallès-Penedès Basin (Casanovas-Vilar et al., 2016a), the latest Aragonian corresponds to the *Democricetodon crusafonti–Hippotherium* interval subzone (from the first local occurrence [FLO] of *Dem. crusafonti* to that of *Hippotherium*), whereas the earliest Vallesian is represented by the *Hippotherium–Cricetulodon hartenbergeri* interval subzone (from the FLO of *Hippotherium* to that of *C. hartenbergeri*). Both subzones belong to the *Hispanomys* assemblage zone (Casanovas-Vilar et al., 2016a), and they are exceptionally based on the equid *Hippotherium* because the respective micromammal assemblages have been considered indistinguishable in taxonomic composition.

The presence of *Megacricetodon ibericus* is not informative regarding the placement of the Aragonian/Vallesian boundary in the Vallès-Penedès Basin, because it is not only recorded from the late Aragonian (Casanovas-Vilar et al., 2016a) but also from the earliest Vallesian sites of Creu de Conill 20 and 22 (Casanovas-Vilar et al., 2006, 2016a), CM1 and Hostalets Superior (Agustí and Gibert, 1982; Agustí et al., 1985; Casanovas-Vilar et al., 2016a), and tentatively also Can Missert and ECM (Agustí et al., 2005; Alba et al., 2012; Casanovas-Vilar et al., 2016a). Similarly, despite its later appearance in the Calatayud-Montalbán Basin, *M. ibericus* s.s. is already recorded there from unambiguously late Aragonian (zone G3) sites (Álvarez Sierra et al., 2003; Van Dam et al., 2014; Oliver Pérez, 2015), persisting until the early Vallesian site of Nombrevilla 1 at ~10.8 Ma (Daams and Freudenthal, 1988; Álvarez Sierra et al., 2003; Van der Meulen et al., 2003; Oliver Pérez, 2015).

3.2. The Cricetulodon *event*

The cricetid *Cricetulodon hartenbergeri* is first recorded at ~10.6 Ma (zone I) in the Calatayud-Montalbán Basin (Van Dam et al., 2014) and at ~10.3 Ma in the Vallès-Penedès (Autopista de Rubí-Terressa 8 locality, with an interpolated age of 10.34 Ma; Casanovas-Vilar et al, 2016a). An isolated M^1 from Hostalets Inferior, originally ascribed to *Democricetodon nemoralis* by Agustí (1981) but no longer present in the ICP collections, was subsequently attributed to *Cricetulodon hartenbergeri* by Agustí and Gibert (1982: Pl. II Fig. 5; see also Agustí et al., 1985; Alba et al., 2006). However, this specimen is slightly larger than the M^1s of *C. hartenbergeri* and we concur with Agustí (1981) that, despite the

presence of a double protolophule (very common in *C. hartenbergeri* and much rarer in *Dem. nemoralis*), it better fits with the latter species, which is first recorded in the ACM composite section at ACM/C6-C2, with an interpolated age of 11.60 Ma. On the other hand, no *Cricetulodon* material has been recovered from Can Mata—not even from well-sampled ECM localities (ECM/VCE-B2 and ECM/VCE-C1; Casanovas-Vilar et al., 2016a), which have an estimated age of ~10.8 and ~10.7 Ma, respectively. This supports the hypothesis that a major turnover of small mammal faunas, characterized by the appearance of *C. hartenbergeri* and the disapperace of *Dem. crusafonti* and *M. ibericus*, did not occur until much later than the Aragonian/Vallesian boundary.

3.3. The Hispanomys *succession across the Aragonian/Vallesian boundary*

Hispanomys species offer some prospects to distinguish between the latest Aragonian and the earliest Vallesian based on micromammals. Casanovas-Vilar et al. (2016a: 209) already noted that "*Hispanomys* species could also be of great use in refining the diagnoses for some zones and their boundaries", although they did not specifically note its potential utility for characterizing the Aragonian/Vallesian transition. The succession of *Hispanomys* species in the Vallès-Penedès Basin is different from that in other Iberian basins. In the Calatayud-Montalbán Basin, *Hispanomys lavocati* co-occurs with *M. ibericus* and *Dem. crusafonti* in MN7+8 (zone G3) sites dating to ~11.9–11.8 Ma (López-Guerrero et al., 2014, 2019; Van Dam et al., 2014), whereas localities dating to zone H (Nombrevilla 9, 10, and 1) are characterized by the appearance of *Hispanomys nombrevillae* (López-Guerrero et al., 2014, 2019; Van Dam et al., 2014; García-Paredes et al., 2016). The latter species is also recorded in early Vallesian sites from the Duero Basin before the appearance of *Hispanomys aragonensis* (see Castillo et al., 2018). In summary, in both the Calatayud-Montalbán and Duero basins, *His. lavocati* is restricted to zone G3 (latest Aragonian), *His. nombrevillae* to zone H (around the Aragonian/Vallesian transition), and *His. aragonensis* to zone I (early Vallesian; Castillo et al., 2018; López-Guerrero et al., 2019).

In the Vallès-Penedès Basin, *His. lavocati* co-occurs with *M. ibericus* and *Dem. crusafonti* since it is first recorded from ACM at ~11.6 Ma, as well as in other MN7+8 sites such as Trinxera del Ferrocarril in Sant Quirze (Casanovas-Vilar et al., 2016a), suggesting that the latter is similar in age to the latest Aragonian localities from ACM. However, unlike in the Calatayud-Montalbán and Duero basins, in the Vallès-Penedès Basin *His. lavocati* persists into the earliest Vallesian and *His. nombrevillae* is not recorded. In contrast, two different species of *Hispanomys* (*Hispanomys dispectus* and *Hispanomys daamsi*) are recorded during

the earliest Vallesian of the Vallès-Penedès Basin. Indeed, in NE Iberia *His. dispectus* is also recorded, together with *M. ibericus*, from various localities of the Empordà Basin (La Bisbal 2, Can Colomer 1, and Abocador de Vacamorta 4; Gibert et al., 1979, 1980; Agustí Ballester, 1980; Llenas et al., 2002; Casanovas-Vilar et al., 2010) that are correlated to the earliest Vallesian (Casanovas-Vilar et al., 2010; Tosal et al., 2022). In the Vallès-Penedès Basin, this species was originally reported from Hostalets Inferior, Can Feliu, Castell de Barberà, and Hostalets Superior (Agustí Ballester, 1980), and subsequently from CM1, Can Valls in Masquefa, and Can Missert (Agustí et al., 1985), Autopista de Rubí-Terrassa km 11 and Can Coromines 2 (Agustí et al., 1997), and Creu de Conill 20 and 22 (Agustí et al., 1997; Casanovas-Vilar et al., 2006). The material from Can Missert was later used by Agustí et al. (2005) to erect a *His. daamsi*, to which the material from Castell de Barberà was also reassigned (Casanovas-Vilar et al., 2016a; Alba et al., 2019). Despite earlier preliminary claims (Alba et al., 2006, 2011; Casanovas-Vilar et al., 2008), ACM localities record *Hispanomys* cf. *aguirrei*, *Hispanomys decedens*, and *His. lavocati* (depending on the locality) but not *His. daamsi* (see Casanovas-Vilar et al., 2016a). Similarly, we have been unable to confirm the citation of *His. dispectus* from the later Vallesian locality Can Coromines 2, which is correlated to C5n.1r (Agustí et al., 1997), indicating an age of ~10.0–9.9 Ma, as the only cricetid specimen from this locality found in the ICP collections (the M_3 IPS18100) cannot be assigned to genus (authors' observation).

All the localities conclusively recording either *His. dispectus* (Hostalets Inferior and Superior, CM1, Can Feliu, Can Valls, Creu de Conill 20 and 22, and Autopista de Rubí-Terrassa km 11) or *His. daamsi* (Castell de Barberà and Can Missert) are currently considered earliest Vallesian in age (Casanovas-Vilar et al., 2016b)—including Autopista de Rubí-Terrassa km 11, which is correlated to C5n.2n (Agustí et al., 1997) with an interpolated age of 10.98 Ma (Casanovas-Vilar et al., 2016a)—with the sole exception of Hostalets Inferior. However, the fact that the micromammal assemblage from Hostalets Inferior includes material from CM1 (presumably in most instances not labeled as such), which is here conclusively dated to the earliest Vallesian, makes it uncertain the presence of either species in the late Aragonian levels of this area (or elsewhere). This is further supported by the absence of both species from ACM, suggesting that they might be characteristic of the early Vallesian or, at most, the Aragonian/Vallesian transition more broadly. Later early Vallesian localities from ECM record *His. aragonensis* instead (Alba et al., 2012; Casanovas-Vilar et al., 2016a), which is first conclusively recorded at ECM/VCE-B2 at ~10.8 Ma (updated from Casanovas-Vilar et al., 2016a), i.e., slightly earlier than in the Calatayud-

Montalbán Basin, where it is first recorded from Nombrevilla 13 at ~10.7 Ma (López-Guerrero et al., 2014; Van Dam et al., 2014). This supports that *His. dispectus* may be restricted to early MN9, thus potentially being—together with *H. daamsi*—a biochronological marker of the Vallesian in its type area. Further refinements will probably be possible once the large sample of *Hispanomys* remains from ACM and ECM (including >4000 specimens) is studied in detail. The study of the micromammal remains recently recovered from the uppermost sectors of the ACM composite section (ACM/C12, ACM/C13, ACM/C14 and ACM/PTA)—jointly extending from 11.4 to 11.1 Ma (from C5r.2r to C5r.1r)—will hopefully show, in the future, whether *His. dispectus* makes it first appearance before the Aragonian/Vallesian boundary or coinciding with the earliest Vallesian.

SOM S4

Biochronological remarks about large mammals

4.1. Age of the earliest hipparionins from China

In the earliest Vallesian, China records *Hippotherium weihoense*, which is characteristic of the Guonigou Fauna of the Linxia Basin and co-occurs with '*Hipparion*' *dongxiangense* (~11.2–11.1 Ma; Deng et al., 2004, 2013; Sun et al., 2022). The Guonigou Fauna is correlated to the early Bahean Asian Land Mammal Age, correlative with the early Vallesian (Deng et al., 2013). Fang et al. (2016) reviewed the tectonosedimentary evolution of the Linxia Basin based on new paleomagnetic analyses, suggesting an age of ~11.5 Ma for the first occurrence of hipparionins in the Guonigou Fauna, thus being slightly older than the record of *Hippotherium* in the Vienna and Vallès-Penedès basins (see also Sun et al., 2022). However, the Guonigou hipparionin record lacks documentation of specimens as well as specific stratigraphic occurrence and magnetostratigraphic correlation within the Linxia Basin, and as such it needs further documentation to be adequately vetted. Indeed, the magnetostratigraphy provided by Fang et al. (2016: Fig. 7) is missing many relevant subchrons, the Chinese *Hippotherium* datum being correlated to a reverse polarity magnetozone interpreted as C5r.1r–C5r.2r (Fang et al., 2016). These subchrons span from 11.59 to 11.15 Ma and include C5r.1n, when the earliest *Hippotherium* is recorded in the Vallès-Penedès Basin. The inability to detect these polarity reversals questions Fang et al.'s (2016) unambiguous magnetostratigraphic correlation of the Chinese *Hipparion* datum with C5r.2r. Alternative correlations cannot be thus entirely discounted, including C5r.1r, which could imply a younger age roughly coeval with the European *Hippotherium* datum.

4.2. Hipparionins from the Duero Basin

In the Duero Basin, hipparionins are recorded together with *Decennatherium* in El Lugarejo, Ávila (Crusafont Pairó et al., 1968; Morales et al., 1981) and in the much better-known site of Los Valles de Fuentidueña, Segovia, which also records *Machairodus* (Crusafont Pairó, 1952; Crusafont-Pairó and Ginsburg, 1973; Alberdi, 1981; Alberdi et al., 1981; Ginsburg et al., 1981; Morales and Soria, 1981; Ríos et al., 2016; Fernández-Monescillo et al., 2019). Both sites are considered similar in age, as supported by similarities in large mammal composition (the giraffid, hipparionin, and *Hispanomeryx* species; Crusafont Pairó et al., 1968; Alberdi, 1974, 1981; Morales et al., 1981; Sánchez and Morales, 2006), being sometimes correlated to zone H (Sánchez and Morales, 2006). However, there are no micromammals from El Lugarejo, while the small mammals from Los Valles de

Fuentidueña (Agustí Ballester, 1978; Alberdi et al., 1981; Sesé Benito and López Martínez, 1981) do not provide a precise dating. The *Hispanomys* species from the latter site, in particular, shows similarities with both *His. aragonensis* and *His. nombrevillae*, whereas a species assignment is neither possible for a member the *Megacricetodon minor–Megacricetodon minutus* lineage (Sesé Benito and López Martínez, 1981; Castillo et al., 2018)—the latter species considered here a senior synonym of *Megacricetodon debruijni*. Only the lack of *Cricetulodon* indicates that Los Valles de Fuentidueña should be correlated to zone H (early MN9) instead of zone I (see Van Dam et al., 2014).

The hipparionin recorded in these localities from the Duero Basin was originally considered by Crusafont Pairó et al. (1968) an archaic form probably different from *Hippotherium catalaunicum*. It was subsequently described as *Hippotherium primigenium melendezi* by Alberdi (1974, 1981), who also considered *Hip. catalaunicum* as a subspecies of *Hip. primigenium*. The hipparionin from the Duero Basin is smaller and more gracile than *Hip. catalaunicum*, but based on the cranial evidence from El Lugarejo, Bernor et al. (1980, 1990) first referred it to 'Group 1' (i.e., *Hippotherium*). Nevertheless, differences in the morphology of the preorbital fossa noted by Bernor and Hussain (1985), who considered it a distinct species, eventually led to its transferral to *Hipparion* s.s. (Bernor et al., 1996). In contrast, other authors have considered this species to be conspecific with the Turolian species *Hipparion concudense* (Forstén, 1982; Pesquero and Alberdi, 2012), which Zouhri and Bensalmia (2005) referred to *Cremohipparion*. This is not only at odds with the Vallesian age of these sites, but also with the morphology displayed by the cranium from El Lugarejo, which rather resembles those of *Hipparion* s.s. (group 3 of Woodburne and Bernor, 1980), first recorded at MN10 in Iran (Bernor et al., 2017). Detailed comparisons would be required to determine the taxonomic identify of the hipparionin species from El Lugarejo and Los Valles de Fuentidueña, but differences relative to *Hippotherium* from both the Vallès-Penedès and Calatayud-Montalbán basins suggest that an earliest Vallesian age is unlikely.

4.3. Earliest Vallesian giraffids from the Vallès-Penedès Basin

Crusafont Pairó (1952) noted dental similarities between the CM2 giraffid material and the somewhat smaller *Palaeotragus quadricornis* (currently in *Schansitherium*; Solounias, 2007), hypothesizing that the former might belong to a new species, and refrained from including it in *Decennatherium pachecoi*—which he described based on the Vallesian material from other Spanish localities (see also Ríos et al., 2016). Ríos et al. (2016, 2017) considered that this genus is only recorded conclusively from MN9 and MN10 localities of Spain (Catalatayud-

Montalbán, Duero, and Madrid basins; Ríos et al., 2016, 2017). However, more recently it has also been reported from the Siwaliks in Pakistan (Ríos et al., 2019). The latter material is Late Miocene in age (10.1–8.2 Ma, MN10–MN11) and more derived than *Dec. pachecoi*, except for some ossicone fragments from locality Y503 (13.5 Ma) that have been assigned with doubts to cf. *Decennatherium* (Ríos et al., 2019). The latter occurrence supports the view that *Dec. pachecoi* and probably '*Palaeotragus*' sp. from the Vallès-Penedès Basin are local endemisms that originated from a dispersal event from the east.

The earliest well-dated record of giraffids in the Vallès-Penedès Basin corresponds to the earliest Vallesian site of Castell de Barberà (~11.2 Ma), followed by the recent find reported here from ACM/C13/C14-A (~11.1 Ma, probably roughly coeval to the remains from CM2 described by Crusafont-Pairó, 1952) and ECM/VCE-Bb (~10.9 Ma). Besides these specimens, giraffid remains traditionally assigned to *Palaeotragus* have also been cited from the Vallès Sector of the Vallès-Penedès Basin—sites of Can Feliu, Can Missert, Can Poncic 2, Castell de Barberà, les Martines, Poble Nou de Sant Quirze, Sant Miquel de Toudell, and Santiga (Crusafont Pairó, 1952, 1953, 1965; Crusafont and Truyols, 1954; Crusafont-Pairó and Golpe, 1972; Crusafont-Pairó and Golpe-Posse, 1972; Golpe-Posse, 1974; Crusafont-Pairó and Golpe-Posse, 1974a; Crusafont Pairó, 1975, 1982; Agustí et al., 1985, 2005). Some of these sites (Sant Miquel de Toudell and Santiga) are clearly Vallesian (e.g., Casanovas-Vilar et al., 2016a, 2016b), but the age of most of the remaining ones has proven controversial due to the absence of *Hippotherium* coupled with the lack of magnetostratigraphic data and clear differences between the latest Aragonian and earliest Vallesian rodent assemblages (but see SOM S2.3). Such controversies are best exemplified by Castell de Barberà, whose correlation to the latest Aragonian was maintained despite the find of a hipparionin fragment (Crusafont-Pairó and Golpe-Posse, 1974b; see also Rotgers and Alba, 2011), until the find of additional *Hippotherium* remains and magnetostratigraphic data more unambiguously supported a Vallesian age (Alba et al., 2019).

Among the aforementioned localities of ambiguous age with '*Paleotragus*' sp., only the Vallesian dating of les Martines in Terrassa, based on the regional context (Crusafont Pairó, 1952, 1953; Crusafont and Truyols, 1954), has remained uncontroversial. Indeed, the location of the clay quarry where the giraffid remains were recovered in unknown, but the area of les Martines is near that of Creu de Conill, so that an early Vallesian age is plausible. Can Feliu (Crusafont and Truyols, 1954), Can Poncic 2 (Crusafont and Truyols, 1956), and Can Missert (Crusafont-Pairó and Golpe-Posse, 1974a) were originally considered Vallesian as well, whereas Poble Nou de Sant Quirze was first considered (with doubts) pre-Vallesian

(Crusafont and Truyols, 1956), but subsequently dated to the Vallesian by Crusafont Pairó (1962) based on the fact that it was calculated to be 30 m stratigraphically above Trinxera del Ferrocarril (which is likely equivalent in age to the uppermost latest Aragonian portion of the ACM sequence; see SOM 2.3). Following the definition of a new pre-Vallesian biozone characterized by the lack of hipparionins and the presence of giraffids (Crusafont Pairó and Golpe Posse, 1971), most of the aforementioned localities (CM2, Can Poncic 2, Castell de Barberà, Poble Nou de Sant Quirze, and Can Missert) were considered pre-Vallesian (Crusafont-Pairó and Golpe, 1972; Golpe-Posse, 1972, 1974; Crusafont Pairó, 1975; Agustí et al., 1985). Also on this basis, Agustí et al. (1985) considered that CM1 predated CM2, given the lack of giraffids in the former.

The definition of the above-mentioned biozone (Crusafont Pairó and Golpe Posse, 1971) prompted the definitive abandonment of Crusafont Pairó's (1950) original concept of the Vallesian based on the presence of both hipparionins and giraffids, in favor of the view that only the giraffid *Decennatherium* (but not '*Palaeotragus*') would be indicative of the Vallesian (Agustí et al., 1985, 1997, 2001). Agustí and Moyà-Solà (1991: 111) even considered that "no other dispersal event is associated with the appearance of *Hipparion* in Europe, the entry of this equid being an isolated datum", while Agustí (1999: 103) remarked that "the latest Aragonian and earliest Vallesian faunas in the Vallès-Penedès share the same small and large mammal elements". These assertions are surprising, given that Agustí et al. (1997) considered the dispersal of *Hippotherium* and *Machairodus* to be synchronous. Notwithstanding the latter, the notion that giraffids dispersed into the Vallès-Penedès Basin before the entry of *Hippotherium* was thus perpetuated by Agustí and colleagues (Agustí and Moyà-Solà, 1990; Agustí et al., 1997, 2005; Agustí, 1999) and further extended to Western Europe as a whole by Agustí et al. (2001), who considered that, unlike *Hippotherium* and the felid *Machairodus*, the giraffid *Palaeotragus* dispersed during MN7+8. More recently, however, an earliest Vallesian age was favored for Can Missert, Can Feliu, Can Poncic 2, and Castell de Barberà (Robles et al., 2011; Casanovas-Vilar et al., 2016a, 2016b; Alba et al., 2019). Only Poble Nou de Sant Quirze and CM2 remained as putative latest Aragonian sites from the Vallès-Penedès Basin where giraffids are recorded. However, the fauna from Poble Nou de Sant Quirze is only poorly known, whereas our results further indicate that a latest Aragonian age is no longer tenable for CM2, as CM1 correlates to the Vallesian despite the lack of *Hippotherium*. Furthermore, our results indicate that CM1 is penecontemporaneous with the oldest well-dated record of giraffids in the area, which in turn slightly postdates the earliest record of *Hippotherium* in the Vallès-Penedès Basin. At ACM, giraffids have yet to

be found in the late Aragonian levels despite the huge sampling effort (Alba et al., 2006, 2017), thus challenging the traditional notion (e.g., Crusafont Pairó and Golpe Posse, 1971; Golpe-Posse, 1974; Crusafont Pairó, 1975; Agustí et al., 1985, 1997, 2001) that giraffids dispersed into the Vallès-Penedès Basin before hipparionin equids. Rather the contrary, our results suggest that giraffids and hipparionins might have dispersed at approximately the same time, as originally considered by Crusafont Pairó (1950).

4.4. Other Vallesian taxa of eastern origin

The machairodontine felid *Machairodus aphanistus* is one of the large mammal species that first appears in the Iberian Peninsula and elsewhere in Europe coinciding with the beginning of the Vallesian (Agustí et al., 1997; Agustí, 1999; Agustí and Antón, 2002). The geographic and evolutionary origin of *Machairodus* is somewhat uncertain (Werdelin et al., 2010; Morlo et al., 2020) but has been related to the more plesiomorphic sabertoothed cat '*Miomachairodus' pseudailuroides*, which is first recorded in the late Aragonian (MN7+8) of Turkey (Schmidt-Kittler, 1976; de Beaumont, 1978; Werdelin et al., 2010; Morlo et al., 2020). This would support the view that *Machairodus* dispersed into Western Europe from the east at the beginning of the Vallesian (Agustí et al., 1997, 2001), rather than locally evolving from a *Pseudaelurus* ancestor. Another relevant example refers to the suine *P. palaeochoerus*, whose first appearance datum was until recently correlated to the late MN7+8 (Van der Made and Moyà-Solà, 1989; Van der Made et al., 1999; Agustí et al., 2001; Fortelius et al., 2005; Alba et al., 2006). However, this was in part due to the incorrect dating of some sites (e.g., Castell de Barberà, where *P. palaeochoerus* is unambiguously recorded; Pickford, 2016a), and also—as in the Vallès-Penedès sites of Sant Quirze (Van der Made and Moyà-Solà, 1989; Van der Made, 1990a, 1990b) and ACM (Alba et al., 2006, 2011)—owing to the confusion with a large tetraconodontine currently referred to *Parachleuastochoerus valentini* by Pickford (2014, 2016a, 2016b). Although there is disagreement about the taxonomic validity of the latter species (Van der Made, 2020), *P. palaeochoerus* is currently considered to be conclusively recorded only from MN9 localities (Pickford, 2016a). The genus is however already recorded in the Middle Miocene of Asia (Harris and Liu, 2007), from where it would have dispersed into Europe (Agustí, 2015).

In the Vallès-Penedès Basin, the earliest published record of *Machairodus* corresponds to Can Mata (Madurell-Malapeira et al., 2014), but the lack of stratigraphic details precludes confirming whether it predates or postdates the Aragonian/Vallesian boundary. The citation of *Machairodus* from the earliest Vallesian locality of Creu de Conill 20 (Agustí et al., 1997;

Agustí and Galobart, 1998; Casanovas-Vilar et al., 2006), was dismissed by Madurell-Malapeira et al. (2014). However, recent fieldwork at Creu de Conill 20 (Almécija et al., 2019) has demonstrated the co-occurrence of *Machairodus*, *Propotamochoerus* and *Hippotherium* coinciding with the first appearance datum of the latter taxon in the Vallès-Penedès Basin. Unfortunately, our efforts to locate within the ICP collections the suid remains that led to the citation of *P. palaeochoerus* from CM1 (e.g., Golpe-Posse, 1974; Agustí et al., 1985) have been unsuccessful. Only Golpe-Posse (1971), in her unpublished dissertation, listed catalog numbers for the specimens from Hostalets assigned to this taxon, but she did not note which specimens came from CM1 or even distinguish between Hostalets Inferior and Superior. As a result, it is currently impossible to confirm whether *P. palaeochoerus* is recorded there (as opposed to stratigraphically superior levels customarily included in Hostalets Superior), or whether the previous citations are just another confusion with *Pa. valentini*, as argued by Pickford (2016a, 2016b).

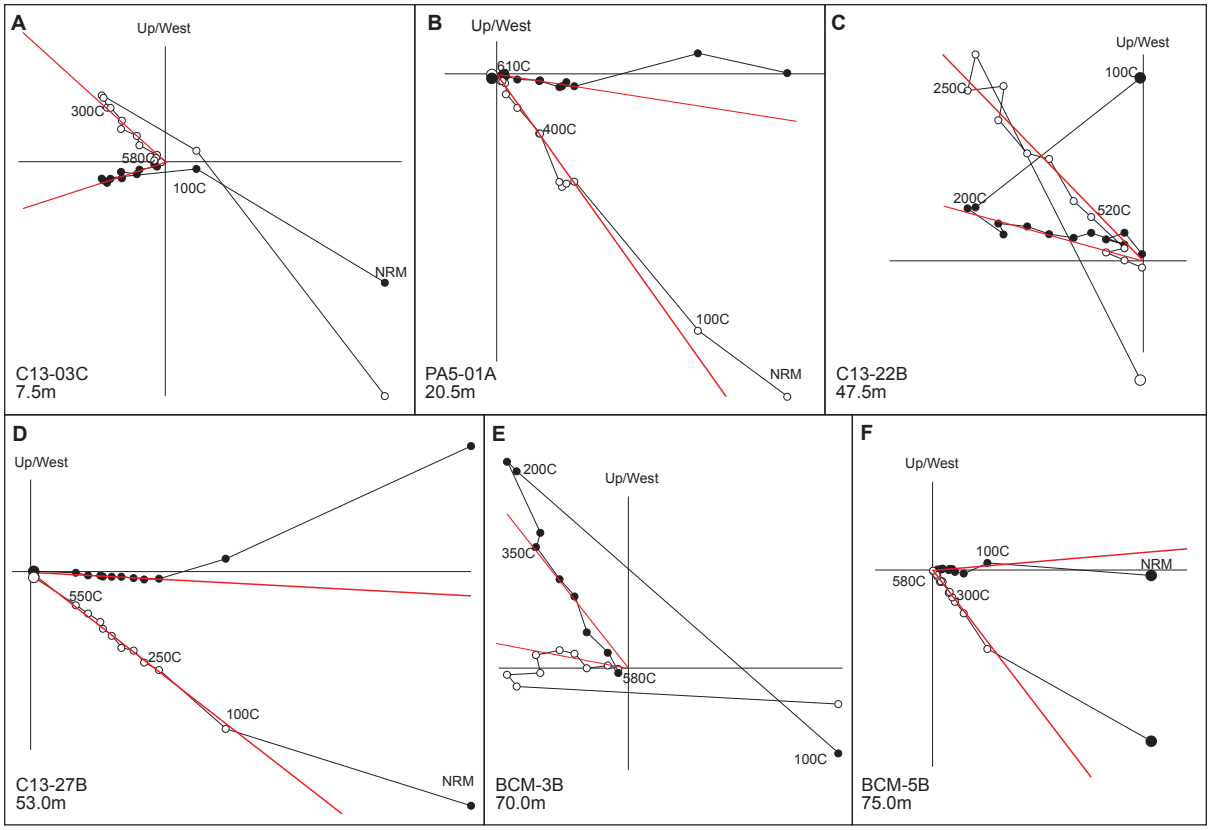

SOM Figure S1. Examples of stepwise thermal demagnetization of samples representative of all recorded magnetozones in the Abocador de Can Mata composite section. Diagrams represent orthogonal projections of vector endpoint demagnetization data; black and white dots represent the projection onto the horizontal and vertical planes, respectively. Red lines represent least-squares fits that define the characteristic paleomagnetic direction. Stratigraphic position in meters is indicated in the lower left corner of each diagram.

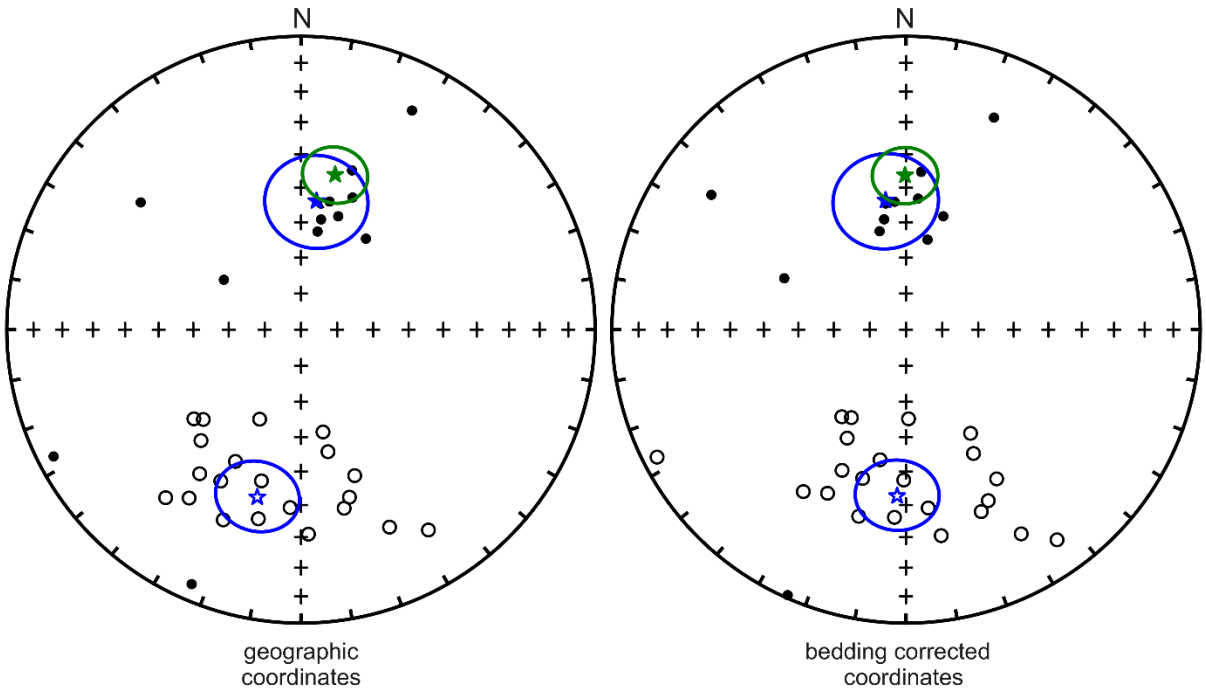

SOM Figure S2. Equal area stereonet projection of paleomagnetic directions and the mean normal and reversed polarity directions in geographic and bedding corrected coordinates (blue stars). Green star represents the mean direction after conversion of all the directions to normal polarity. See also SOM Table S3 for numerical values and Fisher statistics parameters.

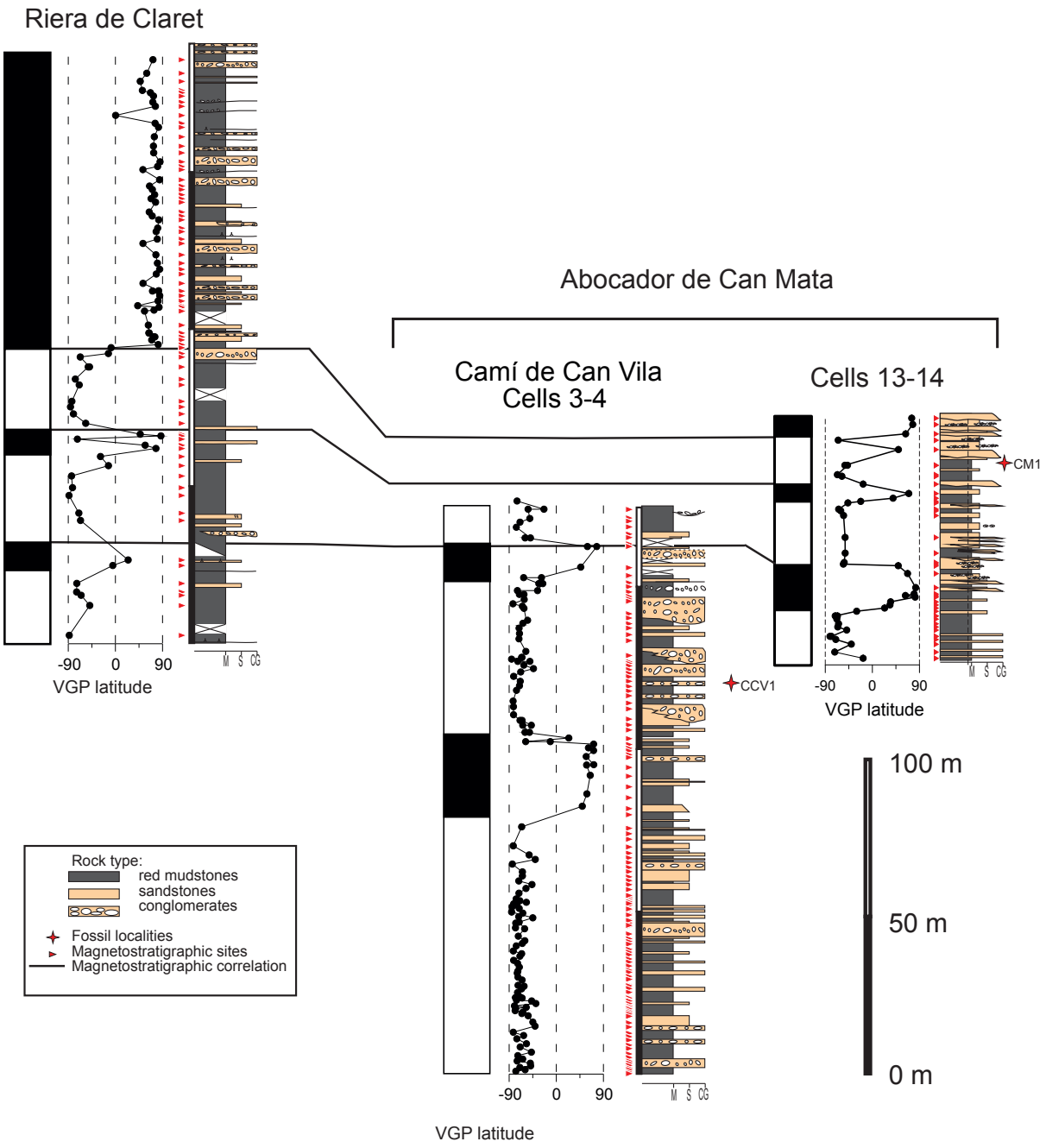

SOM Figure S3. Magnetostratigraphic correlation of the new Cells 13–14 section, where Can Mata 1 is located (denoted by a four-pointed red star), with the Camí de Can Vila–Cells 3–4 (Abocador de Can Mata) and the Riera de Claret sections (after Moyà-Solà et al., 2009 and Alba et al., 2017, with some corrections). Sideways triangles denote the stratigraphic position of paleomagnetic samples. Abbreviations: M = mudstones; S = sandstones; CG = conglomerates; VGP = virtual geomagnetic pole.

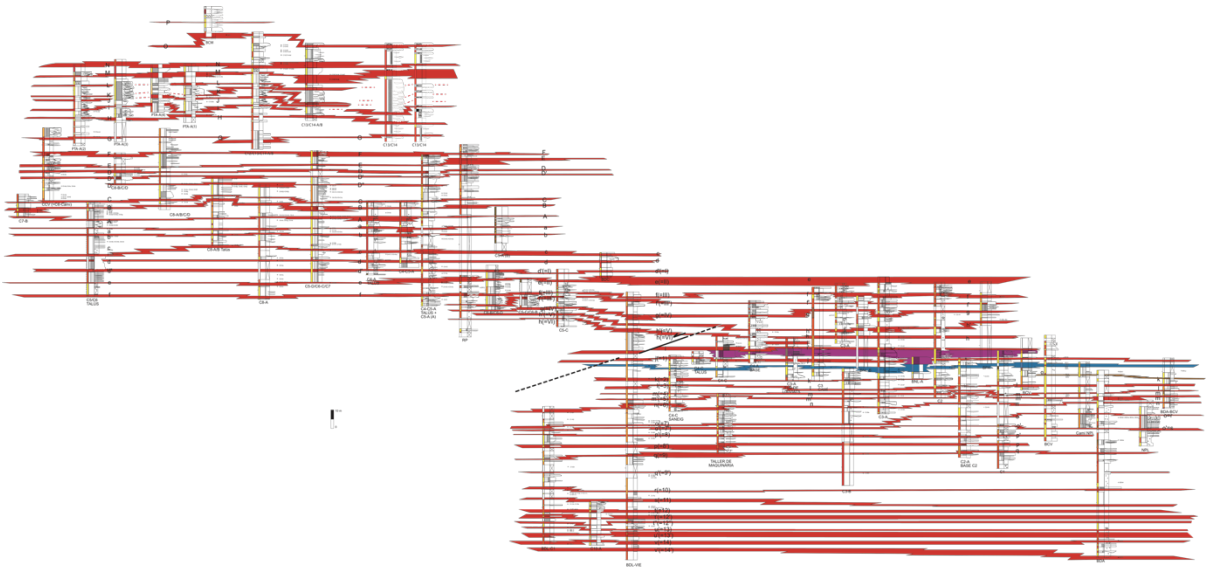

SOM Figure S4. (The source image is provided separately in much higher resolution as a PDF file). Detailed lithostratigraphic panel showing the correlation between the 51 local sections sampled at Abocador de Can Mata, updated after Alba et al. (2017). The used correlation levels and the defined fossil localities (SOM Table S4) are shown. Correlation levels are denoted by red subhorizontal stripes that cross different sections (except for level α, depicted in blue). Each section is represented by a column depicting the following details (from left to right): stratigraphic thickness (in meters, all to the same scale); approximate coloration (streaked patterns represent mixed colorations); approximate granulometric composition (white = mudstones; light gray = sandstones; darker gray = conglomerates); and rock hardness and type of contact with overlying and underlying strata (see also the symbols' legend within the figure).

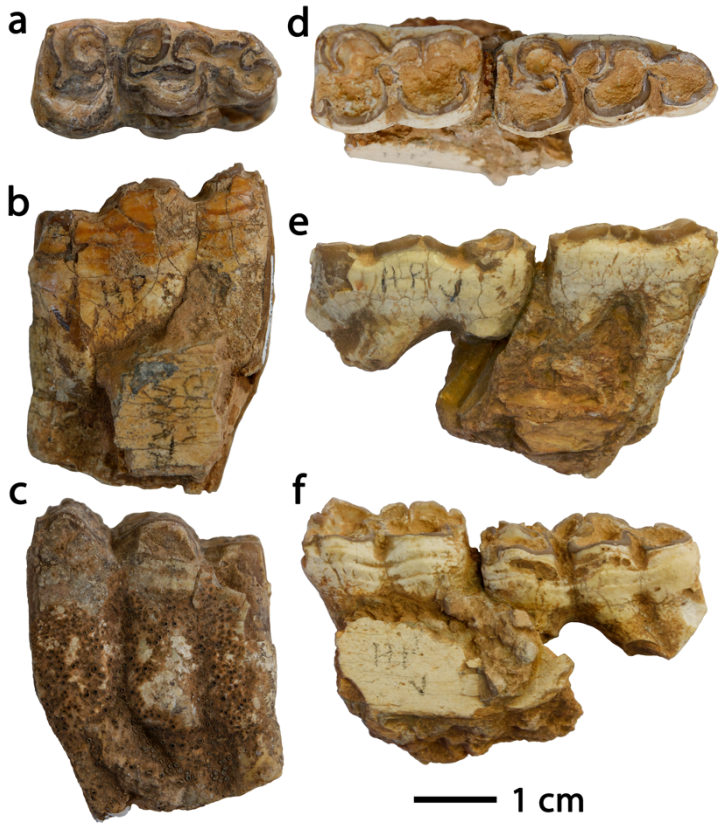

SOM Figure S5. Remains of *Hippotherium* sp. from the area of els Hostalets de Pierola: a–c) IPS124307, left M_3 in occlusal (a), lingual (b), and buccal (c) views; d–f) IPS30897, left M_2–M_3 in occlusal (d), lingual (e), and buccal (f) views. IPS30897 comes in all probability from the locality of Can Mata 3.

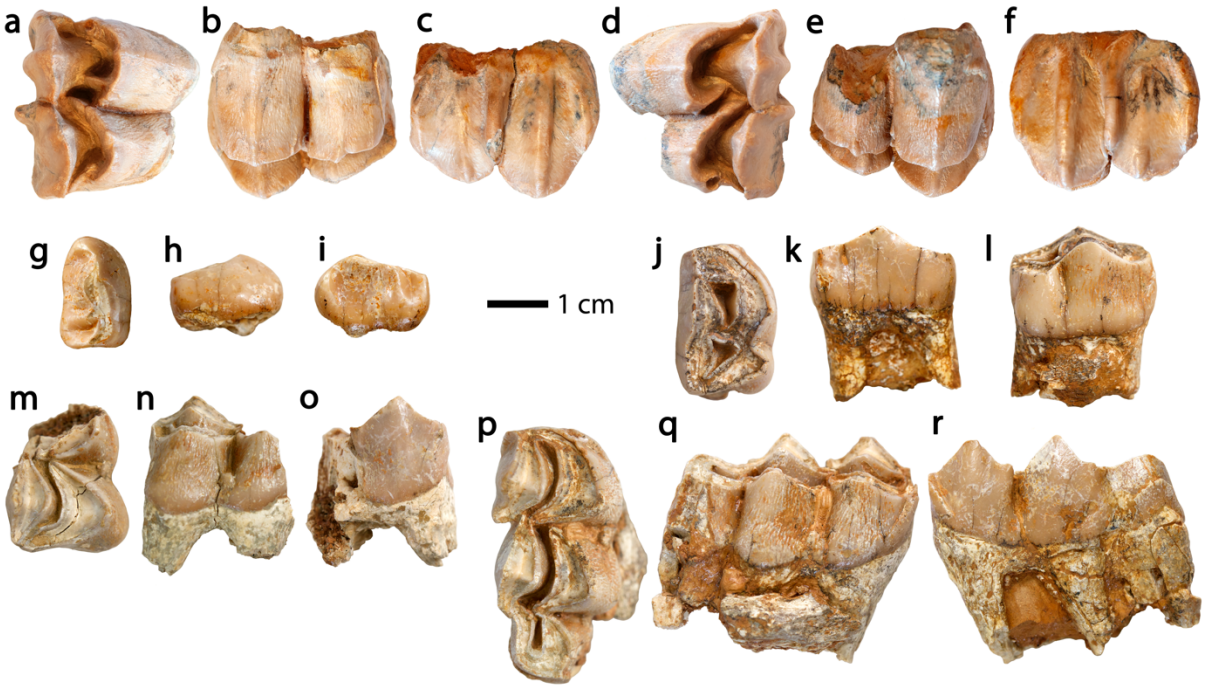

SOM Figure S6. Dental remains of Giraffidae indet. from els Hostalets de Pierola. a–f) IPS121859, right (a–c) and left (d–f) M^3 germs from ACM/C13/C14-A (meter 283 of the ACM composite section; interpolated age of 11.11 Ma), in occlusal (a, d), lingual (b, e), and buccal (c, f) views. g–i) IPS88203, right P_2 from ECM/VCE-Bb (~10.9 Ma), in occlusal (g), buccal (h), and lingual (i) views. j–r) IPS88086, right P_4 (j–l), partial right M_1 (m–o), and right M_3 (p–r) from ECM/VCE-Bb (~10.9 Ma), in occlusal (j, m, p), buccal (k, n, q), and lingual (l, o, r) views.

SOM Table S1

Magnetic susceptibility (*10^{-06} SI) after each demagnetization step (in °C).

Sample	sus ini	100	200	250	300	350	400	440	480	520	550	580	610	630
BCM-1B	865	870	875	870	880	930	935	1015	955	905	820	—	—	—
BCM-2A	245	240	240	240	295	385	385	480	360	230	240	220	210	200
BCM3B	595	595	600	585	630	690	695	760	725	240	570	550	535	515
BCM4C	255	255	250	255	305	395	400	500	495	475	315	280	265	—
BCM-5B	560	560	560	550	570	620	625	760	775	310	725	625	590	490
BCM-6A	230	230	230	225	240	295	330	400	410	305	395	310	290	275
PTA-1.1A	430	430	430	420	420	430	455	470	455	845	375	—	—	—
PTA-2.1A	265	265	260	260	260	260	300	300	260	260	215	210	205	200
PTA-3.1A	250	250	250	250	245	245	340	355	285	605	220	215	215	205
PTA-4.1A	495	495	495	500	500	490	615	630	550	390	440	430	420	410
PTA-5.1A	330	330	330	330	330	330	435	450	370	765	290	280	275	265
PTA-6.1A	320	315	315	315	320	320	460	475	390	400	280	270	265	255
C13-1A	250	250	255	250	245	255	300	340	370	300	260	250	245	—
C13-2A	365	365	365	365	365	395	465	520	505	385	345	320	305	—
C13-3C	310	305	310	300	310	350	400	450	400	310	285	265	250	250
C13-4A	185	185	185	185	200	260	330	365	270	205	185	—	—	—
C13-5C	235	235	235	235	260	340	415	460	385	290	265	255	255	—
C13-6A	360	360	360	355	365	415	460	485	415	345	325	310	300	—
C13-7C	260	255	260	255	275	345	415	450	365	275	250	230	220	—
C13-8A	220	215	220	215	230	305	375	415	350	245	215	195	185	185
C13-9A	275	275	275	270	270	310	365	415	375	300	280	—	—	—
C13-10B	255	255	255	255	255	295	370	470	455	330	275	—	—	—
C13-11B	270	270	270	270	270	295	370	420	520	440	315	260	240	245
C13-12A	245	240	245	245	240	250	290	300	405	425	330	—	—	—
C13-13A.A	400	400	400	405	395	395	405	435	470	490	445	—	—	—
C13-13B	430	425	430	430	430	420	430	495	510	525	530	380	360	360
C13-14A.B	220	220	220	220	220	220	225	265	295	345	380	230	215	220
C13-14B-A	205	205	205	200	205	200	205	235	255	300	330	225	210	215
C13-15A	430	430	430	430	420	430	465	510	550	485	405	395	375	360
C13-16A	285	285	290	285	285	315	390	465	470	330	285	290	275	240
C13-17B	280	280	280	275	285	330	395	455	400	295	265	270	270	225
C13-18A	290	290	290	285	290	330	365	395	345	270	245	250	250	215
C13-19B	355	355	355	345	360	425	495	545	450	350	315	320	—	—

C13-20A	510	515	515	505	515	565	610	640	580	500	475	460	—	—
C13-21A	400	400	400	395	410	470	530	575	510	400	370	350	340	325
C13-22B	625	625	625	615	625	685	740	785	685	610	580	550	540	525
C13-23B	480	485	485	480	485	535	595	645	640	530	475	460	435	420
C13-24A	260	260	260	255	270	335	420	505	500	360	290	245	—	—
C13-25B	310	310	315	310	315	360	440	515	535	415	325	275	—	—
C13-26B	275	275	275	275	275	305	395	480	530	470	340	275	255	250
C13-27B	370	370	370	370	360	370	400	440	475	475	380	305	290	285
C13-28A	395	395	400	395	385	390	405	430	455	480	445	340	—	—
C13-29C	365	365	365	365	355	355	385	440	485	540	535	350	310	300
C13-30A	450	450	450	455	450	445	455	495	520	570	585	—	—	—
C13-31A	795	795	800	775	785	790	845	850	850	895	915	905	—	—
C13-32A	880	880	895	860	865	885	950	955	955	960	975	995	—	—

Abbreviation: sus ini = initial susceptibility; BCM = Bretxa de Can Mata [Can Mata Breccia]; C1–C13 = Cel·la 13 [Cells 13]; PTA = Préstec de Terres de l'Abocador [Landfill Earth Loan].

SOM Table S2

Directions of the characteristic components in geographic and stratigraphic coordinates calculated for each individual sample.

Sample	Level	Dg	Ig	Ds	Is	VGPlat	int	MAD	Q	T range
PTA1-1A	0.5	242.8	06.1	242.8	-05.5	-17.7	229.6	7.6	2	250–480
C13-1A	2.5	204.7	-62.5	178.4	-65.2	-71.9	260.3	6.9	2	300–520
PTA2-1A	5.0	203.2	06.3	204.0	01.1	-40.2	200.8	9.0	1	350–630
C13-2A	6.5	183.5	-39.1	172.9	-38.7	-69.9	732.4	3.2	2	250–480
C13-3C	7.5	167.9	-60.8	148.2	-55.8	-81.0	509.0	3.7	1	300–580
PTA3-1A	7.5	167.5	-55.0	151.5	-50.3	-78.3	202.0	14.3	2	* 350–550
C13-4A	9.5	230.2	-50.8	216.3	-59.8	-49.1	118.2	11.9	2	* 300–440
C13-5C	10.5	166.4	-37.5	157.6	-33.4	-66.1	297.5	6.4	2	250–520
C13-6C	11.5	177.9	-30.9	170.3	-29.5	-64.6	292.0	9.2	2	250–480
C13-7C	13.0	159.8	-46.0	148.8	-40.3	-68.0	289.7	4.6	1	250–520
C13-8A	14.0	163.9	-40.3	154.4	-35.6	-66.7	641.5	8.0	2	250–520
PTA4-1A	14.0	194.6	-45.8	180.9	-47.5	-71.0	3136.5	2.8	1	300–580
C13-9A	15.5	225.0	04.3	224.9	-04.9	-30.0	61.0	20.5	3	* 250–520
C13-10B	16.5	090.4	56.3	090.5	69.3	23.4	98.5	8.4	3	300–440
C13-11B	17.5	265.3	74.3	267.4	61.3	33.6	180.7	9.9	3	300–480
C13-12A	18.5	054.6	25.2	049.9	35.5	34.9	166.6	20.5	3	250–400
C13-13B	20.0	010.3	58.7	348.8	58.5	81.8	1334.5	4.7	1	250–580
PTA5-1A	20.5	035.5	58.8	013.4	64.2	63.2	1057.3	2.7	1	400–610
C13-14A	21.0	009.0	54.2	350.9	54.1	79.8	444.8	5.1	1	300–550
C13-15A	23.0	009.6	62.2	345.0	61.6	82.8	1808.0	4.4	1	300–580
C13-16A	27.5	017.7	42.5	005.5	45.1	67.2	421.8	6.0	1	300–550
C13-17B	30.0	026.8	17.4	022.5	22.8	49.4	724.7	2.8	1	250–520
PTA6-1A	30.5	155.9	-27.2	150.6	-21.3	-55.4	535.1	6.3	1	300–580
C13-18A	31.0	222.0	-47.9	208.4	-55.4	-53.8	434.3	6.4	2	300–550
C13-19B	34.0	227.3	-52.8	211.8	-61.1	-52.0	951.1	3.3	1	300–550
C13-20A	39.0	213.5	-31.8	205.6	-38.2	-52.1	1191.0	3.7	1	250–480
C13-21A	46.0	215.0	-39.8	204.4	-46.3	-55.0	243.4	7.2	2	250–480
C13-22B	47.5	207.8	-41.3	196.2	-46.2	-60.5	1624.0	4.6	1	250–520
C13-23B	48.0	192.7	-34.3	183.5	-36.1	-64.5	539.9	6.7	2	* 350–610
C13-24A	50.0	218.8	-27.4	212.3	-35.0	-46.8	138.3	21.3	2	250–520
C13-25B	50.5	265.8	-48.7	264.2	-61.6	-22.2	224.1	12.1	3	250–440
C13-26B	51.5	308.5	31.0	304.8	20.5	39.5	305.8	9.2	1	300–580

C13-27B	53.0	021.3	50.0	005.2	53.0	69.6	2583.0	1.4	1	250–550
C13-28a	56.0	235.6	25.4	238.2	14.5	-17.7	105.0	8.1	3	300–440
C13-29C	58.5	202.2	-30.7	194.2	-34.7	-58.2	455.8	8.3	2	400–550
C13-30A	59.0	199.4	-43.4	186.7	-46.3	-66.9	168.8	22.5	3	250–440
BCM-1B	62.0	147.6	-20.3	144.4	-12.9	-47.6	140.0	34.9	2	* 350–520
C13-32A	62.0	222.9	-46.8	210.0	-54.6	-52.6	678.7	18.4	3	250–440
BCM-2A	67.0	303.0	64.5	292.9	52.9	49.8	146.3	16.2	2	520–580
BCM-3B	70.0	206.4	-48.5	191.3	-52.7	-65.3	978.2	5.0	1	350–580
BCM-4C	72.0	341.4	37.2	333.1	32.1	63.6	97.1	11.5	3	250–400
BCM-5B	75.0	012.6	53.1	354.9	53.9	77.1	2162.6	2.8	1	300–580
BCM-6A	77.0	018.1	56.6	018.1	56.6	75.2	370.0	3.8	2	350–580

Abbreviations: level = stratigraphic position (m); Dg = declination in geographic coordinates; Ig = inclination in geographic coordinates; Ds = declination in stratigraphic coordinates; Is = inclination in stratigraphic coordinates; VGPlat = latitude of the virtual geomagnetic pole; int = intensity (E 10^{-6} A/m); MAD = maximum angular deviation; Q = quality; T range = temperature interval selected to calculate the characteristic component forced to origin, unless specified by *, which means not forced to origin; BCM = Bretxa de Can Mata [Can Mata Breccia]; C1–C13 = Cel·la 13 [Cells 13]; PTA = Préstec de Terres de l'Abocador [Landfill Earth Loan].

SOM Table S3

Mean directions and their Fisher statistics parameters. See also SOM Figure S2.

		Geographic coordinates				Bedding corrected coordinates			
Polarity	*n*	Dg	Ig	k	α95	Dg	Ig	k	α95
Normal	11	006.9	53.6	12.3	13.6	351.0	53.2	11.8	13.9
Reverse	23	194.6	-40.7	9.1	10.6	183.1	-42.7	9.1	10.6
All to normal	34	012.4	45.0	9.6	8.4	359.6	46.3	9.6	8.4

Abbreviations: *n* = number of samples; Dg = declination in geographic coordinates; Ig = inclination in geographic coordinates; k = precision parameter; α95 = alpha 95.

SOM Table S4

List of fossil localities at Abocador de Can Mata (ACM), in chronological order from youngest to oldest (top to bottom), updated from Alba et al. (2017). Their stratigraphic position within the composite series, their correlated geomagnetic subchron, and their interpolated and estimated ages are provided. Each locality is designated by the ACM acronym, followed by a slash, the acronym of each sector (named after the various cells and other structures of the landfill), sometimes a slash and an uppercase letter denoting a division in subsectors, and a few additional letters and/or numbers designating the particular locality. Primate-bearing localities are bolded. Alternative locality names are given within parentheses for the sake of completeness in relation to field reports and museum inventories. See SOM Table S5 for a list of ACM subsectors and their age ranges.

Locality	Stratigraphic position (m)	Subchron	Interpolated age (Ma)	Estimated age (Ma)
CM3[a]	292	C5r.1r	11.06	11.1
CM1[a]	284	C5r.1r	11.11	11.1
ACM/C13-A2[a]	279	C5r.1r	11.14	11.1
ACM/C13-A3[a]	278	C5r.1r	11.14	11.1
ACM/C13-A5 (=ACM/C13/C14-Ag)[a]	276	C5r.1n	11.16	11.2
ACM/C13/C14-Af[a]	275	C5r.1n	11.17	11.2
ACM/C13/C14-Ad[a]	274	C5r.1n	11.18	11.2
ACM/C13-A6 (=ACM/C13/C14-Ah)	270	C5r.2r [2/2]	11.20	11.2
ACM/C14-Ba	269	C5r.2r [2/2]	11.20	11.2
ACM/PTA-A1 (=ACM/PTA-Ac)	268	C5r.2r [2/2]	11.21	11.2
ACM/PTA-A2	268	C5r.2r [2/2]	11.21	11.2

ACM/C14-Bb	266	C5r.2r [2/2]	11.21	11.2
ACM/C14-B1	266	C5r.2r [2/2]	11.21	11.2
ACM/C13/C14-Aa	264	C5r.2r [2/2]	11.22	11.2
ACM/C13-A1 (=ACM/C13-Ab)	263	C5r.2r [2/2]	11.22	11.2
ACM/C13-A7	263	C5r.2r [2/2]	11.22	11.2
ACM/C13/C14-Ai	263	C5r.2r [2/2]	11.22	11.2
ACM/C13-Aa	262	C5r.2r [2/2]	11.23	11.2
ACM/C13/C14-Ab	262	C5r.2r [2/2]	11.23	11.2
ACM/C13/C14-Aj	260	C5r.2r [2/2]	11.23	11.2
ACM/C13-A4 (=ACM/C13/C14-Ae)	254	C5r.2r [2/2]	11.25	11.3
ACM/C12-A1(=ACM/C12-Ab)	252	C5r.2r [2/2]	11.26	11.3
ACM/PTA-Aa	251	C5r.2r-1	11.26	11.3
ACM/C12-Ba	248	C5r.2r-1	11.28	11.3
ACM/PTA-Ab	245	C5r.2r-1	11.29	11.3
ACM/PTA-Ad	243	C5r.2r-1	11.29	11.3
ACM/C13/C14-Ac	241	C5r.2r-1	11.30	11.3
ACM/PTA-A3 (=ACM/PTA-Ae)	232	C5r.2r [1/2]	11.36	11.4
ACM/C12-Aa	230	C5r.2r [1/2]	11.38	11.4
ACM/CCV1	221	C5r.2r [1/2]	11.45	11.5
ACM/C8-B1	212	C5r.2r [1/2]	11.53	11.5
ACM/C6-Cc	212	C5r.2r [1/2]	11.53	11.5

ACM/C8-Ca	211	C5r.2r [1/2]	11.54	11.5
ACM/C8-Bb	211	C5r.2r [1/2]	11.54	11.5
ACM/C6-Ca	211	C5r.2r [1/2]	11.54	11.5
ACM/C8-Bd	210	C5r.2r [1/2]	11.54	11.5
ACM/C8-Be	210	C5r.2r [1/2]	11.54	11.5
ACM/C6-Aa	209	C5r.2r [1/2]	11.55	11.6
ACM/C8-Ba	209	C5r.2r [1/2]	11.55	11.6
ACM/C8-Bi	209	C5r.2r [1/2]	11.55	11.6
ACM/C8-Br	207	C5r.2r [1/2]	11.57	11.6
ACM/C8-Bc	204	C5r.2n	11.59	11.6
ACM/C8-Ae	204	C5r.2n	11.59	11.6
ACM/C8-Bm	204	C5r.2n	11.59	11.6
ACM/C8-Bq	204	C5r.2n	11.59	11.6
ACM/C5-Ad	203	C5r.2n	11.59	11.6
ACM/C6-Ac	203	C5r.2n	11.59	11.6
ACM/C6-Ab	203	C5r.2n	11.59	11.6
ACM/C6-C1	203	C5r.2n	11.59	11.6
ACM/C8-Bn	203	C5r.2n	11.59	11.6
ACM/C8-Bo	203	C5r.2n	11.59	11.6
ACM/C8-Bh	203	C5r.2n	11.59	11.6
ACM/C8-Bs	203	C5r.2n	11.59	11.6

ACM/C6-C2	202	C5r.2n	11.60	11.6
ACM/C8-B3 (=ACM/C8-Bk)	202	C5r.2n	11.60	11.6
ACM/C8-Bp	202	C5r.2n	11.60	11.6
ACM/C8-Bv	202	C5r.2n	11.60	11.6
ACM/C8-By	202	C5r.2n	11.60	11.6
ACM/C8-Bf	201	C5r.2n	11.60	11.6
ACM/C8-Ac	201	C5r.2n	11.60	11.6
ACM/C8-Ad	201	C5r.2n	11.60	11.6
ACM/C6-C4	201	C5r.2n	11.60	11.6
ACM/C8-Bg	200	C5r.2n	11.60	11.6
ACM/C6-C3 (=ACM/C6-Cd)	200	C5r.2n	11.60	11.6
ACM/C8-B2 (=ACM/C8-Bj)	200	C5r.2n	11.60	11.6
ACM/C8-Ab	198	C5r.2n	11.61	11.6
ACM/C6-Ad	198	C5r.2n	11.61	11.6
ACM/C5-Ac	198	C5r.2n	11.61	11.6
ACM/C6-C5 (=ACM/C6-Ce)	197	C5r.2n	11.61	11.6
ACM/C6-A2	197	C5r.2n	11.61	11.6
ACM/C6-A1	197	C5r.2n	11.61	11.6
ACM/C8-Bt	197	C5r.2n	11.61	11.6
ACM/C8-Bd'	197	C5r.2n	11.61	11.6
ACM/C5-Dc	196	C5r.2n	11.61	11.6

ACM/C8-Aj	195	C5r.2n	11.61	11.6
ACM/C8-A4	194	C5r.2n	11.62	11.6
ACM/C5-A1 (=ACM/C5-Aa)	194	C5r.2n	11.62	11.6
ACM/C8-Bl	194	C5r.2n	11.62	11.6
ACM/C8-B4 (=ACM/C8-Bw)	194	C5r.2n	11.62	11.6
ACM/C8-Bx	192	C5r.2n	11.62	11.6
ACM/C6-Cb	192	C5r.2n	11.62	11.6
ACM/C4-Ad	192	C5r.2n	11.62	11.6
ACM/C6-Ah	191	C5r.2n	11.62	11.6
ACM/C7-Ba	190	C5r.2n	11.63	11.6
ACM/C6-A4	190	C5r.2n	11.63	11.6
ACM/C5-Db	189	C5r.2n	11.63	11.6
ACM/C6-Af	189	C5r.2n	11.63	11.6
ACM/C5-Dm	188	C5r.2n	11.63	11.6
ACM/C5-D1 (=ACM/C5-Da)	188	C5r.2n	11.63	11.6
ACM/C4-Aa	188	C5r.2n	11.63	11.6
ACM/C5-Dg	187	C5r.2n	11.63	11.6
ACM/C5-D2 (=ACM/C5-De)	187	C5r.2n	11.63	11.6
ACM/C8-A3 (=ACM/C8-Ah)	187	C5r.2n	11.63	11.6
ACM/C8-Ai	187	C5r.2n	11.63	11.6
ACM/C8-A1	186	C5r.2n	11.64	11.6

ACM/C5-Dl	186	C5r.2n	11.64	11.6
ACM/C5-Dk	186	C5r.2n	11.64	11.6
ACM/C7-Aa	186	C5r.2n	11.64	11.6
ACM/C8-A2 (=ACM/C8-Aa)	185	C5r.2n	11.64	11.6
ACM/C7-Ab	185	C5r.2n	11.64	11.6
ACM/C8-Ak	185	C5r.2n	11.64	11.6
ACM/C8-Af	185	C5r.2n	11.64	11.6
ACM/C8-Ag	185	C5r.2n	11.64	11.6
ACM/C6-A5 (=ACM/C6-Ag)	184	C5r.2n	11.64	11.6
ACM/C5-D3	183	C5r.2n	11.64	11.6
ACM/C5-Dd	183	C5r.2n	11.64	11.6
ACM/C6-Ai	183	C5r.2n	11.64	11.6
ACM/C5-D4 (=ACM/C5-Df)	182	C5r.2n	11.65	11.6
ACM/C5-A4 (=ACM/C5-Ab)	181	C5r.2n	11.65	11.6
ACM/C8-Am	180	C5r.2n	11.65	11.7
ACM/C7-Bc	180	C5r.2n	11.65	11.7
ACM/C6-Ae	180	C5r.2n	11.65	11.7
ACM/C7-Ca	179	C5r.2n	11.65	11.7
ACM/C5-A7	179	C5r.2n	11.65	11.7
ACM/C8-B*	178.5	C5r.2n	11.65	11.7
ACM/C5-D7 (=ACM/C5-Dn)	178	C5r.2n	11.65	11.7

ACM/C5-A3	178	C5r.2n	11.65	11.7
ACM/C8-Bu	176	C5r.3r	11.66	11.7
ACM/C8-Ba'	176	C5r.3r	11.66	11.7
ACM/C8-Bc'	176	C5r.3r	11.66	11.7
ACM/C5-A5 (=ACM/C5-Ae)	174	C5r.3r	11.67	11.7
ACM/C6-A3	173	C5r.3r	11.67	11.7
ACM/C5-A6 (=ACM/C5-Af)	173	C5r.3r	11.67	11.7
ACM/C7-Bb	172	C5r.3r	11.68	11.7
ACM/C7-A1	171	C5r.3r	11.68	11.7
ACM/C7-A2	171	C5r.3r	11.68	11.7
ACM/C8-Bb'	171	C5r.3r	11.68	11.7
ACM/C8-Be'	171	C5r.3r	11.68	11.7
ACM/C8-Ar	170	C5r.3r	11.69	11.7
ACM/C8-Al	170	C5r.3r	11.69	11.7
ACM/C7-Bd	168	C5r.3r	11.70	11.7
ACM/C8-Bz	168	C5r.3r	11.70	11.7
ACM/C6-Aj	167	C5r.3r	11.70	11.7
ACM/C4-A1 (=ACM/C4-Ae)	166	C5r.3r	11.70	11.7
ACM/C5-D5 (=ACM/C5-Dh)	166	C5r.3r	11.70	11.7
ACM/C5-Di	165	C5r.3r	11.71	11.7
ACM/C8-As	164	C5r.3r	11.71	11.7

ACM/C4-Ac	163	C5r.3r	11.72	11.7
ACM/C8-Ap	162	C5r.3r	11.72	11.7
ACM/C8-Aq	160	C5r.3r	11.73	11.7
ACM/C4-A3	159	C5r.3r	11.73	11.7
ACM/C5-Dj	158	C5r.3r	11.74	11.7
ACM/C6-Ak	157	C5r.3r	11.74	11.7
ACM/C4-Ab	157	C5r.3r	11.74	11.7
ACM/C5-Ag	155	C5r.3r	11.75	11.8
ACM/C8-Av	154	C5r.3r	11.75	11.8
ACM/C8-Ao	153	C5r.3r	11.76	11.8
ACM/C4-A4	151	C5r.3r	11.77	11.8
ACM/C8-At	151	C5r.3r	11.77	11.8
ACM/C8-Au	151	C5r.3r	11.77	11.8
ACM/C5-D6	150	C5r.3r	11.77	11.8
ACM/C6-Bc	150	C5r.3r	11.77	11.8
ACM/C5-A8 (=ACM/C5-Ah)	150	C5r.3r	11.77	11.8
ACM/C6-Bb	149	C5r.3r	11.78	11.8
ACM/C6-Ba	148	C5r.3r	11.78	11.8
ACM/C5-A9 (=ACM/C5-Ai)	148	C5r.3r	11.78	11.8
ACM/C8-An	148	C5r.3r	11.78	11.8
ACM/RP2	148	C5r.3r	11.78	11.8

ACM/C6-Bd	146	C5r.3r	11.79	11.8
ACM/C5-C2 (=ACM/C5-Cb)	146	C5r.3r	11.79	11.8
ACM/C5-C1 (=ACM/C5-Ca)	146	C5r.3r	11.79	11.8
ACM/C4-Cb	145	C5r.3r	11.79	11.8
ACM/BPAa	143	C5r.3r	11.80	11.8
ACM/C4-Cc	142	C5r.3r	11.80	11.8
ACM/C4-C1 (=ACM/C4-Ca)	141	C5r.3r	11.81	11.8
ACM/C4-Af	141	C5r.3r	11.81	11.8
ACM/C5-Cd	137	C5r.3r	11.83	11.8
ACM/C3-AT	134	C5r.3r	11.84	11.8
ACM/C3-A1	133	C5r.3r	11.84	11.8
ACM/C2-A1	133	C5r.3r	11.84	11.8
ACM/C5-C4 (=ACM/C5-Ce)	133	C5r.3r	11.84	11.8
ACM/C5-Cf	133	C5r.3r	11.84	11.8
ACM/BNL-Ba	130	C5r.3r	11.86	11.9
ACM/C5-C3 (=ACM/C5-Cc)	129	C5r.3r	11.86	11.9
ACM/C4-Cd	128	C5r.3r	11.86	11.9
ACM/C3-Aa	126	C5r.3r	11.87	11.9
ACM/C3-A2	126	C5r.3r	11.87	11.9
ACM/C3-Ak	125	C5r.3r	11.88	11.9
ACM/C3-Af	125	C5r.3r	11.88	11.9

ACM/C3-Ae	125	C5r.3r	11.88	11.9
ACM/C4-Ap	124	C5r.3r	11.88	11.9
ACM/C3-A4	121	C5r.3r	11.89	11.9
ACM/C4-C2 (=ACM/C4-Ce)	120	C5r.3r	11.90	11.9
ACM/C3-A5 (=ACM/C3-Ac)	120	C5r.3r	11.90	11.9
ACM/C3-Ah	119	C5r.3r	11.90	11.9
ACM/C4-C3	118	C5r.3r	11.91	11.9
ACM/BCV5	117	C5r.3r	11.91	11.9
ACM/C4-Cf	116	C5r.3r	11.91	11.9
ACM/C3-A3	116	C5r.3r	11.91	11.9
ACM/C3-Ab	114	C5r.3r	11.92	11.9
ACM/C4-Cg	110	C5r.3r	11.94	11.9
ACM/C3-Az	110	C5r.3r	11.94	11.9
ACM/C3-A6 (=ACM/C3-Ad)	110	C5r.3r	11.94	11.9
ACM/BCV4	110	C5r.3r	11.94	11.9
ACM/VIE-C1	109	C5r.3r	11.94	11.9
ACM/C4-Cp	108	C5r.3r	11.95	11.9
ACM/VIE-C2	107	C5r.3r	11.95	12.0
ACM/BCV1 (=ACM/BDA-SW2, ACM/BDA-SW3)	105	C5r.3r	11.96	12.0
ACM/C2-A2	105	C5r.3r	11.96	12.0
ACM/C2-Aa	105	C5r.3r	11.96	12.0

ACM/C3-Ag	104	C5r.3r	11.97	12.0
ACM/C3-Aj	104	C5r.3r	11.97	12.0
ACM/NPLa	103	C5r.3r	11.97	12.0
ACM/BDA1	102	C5r.3r	11.97	12.0
ACM/C3-Ap	102	C5r.3r	11.97	12.0
ACM/BCV3 (=ACM/BDA-SW4)	101	C5r.3r	11.98	12.0
ACM/C3-Aq	100	C5r.3r	11.98	12.0
ACM/C2-A3	100	C5r.3r	11.98	12.0
ACM/C3-Al	98	C5r.3r	11.99	12.0
ACM/C3-An	98	C5r.3r	11.99	12.0
ACM/VIE-C3	98	C5r.3r	11.99	12.0
ACM/C3-A7	95	C5r.3r	12.00	12.0
ACM/VIE-C4	95	C5r.3r	12.00	12.0
ACM/BCV2 (=ACM/BDA-SW1)	90	C5r.3r	12.02	12.0
ACM/C3-Ai	89	C5r.3r	12.03	12.0
ACM/BDA2	88	C5r.3r	12.03	12.0
ACM/BDA7 (=ACM/BDAb)	87	C5r.3r	12.04	12.0
ACM/C2-A4	83	C5An.1n	12.06	12.1
ACM/C3-B2 (=ACM/C3-Bb)	83	C5An.1n	12.06	12.1
ACM/C3-Am	82	C5An.1n	12.07	12.1
ACM/C3-Ba	80	C5An.1n	12.08	12.1

ACM/C1-A1	80	C5An.1n	12.08	12.1
ACM/BDA8 (=ACM/BDAa, ACM/BDAc)	77	C5An.1n	12.11	12.1
ACM/BDA3	77	C5An.1n	12.11	12.1
ACM/C1-A2	76	C5An.1n	12.11	12.1
ACM/C2-Ba	75	C5An.1n	12.12	12.1
ACM/C2-B1	75	C5An.1n	12.12	12.1
ACM/C2-Bb	75	C5An.1n	12.12	12.1
ACM/C2-B2	73	C5An.1n	12.14	12.1
ACM/C1-A3	72	C5An.1n	12.15	12.1
ACM/C1-A5	70	C5An.1n	12.16	12.2
ACM/C1-A4	70	C5An.1n	12.16	12.2
ACM/C2-B3	69	C5An.1n	12.17	12.2
ACM/C3-Bc	67	C5An.1r	12.18	12.2
ACM/C2-Bc	66	C5An.1r	12.19	12.2
ACM/BDAd	65	C5An.1r	12.19	12.2
ACM/C3-Bd	58	C5An.1r	12.22	12.2
ACM/C1-E4	51	C5An.1r	12.25	12.3
ACM/C3-B3	47	C5An.2n	12.27	12.3
ACM/C1-E10	46	C5An.2n	12.28	12.3
ACM/C1-E9 (=ACM/C1-Ef)	45	C5An.2n	12.29	12.3
ACM/BDA4	42	C5An.2n	12.31	12.3

ACM/C1-C1	39	C5An.2n	12.32	12.3
ACM/C1-Ed	38	C5An.2n	12.33	12.3
ACM/C1-Ea	38	C5An.2n	12.33	12.3
ACM/C1-E6	38	C5An.2n	12.33	12.3
ACM/C1-Eb	36	C5An.2n	12.34	12.3
ACM/C1-E5	36	C5An.2n	12.30	12.3
ACM/C1-E3	36	C5An.2n	12.30	12.3
ACM/C1-Fa	35	C5An.2n	12.35	12.4
ACM/C1-C3	34	C5An.2n	12.36	12.4
ACM/C1-E*	~34–46	C5An.2n	12.36–12.28	12.4–12.3
ACM/C1-E2	32	C5An.2n	12.37	12.4
ACM/C1-C4	30	C5An.2n	12.38	12.4
ACM/C1-Ee	30	C5An.2n	12.30	12.4
ACM/C1-E7+8 (=ACM/C1-Ec)	29	C5An.2n	12.39	12.4
ACM/VIE-E1 (=ACM/VIE-Ea)	29	C5An.2n	12.39	12.4
ACM/C1-E1	28	C5An.2n	12.40	12.4
ACM/C1-ET2	26	C5An.2n	12.41	12.4
ACM/C1-ET	26	C5An.2n	12.41	12.4
ACM/C10-A1	25	C5An.2n	12.42	12.4
ACM/C1-Ex	25	C5An.2n	12.42	12.4
ACM/C1-D1	20	C5An.2n	12.45	12.4

ACM/C9-A1	19	C5An.2n	12.45	12.5
ACM/BDL3	16	C5An.2n	12.47	12.5
ACM/BDL2	15,5	C5Ar.1r	12.48	12.5
ACM/BDAe	~11–77	C5Ar.1r–C5An.1n	12.51–12.11	12.5–12.1
ACM/BDA6	11	C5Ar.1r	12.51	12.5
ACM/BDL1	9	C5Ar.1r	12.52	12.5
ACM/BDA5	2	C5Ar.1r	12.56	12.6

Abbreviations: ACM = Abocador de Can Mata [Can Mata Landfill]; BCV = Barranc de Can Vila [Can Vila Ravine]; BDA = Bassa de Decantació d'Aigües Pluvials [Settling Pond of Rainwater]; BDA-SW = Bassa de Decantació d'Aigües Pluvials Sud-Oest [Settling Pond of Rainwater South-West]; BDL = Bassa de Lixiviats [Pond of Leachates]; BNL = Bassa Nova de Lixiviats [New Pond of Leachates]; BPA = Base de la Pila d'Acopi [Base of the Stockpile]; C1–C13 = Cel·les 1–13 [Cells 1–13]; CCV = Camí de Can Vila [Can Vila's Trackway]; CM = Can Mata; NPL= Nova Planta de Lixiviats [New Pond of Leachates]; PTA = Préstec de Terres de l'Abocador [Landfill Earth Loan]; RP = Rasa de Desguàs d'Aigües Pluvials [Rainwater Drainage Ditch]; VIE = Vial Intern d'Explotació [Internal Operating Road].

[a] Vallesian localities according to the earliest appearance of *Hippotherium* in the Vallès-Penedès Basin (Garcés et al., 1996).

SOM Table S5

List of fossiliferous (sub)sectors at Abocador de Can Mata (ACM), in chronological order from youngest to oldest (top to bottom). Their stratigraphic range within the composite series, their correlated geomagnetic subchron(s), and their interpolated and estimated age ranges are provided. Each sector is designated by the ACM acronym, followed by a slash, the acronym of each sector (named after the various cells and other structures of the landfill), and sometimes a slash and an uppercase letter denoting a division in subsectors. Alternative (sub)sector names are given within parentheses for the sake of completeness in relation to field reports and museum inventories. See SOM Table S4 for an updated list of ACM fossil localities.

(Sub)sector	Stratigraphic position (m)	Subchron	Interpolated age (Ma)	Estimated age (Ma)
ACM/C14-B[a]	268–286	C5r.2r [2/2]–C5r.1r	11.21–11.10	11.2–11.1
ACM/PTA-B[a]	268–286	C5r.2r [2/2]–C5r.1r	11.21–11.10	11.2–11.1
ACM/C12-B[a]	245–286	C5r.2r-1–C5r.1r	11.29–11.10	11.3–11.1
ACM/C13-A[a]	238–286	C5r.2r [2/2]–C5r.1r	11.31–11.10	11.3–11.1
ACM/C13/C14-A (=ACM/C14-A)[a]	238–286	C5r.2r [1/2]–C5r.1r	11.31–11.10	11.3–11.1
ACM/PTA-A	224–271	C5r.2r [1/2]–C5r.2r [2/2]	11.43–11.19	11.4–11.2
ACM/C12-A	223–269	C5r.2r [1/2]–C5r.2r [2/2]	11.44–11.20	11.4–11.2
ACM/CCV	195–234	C5r.2n–C5r.2r [1/2]	11.61–11.35	11.6–11.4
ACM/C6-Camí	195–234	C5r.2n–C5r.2r [1/2]	11.61–11.35	11.6–11.4
ACM/RPA-2	72–234	C5An.1n–C5r.2r [1/2]	12.15–11.35	12.2–11.4
ACM/RP	121–225	C5r.3r–C5r.2r [1/2]	11.89–11.42	11.9–11.4
ACM/C6-C	194–222	C5r.2n–C5r.2r [1/2]	11.62–11.45	11.6–11.5
ACM/C8-C	210–221	C5r.2r [1/2]	11.54–11.45	11.5

ACM/C8-B	166–221	C5r.3r–C5r.2r [1/2]	11.70–11.45	11.7–11.5
ACM/VIE-A	166–221	C5r.3r–C5r.2r [1/2]	11.70–11.45	11.7–11.5
ACM/C5-A	138–220	C5r.3r–C5r.2r [1/2]	11.81–11.46	11.8–11.5
ACM/C6-A	143–209	C5r.3r–C5r.2r [1/2]	11.80–11.55	11.8–11.6
ACM/C8-A	141–207	C5r.3r–C5r.2r [1/2]	11.81–11.57	11.8–11.6
ACM/C11-A	141–207	C5r.3r–C5r.2r [1/2]	11.81–11.57	11.8–11.6
ACM/C11-B	141–207	C5r.3r–C5r.2r [1/2]	11.81–11.57	11.8–11.6
ACM/VIE-B	141–207	C5r.3r–C5r.2r [1/2]	11.81–11.57	11.8–11.6
ACM/C5-D	150–200	C5r.3r–C5r.2n	11.77–11.60	11.8–11.6
ACM/C4-A	107–195	C5r.3r–C5r.2n	11.95–11.61	12.0–11.6
ACM/C7-A	168–190	C5r.3r–C5r.2n	11.70–11.63	11.7–11.6
ACM/C7-B	168–185	C5r.3r–C5r.2n	11.70–11.64	11.7–11.6
ACM/C7-C	175–183	C5r.3r–C5r.2n	11.67–11.64	11.7–11.6
ACM/C6-B	136–160	C5r.3r	11.83–11.73	11.8–11.7
ACM/C6-B	136–160	C5r.3r	11.83–11.73	11.8–11.7
ACM/C5-C	126–158	C5r.3r	11.87–11.74	11.9–11.7
ACM/C3-A	79–153	C5An.1n–C5r.3r	12.08–11.76	12.1–11.8
ACM/BPA	106–151	C5r.3r	11.96–11.77	12.0–11.8
ACM/C2-A	55–150	C5An.1r–C5r.3r	12.24–11.77	12.2–11.8
ACM/BNL-B	110–145	C5r.3r	11.94–11.79	11.9–11.8
ACM/BNL-A/B	98–145	C5r.3r	11.99–11.79	12.0–11.8

ACM/VIE-C	88–145	C5r.3r	12.03–11.79	12.0–11.8
ACM/C4-C	80–145	C5An.1n–C5r.3r	12.08–11.79	12.1–11.8
ACM/C4-B	80–142	C5An.1n–C5r.3r	12.08–11.80	12.1–11.8
ACM/C5-B	135–140	C5r.3r	11.83–11.81	11.8
ACM/BCV (=ACM/BDA-SW)	64–122	C5An.1r–C5r.3r	12.20–11.89	12.2–11.9
ACM/C1-A	70–113	C5An.1n–C5r.3r	12.16–11.93	12.2–11.9
ACM/C1-B	50–113	C5An.1r–C5r.3r	12.26–11.93	12.3–11.9
ACM/BNL-A	98–110	C5r.3r	11.99–11.94	12.0–11.9
ACM/C2-Base	55–109	C5An.1r–C5r.3r	12.24–11.94	12.2–11.9
ACM/NPL	62–107	C5An.1r–C5r.3r	12.20–11.95	12.2–12.0
ACM/C3-A/B	79–104	C5An.1n–C5r.3r	12.08–11.97	12.1–12.0
ACM/C3-B	40–104	C5An.2n–C5r.3r	12.32–11.97	12.3–12.0
ACM/BDA	2–102	C5Ar.1r–C5r.3r	12.56–11.97	12.6–12.0
ACM/C2-B	64–78	C5An.1r–C5An.1n	12.20–12.10	12.2–12.1
ACM/C1-E	23–51	C5An.2n–C5An.1r	12.43–12.25	12.4–12,3
ACM/C1-F	33–46	C5An.2n	12.36–12.28	12.4–12.3
ACM/C1-C	28–43	C5An.2n	12.40–12.30	12.4–12.3
ACM/VIE-E	25–35	C5An.2n	12.42–12.35	12.4
ACM/C10-A	8–33	C5Ar.1r–C5An.2n	12.52–12.36	12.5–12.4
ACM/BDL	0–25	C5Ar.1r–C5An.2n	12.58–12.42	12.6–12.4
ACM/C1-D	18–23	C5An.2n	12.46–12.43	12.5–12.4

ACM/C9-A	17–23	C5An.2n	12.47–12.43	12.5–12.4
ACM/VIE-D	17–23	C5An.2n	12.47–12.43	12.5–12.4
ACM/RBL	10–20	C5Ar.1r–C5An.2n	12.51–12.45	12.5

Abbreviations: ACM = Abocador de Can Mata [Can Mata Landfill]; BCV = Barranc de Can Vila [Can Vila Ravine]; BDA = Bassa de Decantació d'Aigües Pluvials [Settling Pond of Rainwater]; BDA-SW = Bassa de Decantació d'Aigües Pluvials Sud-Oest [Settling Pond of Rainwater South-West]; BDL = Bassa de Lixiviats [Pond of Leachates]; BNL = Bassa Nova de Lixiviats [New Pond of Leachates]; BPA = Base de la Pila d'Acopi [Base of the Stockpile]; C1–C13 = Cel·les 1–13 [Cells 1–13]; CCV = Camí de Can Vila [Can Vila's Trackway]; NPL= Nova Planta de Lixiviats [New Pond of Leachates]; PTA = Préstec de Terres de l'Abocador [Landfill Earth Loan]; RBL = Rasa de la Bassa de Lixiviats [Pond of Leachates Ditch]; RP = Rasa de Desguàs d'Aigües Pluvials [Rainwater Drainage Ditch]; RPA-2 = Rasa Perimetral de L'Abocador 2 [Perimetric Ditch of the Landfill 2]; VIE = Vial Intern d'Explotació [Internal Operating Road].

[a] Sectors recording the Aragonian/Vallesian boundary according to the earliest appearance of *Hippotherium* in the Vallès-Penedès Basin (Garcés et al., 1996).

SOM Table S6

List of primate-bearing fossil localities at Abocador de Can Mata (ACM), in chronological order from youngest to oldest (top to bottom), updated from Alba et al. (2017). Their interpolated and estimated ages are provided (for further details, see SOM Table S4).

Locality	Taxon	Interpolated age (Ma)	Estimated age (Ma)
CM1	Dryopithecinae indet.	11.11	11.1
ACM/C8-A4	*Pliobates cataloniae*	11.62	11.6
ACM/C5-D1	*Pliobates cataloniae*, Dryopithecinae indet.	11.63	11.6
ACM/C8-B*	Dryopithecinae indet.	11.65	11.7
ACM/C4-A1	*Pliopithecus canmatensis*	11.70	11.7
ACM/C8-Au	Dryopithecinae indet.	11.77	11.8
ACM/C5-A8	*Pliopithecus canmatensis*	11.77	11.8
ACM/C5-C2	*Pliopithecus canmatensis*	11.79	11.8
ACM/C4-Cb	*Pliopithecus canmatensis*	11.79	11.8
ACM/C5-C4	*Pliopithecus canmatensis*	11.84	11.8
ACM/C5-C3	*Pliopithecus canmatensis*	11.86	11.9
ACM/C3-Ae	*Dryopithecus fontani*	11.88	11.9
ACM/C4-Ap	*Dryopithecus fontani*	11.88	11.9
ACM/BCV5	*Pliopithecus canmatensis*	11.91	11.9
ACM/C3-Az	cf. *Dryopithecus fontani*	11.94	11.9
ACM/BCV4	'*Sivapithecus*' *occidentalis* species inquirenda	11.94	11.9
ACM/C4-Cp	*Anoiapithecus brevirostris*	11.95	11.9

ACM/BCV1	*Pierolapithecus catalaunicus*	11.96	12.0
ACM/C3-Aj	*Anoiapithecus brevirostris*	11.97	12.0
ACM/C3-B2	Pliopithecoidea indet.	12.06	12.1
ACM/C1-E*	*Anoiapithecus brevirostris*	12.36–12.28	12.4–12.3

Abbreviations: See SOM Table S4.

SOM References

Agustí Ballester, J., 1978. El Vallesiense inferior de la Península Ibérica y su fauna de roedores (Mamm.). Acta Geol. Hisp. 13, 137–141.

Agustí Ballester, J., 1980. La asociación de *Hispanomys* y *Cricetodon* (Rodentia, Mammalia) en el Mioceno Superior del Vallès-Penedès (Cataluña, España). Acta Geol. Hisp. 15, 51–60.

Agustí, J., 1981. Roedores miomorfos del Neógeno de Cataluña. Ph.D. Dissertation, Universidad de Barcelona.

Agustí, J., 1999. A critical re-evaluation of the Miocene mammal units in Western Europe: dispersal events and problems of correlation. In: Agustí, J., Rook, L., Andrews, P. (Eds.), The Evolution of Neogene Terrestrial Ecosystems in Europe. Cambridge University Press, Cambridge, pp. 84–112.

Agustí, J., 2015. The biotic environments of the Late Miocene hominids. In: Henke, W., Tattersall, I. (Eds.), Handbook of Paleoanthropology, 2nd ed. Springer, Heidelberg, pp. 1333–1362.

Agustí, J., Gibert, J., 1982. Roedores e insectívoros del Mioceno superior dels Hostalets de Pierola (Vallès-Penedès, Cataluña). Butll. Inf. Inst. Paleontol. Sabadell 14, 19–37.

Agustí, J., Moyà-Solà, S., 1990. Mammal extinctions in the Vallesian (Upper Miocene). Lect. Not. Earth Sci. 30, 425–432.

Agustí, J., Moyà-Solà, S., 1991. Spanish Neogene Mammal succession and its bearing on continental biochronology. Newslett. Stratigr. 25, 91–114.

Agustí, J., Galobart, À., 1998. Noves localitats amb mamífers fòssils en el miocè de la Conca del Vallès-Penedès. Trib. Arqueol. 1996–1997, 9–23.

Agustí, J., Antón, M., 2002. Mammoths, Sabertooths, and Hominids. 65 million Years of Mammalian Evolution in Europe. Columbia University Press, New York.

Agustí, J., Cabrera, L., Moyà-Solà, S., 1985. Sinopsis estratigráfica del Neógeno de la fosa del Vallés-Penedés. Paleontol. Evol. 18, 57–81.

Agustí, J., Cabrera, L., Garcés, M., Parés, J.M., 1997. The Vallesian mammal succession in the Vallès-Penedès basin (northeast Spain): Paleomagnetic calibration and correlation with global events. Palaeogeogr. Palaeoclimatol. Palaeoecol. 133, 149–180.

Agustí, J., Casanovas-Vilar, I., Furió, M., 2005. Rodents, insectivores and chiropterans (Mammalia) from the late Aragonian of Can Missert (Middle Miocene, Vallès-Penedès basin, Spain). Geobios 38, 575–583.

Agustí, J., Cabrera, L., Garcés, M., Krijgsman, W., Oms, O., Parés, J.M., 2001. A calibrated mammal scale for the Neogene of Western Europe. State of the art. Earth Sci. Rev. 52, 247–260.

Alba, D.M., Moyà-Solà, S., Casanovas-Vilar, I., Galindo, J., Robles, J.M., Rotgers, C., Furió, M., Angelone, C., Köhler, M., Garcés, M., Cabrera, L., Almécija, S., Obradó, P., 2006. Los vertebrados fósiles del Abocador de Can Mata (els Hostalets de Pierola, l'Anoia, Cataluña), una sucesión de localidades del Aragoniense superior (MN6 y MN7+8) de la cuenca del Vallès-Penedès. Campañas 2002-2003, 2004 y 2005. Estud. Geol. 62, 295–312.

Alba, D.M., Casanovas-Vilar, I., Robles, J.M., Moyà-Solà, S., 2011. Parada 3. El Aragoniense superior y la transición con el Vallesiense: Can Mata y la exposición paleontological de els Hostalets de Pierola. Paleontol. Evol. Memòria especial 6, 95–109.

Alba, D.M., Carmona, R., Bertó Mengual, J.V., Casanovas-Vilar, I., Furió, M., Garcés, M., Galindo, J., Luján, À.H., 2012. Intervenció paleontològica a l'Ecoparc de Can Mata (els Hostalets de Pierola, conca del Vallès-Penedès). Trib. Arqueol. 2010–2011, 115–130.

Alba, D.M., Casanovas-Vilar, I., Garcés, M., Robles, J.M., 2017. Ten years in the dump: An updated review of the Miocene primate-bearing localities from Abocador de Can Mata (NE Iberian Peninsula). J. Hum. Evol. 102, 12–20.

Alba, D.M., Garcés, M., Casanovas-Vilar, I., Robles, J.M., Pina, M., Moyà-Solà, S., Almécija, S., 2019. Bio- and magnetostratigraphic correlation of the Miocene primate-bearing site of Castell de Barberà to the earliest Vallesian. J. Hum. Evol. 132, 32–46.

Alba, D.M., Gasamans, N., Pons-Monjo, G., Luján, À.H., Robles, J.M., Obradó, P., Casanovas-Vilar, I., 2020. Oldest *Deinotherium proavum* from Europe. J. Vertebr. Paleontol. 40, e1775624.

Alberdi, M.T., 1974. El género *Hipparion* en España. Nuevas formas de Castilla y Andalucía, revisión e historia evolutiva. Instituto Lucas Mallada C.S.I.C., Madrid.

Alberdi, M.T., 1981. El género *Hipparion* en el yacimiento de los Valles de Fuentidueña. Estud. Geol. 37, 425–437.

Alberdi, M.T., López, N., Morales, J., Sesé, C., Soria, D., 1981. Bioestratigrafía y biogeografía de la fauna de mamíferos de los Valles de Fuentidueña. Estud. Geol. 37, 503–511.

Almécija, S., Pina, M., Vinuesa, V., DeMiguel, D., Moyà-Solà, S., Alba, D.M., 2019. Memòria sobre la intervenció paleontològica programada a Creu Conill (Terrassa): Campanyes 2016-2017. Institut Català de Paleontologia Miquel Crusafont, unpublished report.

Álvarez Sierra, M. A., Calvo, J. P., Morales, J., Alonso-Zarza, A., Azanza, B., García Paredes, I., Hernández Fernández, M., van der Meulen, A.J., Peláez-Campomanes, P., Quiralte, V., Salesa, M.J., Sánchez, I.M., Soria, D., 2003. El tránsito Aragoniense-Vallesiense en el área de Daroca-Nombrevilla (Zaragoza, España). Coloquios de Paleontología Vol. Ext. 1, 25–33.

Anquetin, J., Antoine, P.-O., Tassy, P., 2007. Middle Miocene Chalicotheriinae (Mammalia, Perissodactyla) from France, with a discussion on chalicotheriine phylogeny. Zool. J. Linn. Soc. 151, 577–508.

Azanza, B., Menéndez, E., 1990. Los ciervos fósiles del neógeno español. Paleontol. Evol. 23, 75–82.

Bernor, R.L., Hussain, S.T., 1985. An assessment of the systematic, phylogenetic and biogeographic relationships of Siwalik hipparionine horses. J. Vertebr. Paleontol. 5, 32–87.

Bernor, R.L., Woodburne, M.O., Van Couvering, J.A., 1980. A contribution to the chronology of some Old World Miocene faunas based on hipparionine horses. Geobios 13, 705–739.

Bernor, R.L., Tobien, H., Woodburne, M.O., 1990. Patterns of Old World hipparionine evolutionary diversification and biogeographic extension. In: Lindsay, E.H., Fahlbush, V., Mein, P. (Eds.), European Neogene Mammal Chronology. Plenum Press, New York, pp. 263–319.

Bernor, R.L., Koufos, G.D., Woodburne, M.O., Fortelius, M., 1996. The evolutionary history and biochronology of European and Southwest Asian Late Miocene and Pliocene Hipparionine horses. In: Bernor, R.L., Fahlbusch, V., Mittmann, H.-W. (Eds.), The Evolution of Western Eurasian Neogene Faunas. Columbia University Press, New York, pp. 307–338.

Bernor, R.L., Göhlich, U., Harzhauser, M., Semprebon, G.M., 2017. The Pannonian C hipparions from the Vienna Basin. Palaeogeogr. Palaeoclimatol. Palaeoecol. 476, 28–41.

Bernor, R.L., Kaya, F., Kaakinen, A., Saarinen, J., Fortelius, M., 2021. Old world hipparion evolution, biogeography, climatology and ecology. Earth Sci. Rev. 221, 103784.

Casanovas-Vilar, I., Furió, M., Agustí, J., 2006. Rodents, insectivores and paleoenvironment associated to the first-appearing hipparionine horses in the Vallès-Penedès Basin (Northeastern Spain). Beitr. Paläontol. 30, 89–107.

Casanovas-Vilar, I., Alba, D.M., Moyà-Solà, S., Galindo, J., Cabrera, L., Garcés, M., Furió, M., Robles, J.M., Köhler, M., Angelone, C., 2008. Biochronological, taphonomical and

paleoenvironmental background of the fossil great ape *Pierolapithecus catalaunicus* (Primates, Hominidae). J. Hum. Evol 55, 589–603.

Casanovas-Vilar, I., Alba, D.M., Robles, J.M., Galindo, J., Carmona Garcia, R., 2010. Rosegadors del Dipòsit Controlat de Vacamorta (=Can Colomer) (Cruïlles, Baix Empordà). In: Galobart, À. (Ed.), Treballs de Paleontologia. Servei d'Arqueologia i Paleontologia, Barcelona, pp. 129–150.

Casanovas-Vilar, I., Garcés, M., Van Dam, J., García-Paredes, I., Robles, J.M., Alba, D.M., 2016a. An updated biostratigraphy for the late Aragonian and the Vallesian of the Vallès-Penedès Basin (Catalonia). Geol. Acta 14, 195–217.

Casanovas-Vilar, I., Madern, A., Alba, D.M., Cabrera, L., García-Paredes, I., Van den Hoek Ostende, L.W., DeMiguel, D., Robles, J.M., Furió, M., Van Dam, J., Garcés, M., Angelone, C., Moyà-Solà, S., 2016b. The Miocene mammal record of the Vallès-Penedès Basin (Catalonia). C. R. Palevol 15, 791–812.

Castillo, A., López-Guerrero, P., Álvarez-Sierra, M.Á., 2018. New Insights on Cricetodontini (Rodentia, Mammalia) from the Duero Basin, Spain. Hist. Biol. 30, 392–403.

Churcher, C.S., 1978. Giraffidae. In: Maglio, V.J., Cooke, H.B.S. (Eds.), Evolution of African Mammals. Harvard University Press, Cambridge, pp. 509–535.

Colbert, E.H., 1933. A skull and mandible of *Giraffokeryx punjabiensis* Pilgrim. Am. Mus. Nov. 632, 1–14.

Crusafont Pairó, M., 1950. La cuestión del llamado Meótico español. Arrahona 1950, 41–48.

Crusafont Pairó, M., 1952. Los jiráfidos fósiles de España. Mem. Com. Inst. Geol. Prov. 8, 1–239.

Crusafont Pairó, M., 1953. Primer hallazgo de un jiráfido fósil en el Meótico del Vallès. Mem. Com. Inst. Geol. Prov. 10, 11–12.

Crusafont Pairó, M., 1962. Las especies transientes en paleomastología: su importancia en España. Not. Com. Inst. Geol. Min. Esp. 65, 49–60.

Crusafont Pairó, M., 1965. El desarrollo de los caninos en algunos Driopitécidos del Vallesiense en Cataluña. Not. Com. Inst. Geol. Min. Esp. 80, 179–191.

Crusafont Pairó, M., 1975. Topografia paleontològica del Vallès. In: Societat Catalana de Geografia (Ed.), Miscel·lània Pau Vila: Biografia, Bibliografia, Treballs d'Homenatge. Editorial Montblanc-Martín, Granollers, pp. 249–254.

Crusafont Pairó, M., 1982. Novetats paleomastològiques del Vallès-Penedès. Nota preliminar. Acta Geol. Hisp. 14, 354–355.

Crusafont Pairó, M., Golpe Posse, J.M., 1971. Biozonation des Mammifères néogènes d'Espagne. In: V Congrés du Néogène Mediterranéen. Mém. Bur. Recher. Géol. Min. 78, 121–129.

Crusafont-Pairó, M., Golpe, J.M., 1972. Dos nuevos yacimientos del vindoboniense en el Vallés. Acta Geol. Hisp. 7, 71–72.

Crusafont-Pairó, M., Golpe-Posse, J.M., 1972. Algunos nuevos yacimientos de vertebrados del Vallesiense inferior de los alrededores de Sabadell. Acta Geol. Hisp. 7, 69–70.

Crusafont-Pairó, M., Ginsburg, L., 1973. Les carnassiers fossiles de Los Vallès de Fuentiduena (Ségovie, Espagne). Bull. Mus. Nat. Hist. Nat. 131, 29–45.

Crusafont-Pairó, M., Golpe-Posse, J.M., 1973. New pongids from the Miocene of Vallès Penedès Basin (Catalonia, Spain). J. Hum Evol. 2, 17–24.

Crusafont-Pairó, M., Golpe-Posse, J.M., 1974a. Nuevos yacimientos del Terciario continental del N. E. de España. Acta Geol. Hisp. 9 81–83.

Crusafont-Pairó, M., Golpe-Posse, J.M., 1974b. Asociación de *Anchitherium* Mey., 1834, con *Hipparion* Christ, 1832, en el Alto Mioceno del Vallés. Bol. R. Soc. Esp. Hist. Nat. (Geol.) 72, 75–93.

Crusafont, M., Truyols, J., 1954. Catálogo Paleomastológico del Mioceno del Vallés-Penedés y de Calatayud-Teruel. Segundo Cursillo Internacional de Paleontología. Museo de la Ciudad de Sabadell, Sabadell.

Crusafont, M., Truyols, J., 1956. Catálogos paleomastológicos. A) Cuenca del Vallés-Penedés (adiciones). B) Cuenca de Calatayud-Teruel (adiciones). C) Cuenca de La Cerdaña. D) Cuenca de la Seu d'Urgell. E) Cuenca de Tremp. F) Tipos de la fauna española. III Cursillo Internacional de Paleontología. Museo de la Ciudad de Sabadell, Sabadell.

Crusafont Pairó, M., Aguirre, E. de, García, J., 1968. Un nuevo yacimiento de Mamíferos del Mioceno de la meseta española. Acta Geol. Hisp. 3, 22–24.

Daams, R., Freudenthal, M., 1988. Cricetidae (Rodentia) from the type-Aragonian; the genus *Megacricetodon*. Scripta Geol. Special Issue 1, 39–132.

de Beaumont, G., 1978. Notes complementaires sur quelques Félidés (Carnivores). Arch. Sci. Phys. Nat. Géneve 31, 219–227.

Deng, T., Wang, X., Ni, X., Liu, L., 2004. Sequence of the Cenozoic mammalian faunas of the Linxia Basin in Gansu, China. Acta Geol. Sin. 78, 8–14.

Deng, T., Qiu, Z.-X., Wang, B.-Y., Wang, X., Hou S.-K., 2013. Late Cenozoic biostratigraphy of the Linxia Basin, Northwestern China. In: Wang, X., Flynn, L.J.,

Fortelius M. (Eds.), Fossil Mammals of Asia: Neogene Biostratigraphy and Chronology. Columbia University Press, New York, pp. 243–273.

Fang, X., Wang, J., Zhang, W., Zan, J., Song, C., Yan, M., Appel, E., Zhang, T., Wu, F., Yang, Y., Lu, Y., 2016. Tectonosedimentary evolution model of an intracontinental flexural (foreland) basin for paleoclimatic research. Global Planet. Change 145, 78–97.

Fernández-Monescillo, M., Antón, M., Salesa, M.J., 2019. Palaeoecological implications of the sympatric distribution of two species of *Machairodus* (Felidae, Machairodontinae, Homotherini) in the Late Miocene of Los Valles de Fuentidueña (Segovia, Spain). Hist. Biol. 31, 903–913.

Forstén, A. 1982. *Hipparion primigenium melendezi* Alberdi reconsidered. Ann. Zool. Fenn. 19, 109–113.

Fortelius, M., Armour-Chelu, M., Bernor, R. L., Fessaha, N., 2005. Systematics and palaeobiology of the Rudabánya Suidae. Palaeontogr. Ital. 90*,* 259–278.

Garcés, M., Agustí, J., Cabrera, L., Parés, J.M., 1996. Magnetostratigraphy of the Vallesian (late Miocene) in the Vallès-Penedès Basin (northeast Spain). Earth Planet. Sci. Lett. 142, 381–396.

García-Paredes, I., Álvarez-Sierra, M.Á., Van den Hoek Ostende, L., Hernández-Ballarín, V., Hordijk, K., López-Guerrero, P., Oliver, A., Peláez-Campomanes, P., 2016. The Aragonian and Vallesian high-resolution micromammal succession from the Calatayud-Montalbán Basin (Aragón, Spain). C. R. Palevol 15, 781–789.

Gibert, J., Agustí, J., Moyà, S., 1979. Bioestratigrafia de l'Empordà. Butll. Inf. Inst. Paleontol. Sabadell 11, 43–47.

Gibert, J., Agustí, J., Moyà, S., 1980. Nuevos datos sobre la bioestratigrafía del Ampurdán. Bol. Geol. Min. 91, 705–712.

Ginsburg, L., Morales, J., Soria, D., 1981. Nuevos datos sobre los carnívoros de los Valles de Fuentidueña (Segovia). Estud. Geol. 37, 383–415.

Golpe-Posse, J.M., 1971. Suiformes del Terciario español y sus yacimientos. Ph.D. Dissertation, Universidad de Barcelona.

Golpe-Posse, J.M., 1972. Suiformes del Terciario español y sus yacimientos (Tesis doctoral-Resumen) (revisado y reimprimido en Diciembre de 1972). Paleontol. Evol. 2, 1–197.

Golpe-Posse, J.M., 1974. Faunas de yacimientos con suiformes en el Terciario español. Paleontol. Evol. 8, 1–87.

Hamilton, W.R., 1978. Fossil giraffes from the Miocene of Africa and a revision of the phylogeny of the Giraffoidea. Phil. Trans. R. Soc. Lond. B 283, 165–229.

Harris, J.H., Liu, L.-P., 2007. Superfamily Suoidea. In: Prothero, D.R., Foss, E.F. (Eds.), The Evolution of Artiodactyls. Johns Hopkins University Press, Baltimore, pp. 130–150.

Konidaris, G.E., Koufos, G.D., 2019. Late Miocene proboscideans from Samos Island (Greece) revisited: new specimens from old collections. Paläontol. Z. *93*, 115–134.

Llenas, M., Galobart, À., Agustí, J., 2002. Els petits mamífers del neogen i del quaternari inferior. In: Maroto, J., Ramió, S., Galobart, À. (Eds.), Els Vertebrats Fòssils del Pla de l'Estany. Centre d'Estudis Comarcals de Banyoles, Banyoles, pp. 29–42.

López-Guerrero, P., García-Paredes, I., Álvarez-Sierra, M.Á., Peláez-Campomanes, P., 2014. Cricetodontini from the Calatayud–Daroca Basin (Spain): A taxonomical description and update of their stratigraphical distributions. C. R. Palevol 13, 647–664.

López-Guerrero, P., Álvarez-Sierra, M. Á., García-Paredes, I., Carro-Rodríguez, P. M., Peláez-Campomanes, P., 2019. Species of *Hispanomys* from the late Aragonian and early Vallesian (middle-late Miocene) of the Calatayud–Daroca Basin, Zaragoza, Spain. J. Iber. Geol. 45, 163–180.

Madurell-Malapeira, J., Robles, J.M., Casanovas-Vilar, I., Abella, J., Obradó, P., Alba, D.M., 2014. The scimitar-toothed cat *Machairodus aphanistus* (Carnivora: Felidae) in the Vallès-Penedès Basin (NE Iberian Peninsula). C. R. Palevol 13, 569–585.

Mazo, A.V., Van der Made, J., 2012. Iberian mastodonts: Geographic and stratigraphic distribution. Quat. Int. 255, 239–256.

Morales, J., Soria, D., 1981. Los artiodáctilos de los Valles de Fuentidueña (Segovia). Estud. Geol. 37, 477–501.

Morales, J., Moya-Sola, S., Soria, D., 1981. Presencia de la familia Moschidae (Artiodactyla, Mammalia) en el Vallesiense de España: *Hispanomeryx duriensis* novo gen. nova sp. Estud. Geol. 37, 467–475.

Morales, J., Soria, D., Thomas, H., 1987. Les Giraffidae (Artiodactyla, Mammalia) d'Al Jadidah du Miocène Moyen de la Formation Hofuf (Province du Hasa, Arabie Saoudite). Geobios 20, 441–467.

Morlo, M., Nagel, D., Bastl, K., 2020. Evolution of the carnivoran (Carnivora, Mammalia) guild structure across the Middle/Upper Miocene boundary in Germany. Palaeogeogr., Palaeoclimatol. Palaeoecol. 553, 109801.

Moyà-Solà, S., Köhler, M., Alba, D.M., Casanovas-Vilar, I., Galindo, J., Robles, J.M., Cabrera, L., Garcés, M., Almécija, S., Beamud, E., 2009. First partial face and upper dentition of the Middle Miocene hominoid *Dryopithecus fontani* from Abocador de Can

Mata (Vallès-Penedès Basin, Catalonia, NE Spain): taxonomic and phylogenetic implications. Am. J. Phys. Anthropol. 139, 126–145.

Oliver Pérez, A., 2015. Evolution of *Megacricetodon* from the Aragonian and Vallesian (Miocene) of the Iberian Peninsula. Ph.D. Dissertation, Universidad Complutense de Madrid.

Pesquero, M.D., Alberdi, M.T., 2012. New evidence of conspecificity between *Hipparion primigenium melendezi* Alberdi, 1974 from Los Valles de Fuentidueña (Segovia) and *Hipparion concudense concudense* Pirlot, 1956 from Concud (Teruel) Spain. Estud. Geol. 68, 247-260.

Pickford, M., 2014. *Sus valentini* Filhol (1882) from St Gaudens (MN 8–9) France: blighted from the outset but a key to understanding late Middle Miocene Tetraconodontinae (Suidae, Mammalia) of Europe. Mainz. Natwiss. Arch. 51, 167–220.

Pickford, M., 2016a. Biochronology of European Miocene Tetraconodontinae (Suidae, Artiodactyla, Mammalia) flowing from recent revision of the Subfamily. Ann. Naturhist. Mus. Wien A, 118, 175–244.

Pickford, M., 2016b. Revision of European Hyotheriinae (Suidae) and *Doliochoeridae* (Mammalia). Münch. Geowissen. Abh. A 44, 1–270.

Pickford, M., Pourabrishami, Z., 2013. Deciphering Dinotheriensande deinotheriid diversity. Palaeobiodivers. Palaeoenvir. 3, 121–150.

Ríos, M., Sánchez, I. M., Morales, J., 2016. Comparative anatomy, phylogeny, and systematics of the Miocene giraffid *Decennatherium pachecoi* Crusafont, 1952 (Mammalia, Ruminantia, Pecora): state of the art. J. Vertebr. Paleontol. 36, e1187624.

Ríos, M., Sánchez, I.M., Morales, J., 2017. A new giraffid (Mammalia, Ruminantia, Pecora) from the late Miocene of Spain, and the evolution of the sivathere-samothere lineage. PLoS One, 12, e0185378.

Ríos, M., Danowitz, M., Solounias, N., 2019. First identification of *Decennatherium* Crusafont, 1952 (Mammalia, Ruminantia, Pecora) in the Siwaliks of Pakistan. Geobios 57, 97–110.

Robles, J.M., Alba, D.M., Casanovas-Vilar, I., Galindo, J., Cabrera, L., Carmona, R., Moyà-Solà, S., 2011. On the age of the paleontological site of Can Missert (Terrassa, Vallès-Penedès Basin, NE Iberian Peninsula). In: Pérez-García, A., Gascó, F., Gasulla, J.M., Escaso, F. (Eds.), Viajando a Mundos Pretéritos. Ayuntamiento de Morella, Morella, pp. 339–346.

Rotgers, C., Alba, D.M., 2011. The genus *Anchitherium* (Equidae: Anchitheriinae) in the Vallès-Penedès Basin (Catalonia, Spain). In: Pérez-García, A., Gascó, F., Gasulla, J.M., Escaso, F. (Eds.), Viajando a Mundos Pretéritos. Ayuntamiento de Morella, Morella, pp. 347–354.

Sánchez, I.M., Morales, J., 2006. Distribución biocronológica de los Moschidae (Mammalia, Ruminantia) en España. Estud. Geol. 62, 533–546.

Schmidt-Kittler, N., 1976. Raubtiere aus dem Jungtertiär Kleinasiens. Palaeontographica A 155, 1–131.

Sesé Benito, C., López Martínez, N., 1981. Los micromamíferos (Insectivora, Rodentia y Lagomorpha) del Vallesiense inferior de Los Valles de Fuentidueña (Segovia, España). Estud. Geol. 37, 369–381.

Solounias, N., 2007. Family Giraffidae. In: Prothero, D.R., Foss, E.F. (Eds.), The Evolution of Artiodactyls. Johns Hopkins University Press, Baltimore, pp. 257–277.

Sun, B., Liu, Y., Chen, S., Deng, T., 2022. *Hippotherium* Datum implies Miocene palaeoecological pattern. Sci. Rep. 12, 3605.

Tosal, A., Coward, S.R., Casanovas-Vilar, I., Martín-Closas, C., 2022. Palaeoenvironmental reconstruction of the late Miocene macroflora of La Bisbal d'Empordà (Catalonia, Spain). Comparison with small mammals. Rev. Palaeobot. Palynol. 297, 104583.

Van Dam, J.A., Krijgsman, W., Abels, H.A., Álvarez-Sierra, M.Á., García-Paredes, I., López-Guerrero, P., Peláez-Campomanes, P., Ventra, D., 2014. Updated chronology for middle to late Miocene mammal sites of the Daroca area (Calatayud-Montalbán Basin, Spain). Geobios 47, 325–334.

Van der Made, J., 1990a. Iberian Suoidea. Paleontol. Evol. 23, 83–97.

Van der Made, J., 1990b. A range-chart for European Suidae and Tayassuidae. Paleontol. Evol. 23, 99–104.

Van der Made, J., 2020. The Suoidea from the Middle Miocene of Gračanica (Bugojno Basin, Bosnia and Herzegovina)—evolution, taxononomy, and biostratigraphy. Palaeobiodivers. Palaeoenvir. 100, 321–349.

Van der Made, J., Moyà-Solà, S., 1989. European Suinae (Artiodactyla) from the Late Miocene onwards. Boll. Soc. Paleontol. Ital. 28, 329–339.

Van der Made, J., Krakhmalnaya, T., Kubiak, H., 1999. The pig *Propotamochoerus palaeochoerus* from the Upper Miocene of Grytsiv, Ukraine. Estud. Geol. 55, 283–292.

Van der Meulen, A.J., Peláez-Campomanes, P., Daams, R., 2003. Revision of medium-sized Cricetidae from the Miocene of the Daroca-Villafeliche area in the Calatayud-Teruel Basin (Zaragoza, Spain). Coloquios de Paleontología Vol. Ext. 1, 385–411.

Villalta Comella, J.F. de, Crusafont Pairó, M., 1941. Noticia preliminar sobre la fauna de carnívoros del Mioceno continental del Vallés-Penedés. Bol. R. Soc. Esp. Hist. Nat. 39, 201–208.

Villalta Comella, J.F. de, Crusafont Pairó, M., 1943. Los vertebrados del Mioceno continental de la cuenca del Vallés-Panadés (provincia de Barcelona). I. Insectívoros. II. Carnívoros. Bol. Inst. Geol. Min. Esp. 56, 145–336.

Vislobokova, I., 2007. New data on Late Miocene mammals of Kohfidisch, Austria Paleontol. J. 41, 451–460.

Werdelin, L., Yamaguchi, N., Johnson, W.E., O'Brien, S.J., 2010. Phylogeny and evolution of cats (Felidae). In: Macdonald, D., Loveridge, A. (Eds.), The Biology and Conservation of Wild Felids. Oxford University Press, Oxford, pp. 59–82.

Woodburne, M.O., Bernor, R.L., 1980. On superspecific groups of some Old World hipparionine horses. J. Paleontol. 54, 1319–1348.

Zouhri, S., Bensalmia, A., 2005. Révision systemátique des *Hipparion* sensu lato (Perissodactyla, Equidae) de l'ancien monde. Estud. Geol. 61, 61–99.